

## 2-4 Analysis Method

### 2-4-1 Data Processing

The TDIP data processing involves the determination of 3 parameters, i.e., apparent resistivity, chargeability as well as metal factor. The first 2 parameters are calculated directly by the receiver unit during data acquisition. The third one is calculated as a simple relation between the first 2 parameters. These 3 parameters are calculated as follow:

#### a) Apparent resistivity ( $\rho$ )

$$\rho = \pi \frac{V}{I} a n(n+1)(n+2)$$

Where,

- V: Received voltage in volts
- a: A-spacing in meters
- n: N-spacing
- I: Transmitted current in Amp

#### b) Chargeability (M)

$$M = \frac{1}{V_p} \int V_s dt$$

Where,

- V<sub>p</sub>: Primary voltage in volts
- V<sub>s</sub>: Secondary voltage in volts

Here, the secondary voltage is calculated from 55.00 msec to 1555.00 msec.

#### c) Metal factor (MF)

$$MF = \frac{M}{\rho_a} \times 100$$

Where,

- M: Chargeability (mV/V)
- $\rho_a$ : Apparent resistivity ( $\Omega m$ )

### 2-4-2 Topographic Corrections

Since the apparent resistivity is calculated also in function of the location of the current and potential electrodes on a half-infinite plane, it is affected by topography depending on the location of the electrodes. For the case of a dipole-dipole configuration, the apparent resistivity appears to be high

beneath a hill and low beneath a valley. On the other hand, the chargeability values are less affected by topography.

For the present survey, topography corrections were carried out only in the lines 000N and 180S of Ghuzayn North, and in the lines 600N, 400N, 200N and 200S of Doqal area by using a finite element method which assumes a two dimensional half space topography.

### **2-4-3 Two-dimensional Analysis**

For the IP data analysis and according to the standard model, the apparent resistivity distribution and the chargeability distribution are used in combination to make a quantitative analysis of the pseudo-sections and plan maps. The resultant underground model is inferred by making use of the theoretical results given by the model. This is called in general a model simulation.

In the present survey, according to the limitations of the results of the forward modeling and to match the field results, it was used a 2-D inversion model which combines the FEM forward calculations with a non-linear square method. The inconveniences presented by the 1D analysis to make a more realistic layer analysis of the underground structure, are best solved by the approximation made by the 2-D model.

In order to make the model calculations, the geological structure is divided into many small blocks, each of them having initially assigned their own chargeability and resistivity value. The blocks are designed so that small blocks are placed close to the surface and they increase in size as the blocks are located at deeper levels.

## **2-5 Electrical Measurements of Rock Samples**

### **2-5-1 Measurement Method**

Measure of the electrical properties of rock samples were carried out in order to determine the actual electrical properties of the rocks distributed on the survey area. 26 pieces of the rocks collected from the surface were formed into a cubic shape and thereafter, soaked into water for a reasonable amount of days, apparent resistivity as well as chargeability values were measured according to the IP time domain procedures.

## 2-5-2 Results

Results of the electrical property of rocks and ore samples measured in the laboratory are indicated in Table II-2-3. The resistivity values measured in the laboratory ranged from 0.9 to 11343  $\Omega\text{m}$ . The samples Nos. 4, 8, 21 and 23 which correspond to massive sulphide presented extremely low resistivity values of around 1  $\Omega\text{m}$ , while the samples Nos. 5, 6, 12, 13, 14, 16, 18, 25, 15 and 26 indicated intermediate values in the range of 50 to 250  $\Omega\text{m}$ . The samples Nos. 1, 2, 3, 7, 9, 10, 11, 15, 17, 20 and 22 indicated high resistivity values above 300  $\Omega\text{m}$ .

The chargeability values measured in the laboratory ranged between 1.6 to 203 mV/V. The massive sulphide samples indicated high values between 53 and extremely high values of 203 mV/V. Also the network samples Nos. 5 and 17 showed high chargeability values of about 100 mV/V. The samples Nos. 7, 10, 18 and 19 indicated comparatively high values of about 30 mV/V. The samples Nos. 1, 3, 9, 14, 15, 20 and 22 indicated intermediate chargeability values around 10 mV/V.

The samples Nos. 27 and 28 were built by placing 3 selected samples together one after another, i.e., a massive sulphide (low resistivity-high chargeability) sample was placed in the middle of other two which ranged between medium to high resistivity and low to medium chargeability. Though the influence of the massive sulphide sample can be suggested, in both integrated samples, the predominant result indicated rather relatively high resistivity and low chargeability values.

## 2-6 Fardah Area

### 2-6-1 Lines location

Eight IP lines each of 1.5 km long were located on this area along the N28°E direction. The lines 400W and 600W, located towards the west of the area, were displaced 300m southwards in order to avoid the crossing of houses built on this area. The location of the lines are indicated in Fig. II-2-4.

### 2-6-2 Results

Apparent resistivity, chargeability and metal factor pseudo-sections for the 8 IP lines are indicated in Figs. II-2-5, II-2-6 and II-2-7 respectively. Figs. II-2-8, II-2-9, II-2-10 and II-2-11 show the resistivity, chargeability and metal factor maps for  $n=1$  to  $n=4$ .

According to the above mentioned results, it can be inferred that the apparent resistivity values range from 3 to 288  $\Omega\text{m}$ , but showing in general relatively low values of less than 50  $\Omega\text{m}$ . To the NE of the gossanized zone, it can be seen a zone of low resistivity extended along the NW-SE direction. This low resistivity zone presents a width of about 250m below 10  $\Omega\text{m}$  and displaced towards northeast at depth.

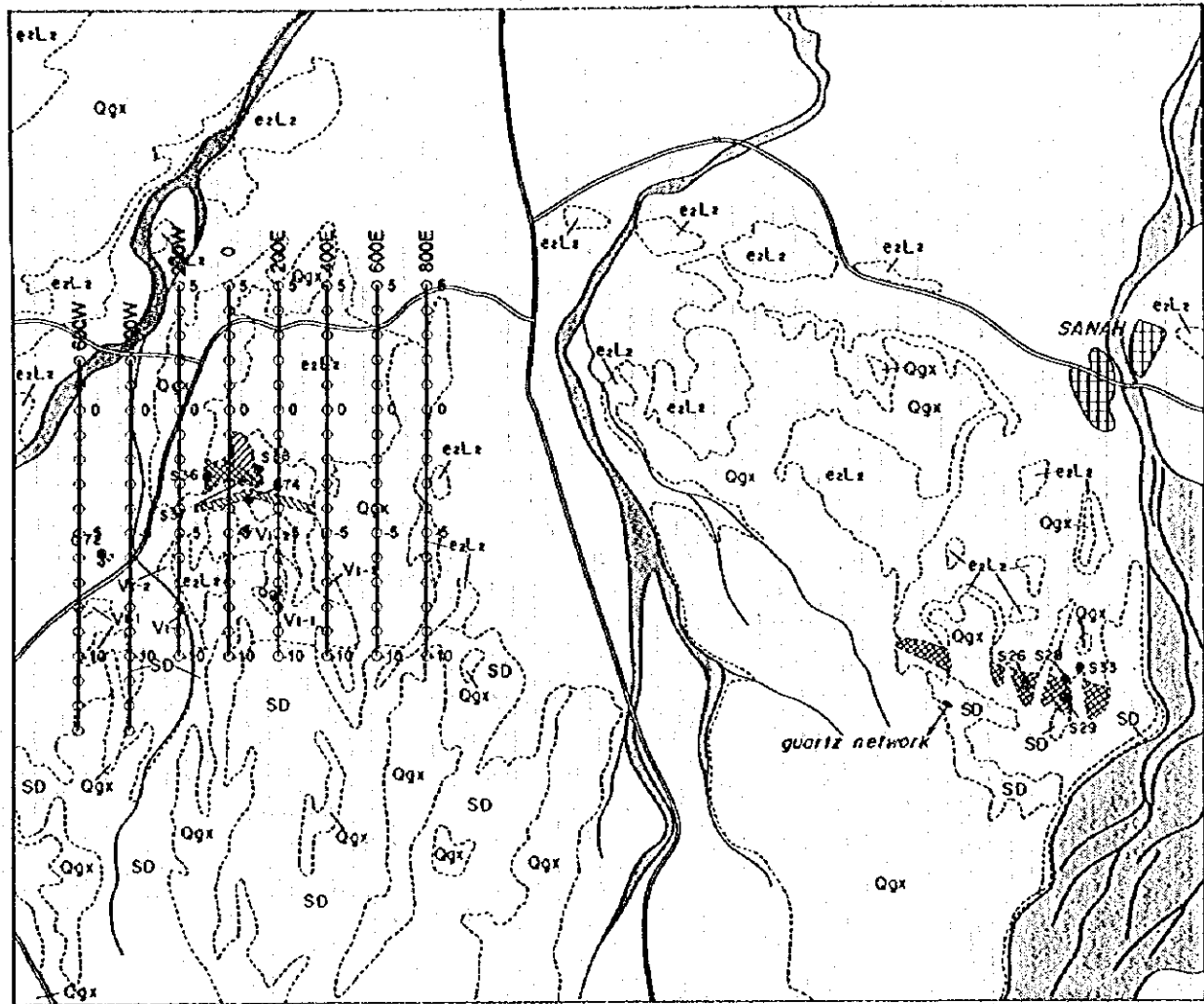
Table II-2-3 Resistivity and chargeability of core samples

No.	Area	Borehole No.	Sampling Depth(m)	Resis. ( $\Omega$ -m)	Charge. (mV/V)	Rock Name	Remarks
1	GG	G2	76.10	654.7	13.1	Pw(VI-1)	Py diss(sl)
2	GG	G2	170.30	454.3	5.1	Pw(VI-1)	Py diss, Py-Qz net, Sili(sl)
3	GG	G3	80.00	817.8	15.2	MI(VI-2)	Py-Cp diss(sl), Sili(sl)
4	GG	G3	140.30	1.1	53.3	Ms	Massive Sulphide
5	GG	G4	83.50	105.3	135.9	Pw(VI-2)	Sph-Cp net, Py diss(in), Sili(sl)
6	GG	G4	212.00	79.1	6.6	Pw(VI-2)	Py diss(sl), Py str
7	GG	G5	86.10	1000.0	34.6	Pw(VI-2)	Py diss, Py vein
8	GG	G5	165.40	0.9	177.6	Ms	Massive Sulphide
9	GG	G5	238.30	693.1	11.3	BaDy	Py diss, Sili(sl)
10	GG	G6	164.80	626.4	27.0	MI(VI-2)	Py diss(sl), Cp-Epi-Cal vein
11	GG	G7	28.10	930.5	5.1	Calc(Q)	
12	GG	G7	194.00	57.2	1.6	MI(VI-2)	Py diss(sl)
13	GG	G7	252.90	70.1	2.1	Pw(VI-2)	Py diss(sl)
14	GG	G8	115.60	225.6	12.0	MI(VI-2)	Py diss(sl), Cp-Py-Cal vein
15	GG	G9	52.70	489.0	16.3	Pw(VI-2)	Py diss
16	GG	G10	50.00	124.1	3.1	GaDy	
17	GG	G11	163.90	1134.0	104.1	Js	Hm, Py, Cp
18	GG	G12	64.00	248.7	31.5	Pw(VI-2)	Py diss, Py-Chl vein
19	GG	G13	167.80	81.2	32.1	Pw(VI-1)	Py diss(in), Py-Qz net, Sili(in)
20	GG	G14	80.00	423.0	11.4	BaDy	Py diss(sl), Py fine net
21	GG	G14	150.00	1.8	202.9	Ms	Massive Sulphide
22	GG	G15	52.50	327.0	14.6	Pw(VI-2)	Py diss, Sili
23	GG	G15	207.55	1.2	149.6	Ms	Massive Sulphide
24	GG	G16	45.25	253.5	3.7	MI(VI-2)	Py diss(sl)
25	DA	D1	31.20	147.7	6.7	Cata	Brecciated
26	DA	D4	37.50	221.9	7.6	MI(VI-2)	Py diss(sl), Py-Cal vein
27		14+23+7		261.4	33.0		
28		14+23+2		126.8	9.2		

Notes

- |                                  |                      |
|----------------------------------|----------------------|
| GG : Ghuzayn Gossan              | Py : Pyrite          |
| DA : Daris                       | Cp : Calcopryrite    |
|                                  | Sph : Sphalerite     |
| Resis. : Resistivity             | Epi : Epidote        |
| Charge. : Chargeability          | Cal : Calcite        |
|                                  | Hm : Hematite        |
| Pw : Pillow lava(basalt)         | Chl : Chlorite       |
| MI : Massive lava(basalt)        | Qz : Quartz          |
| MS : Massive sulphide            |                      |
| Js : Jasper                      | diss : dissemination |
| BaDy : Basalt ~ doleritic lava   | net : network        |
| GaDy : Gabbroic lava             | vein : veinlets      |
| Calc : Calcrete                  | (sl) : slight        |
| Cata : Cataclastic volcanic rock | (in) : intense       |
|                                  | Sili : Silicified    |
| VI-1 : Lower Extrusives 1        |                      |
| VI-2 : Lower Extrusives 2        |                      |
| Q : Quaternary                   |                      |

### Fardah-Sanah Area



**LITHOLOGY**

- Wadi sediments and sub-recent alluvial fans; terraces
- Qgx Ancient alluvial fans; terraces
- TERTIARY**
- ezLz Upper nodular limestone
- SANAH OPHIOLITE**  
Sanah Volcanic Rocks
- Y<sub>1-2</sub> Lower extrusives 2
- Y<sub>1-1</sub> Lower extrusives 1
- Sheeted-dyke complex**
- SD Sheeted dykes; dolerite

**MINERALIZATION**

- Gossan
- Argillized zone
- Gossanized metalliferous sediments
- Other symbols**
- S36 Sample location
- Road
- Wadi

○—○—○ TDIP Survey Lines

0 1 2 km

Fig. II-2-4 IP line locations in Fardah area

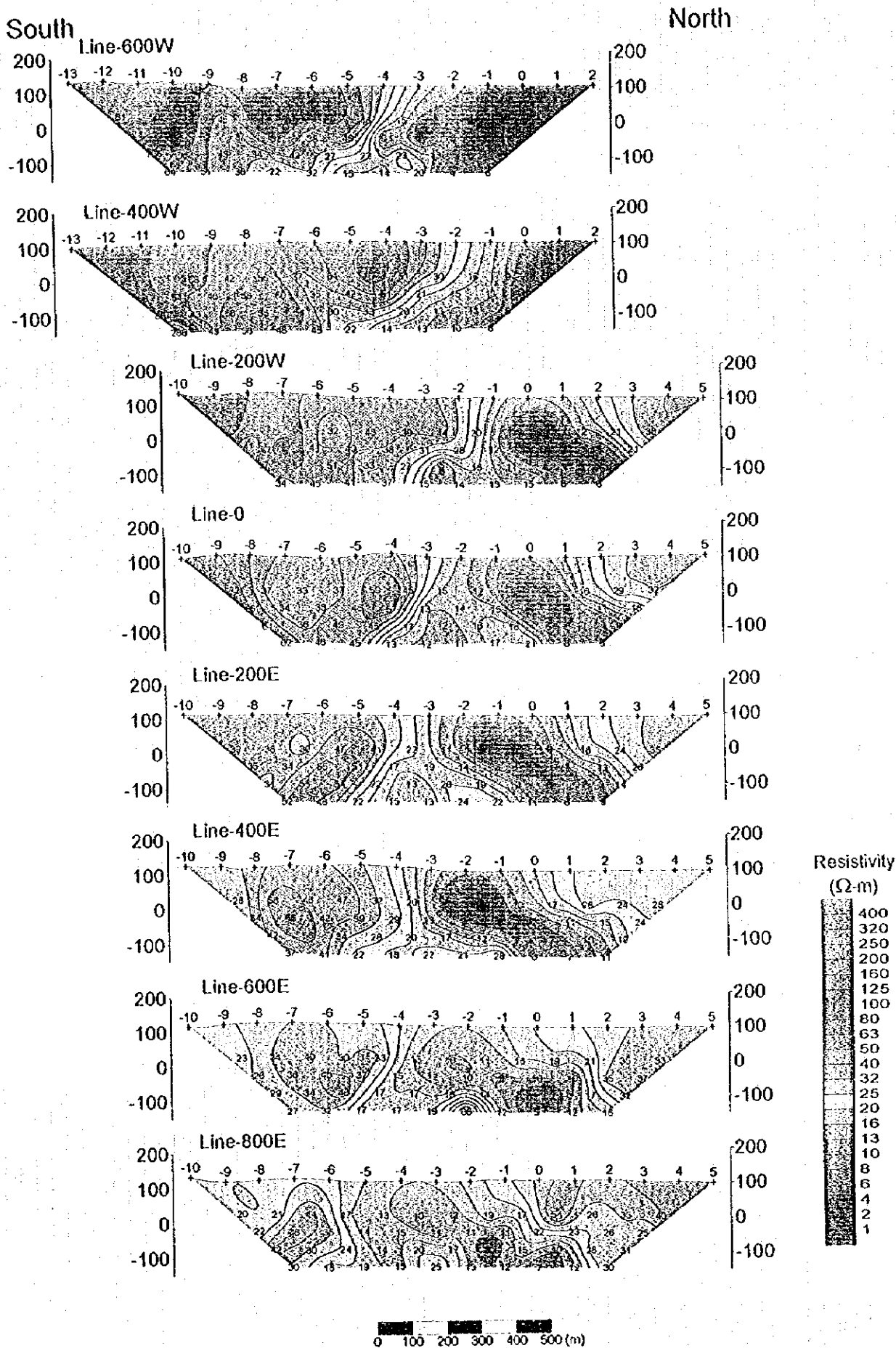


Fig.II-2-5 Apparent resistivity pseudo-sections in Pardah area 3a

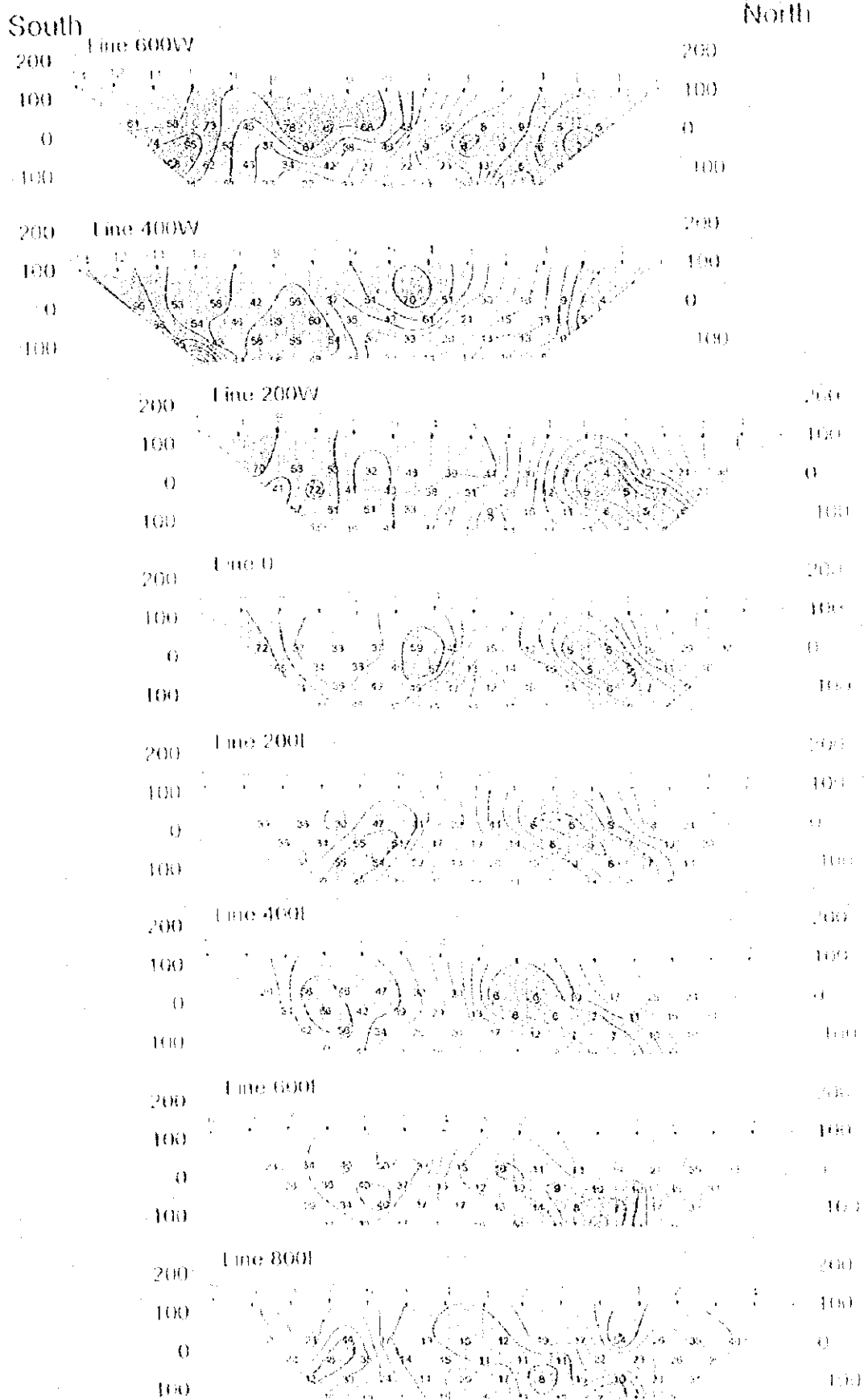
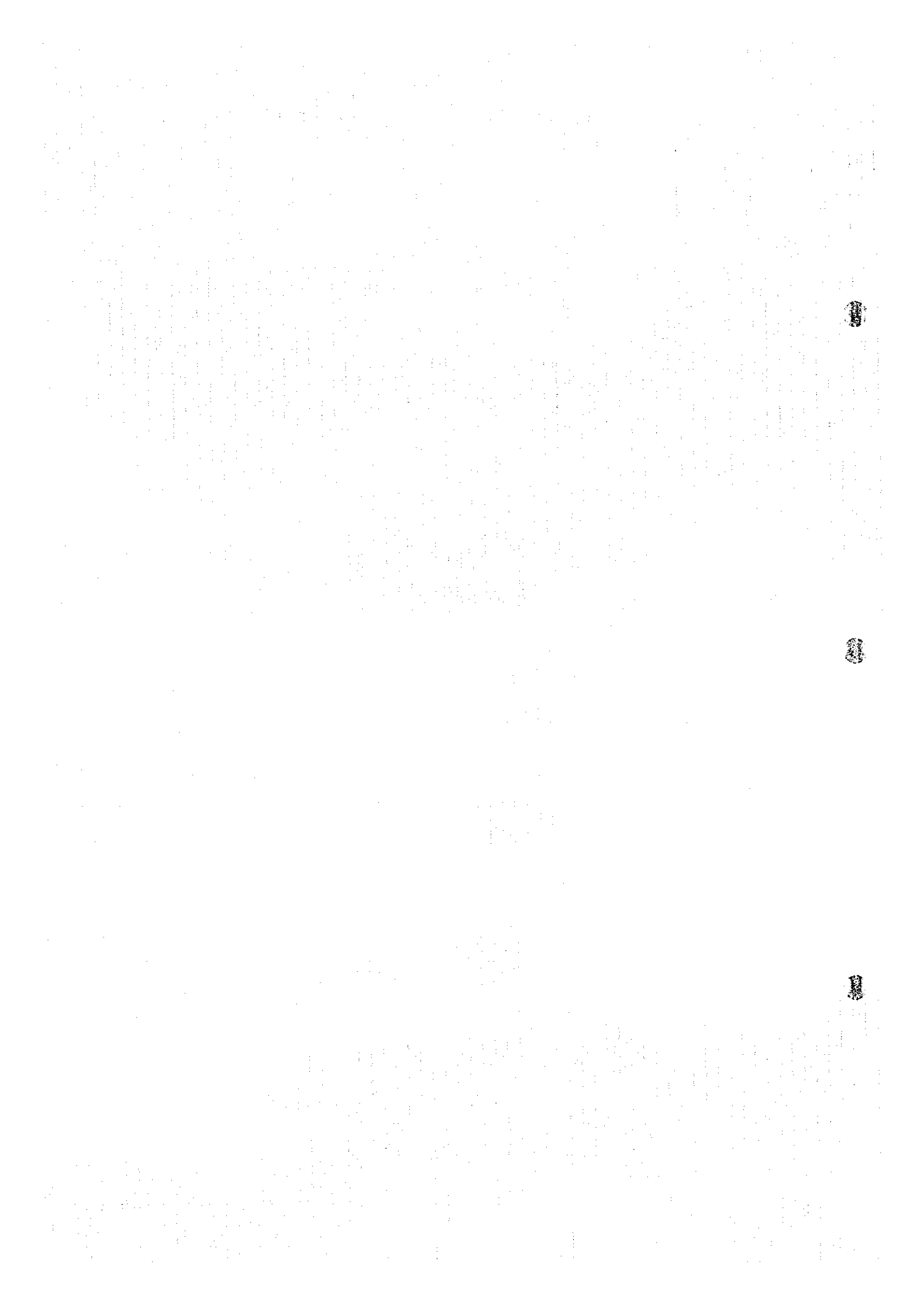


Fig. II.2.3 Apparent resistivity profiles in Enderbury





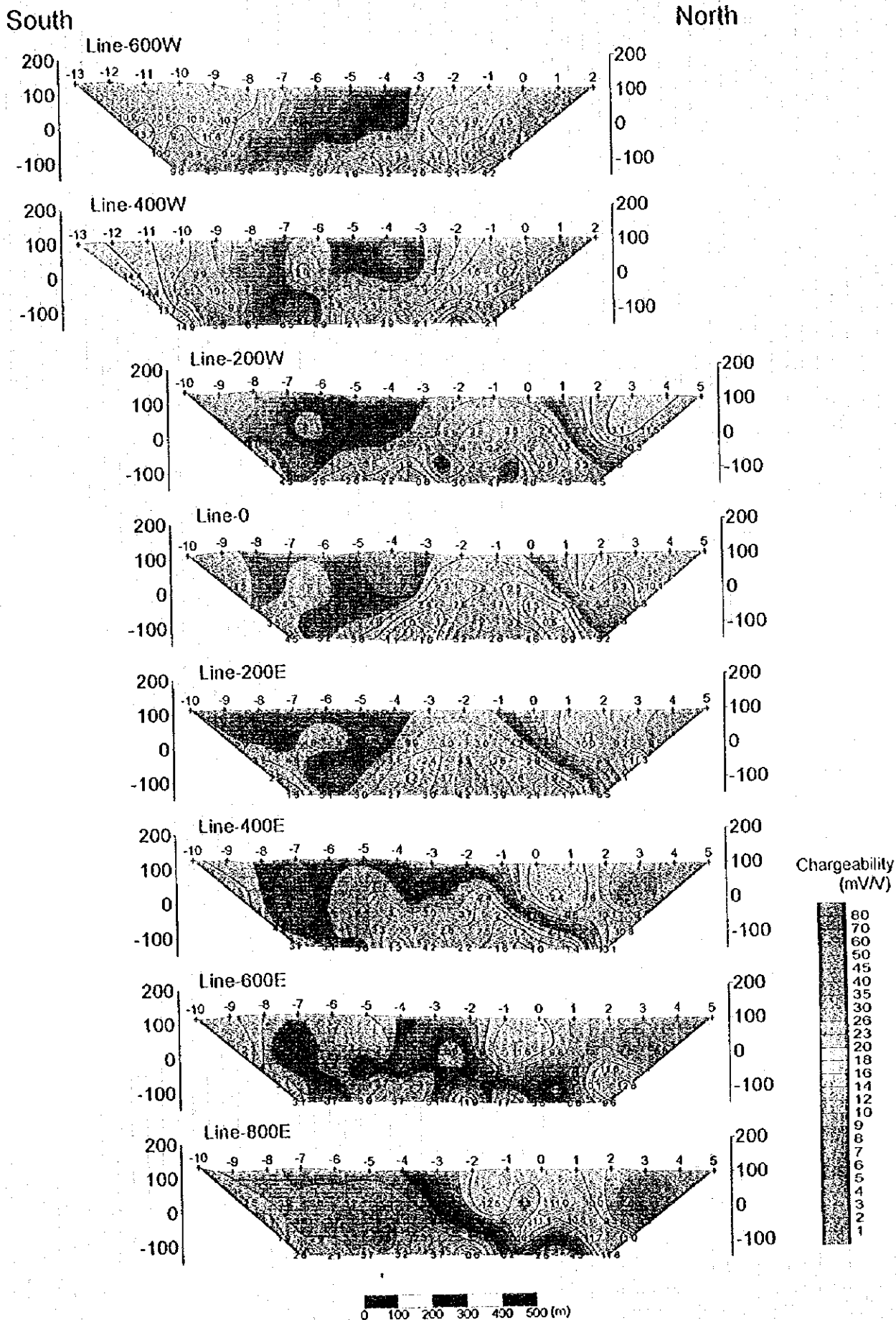
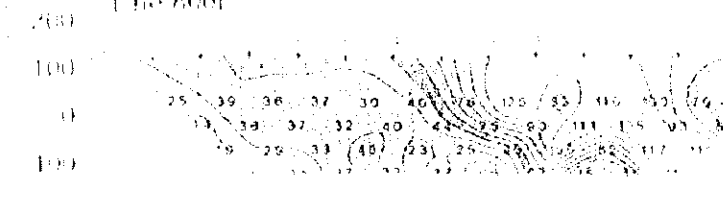
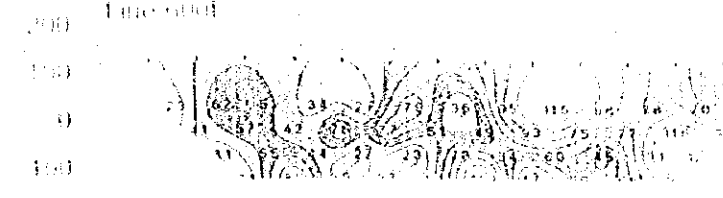
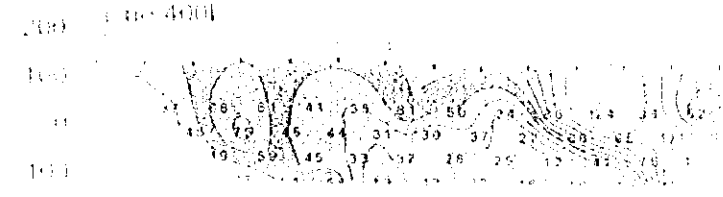
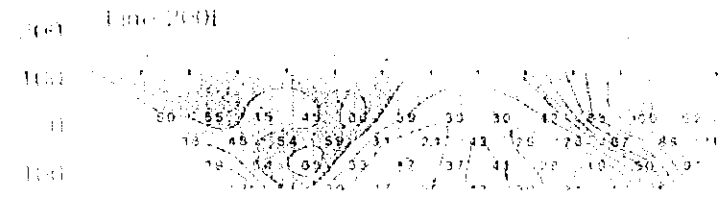
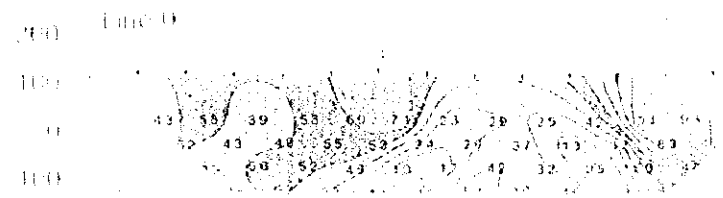
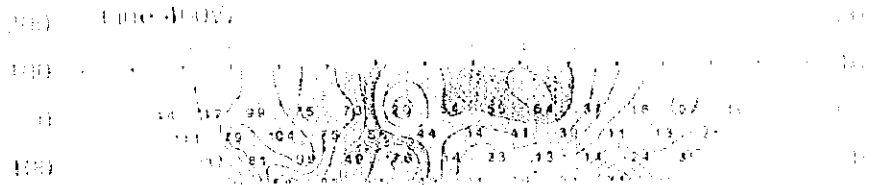
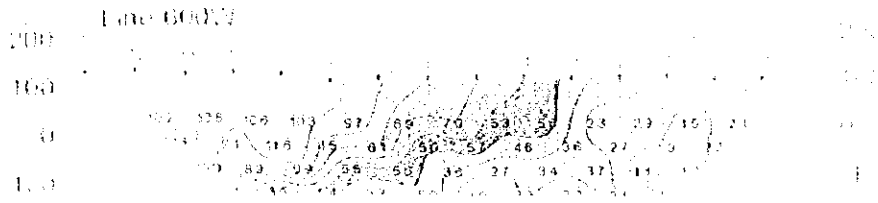


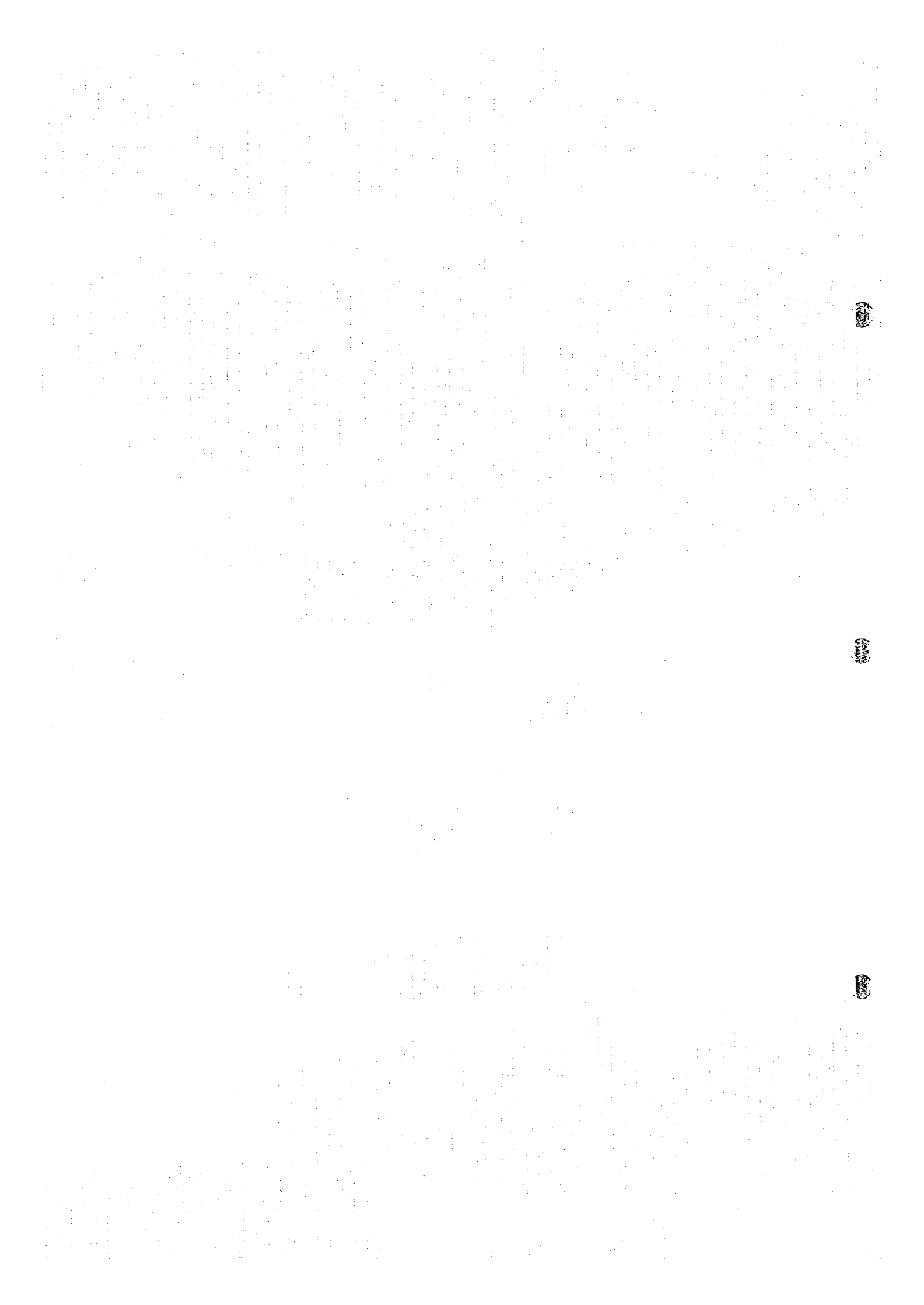
Fig.II-2-6 Chargeability pseudo-sections in Fardah area

South

North



Scale 1:1000



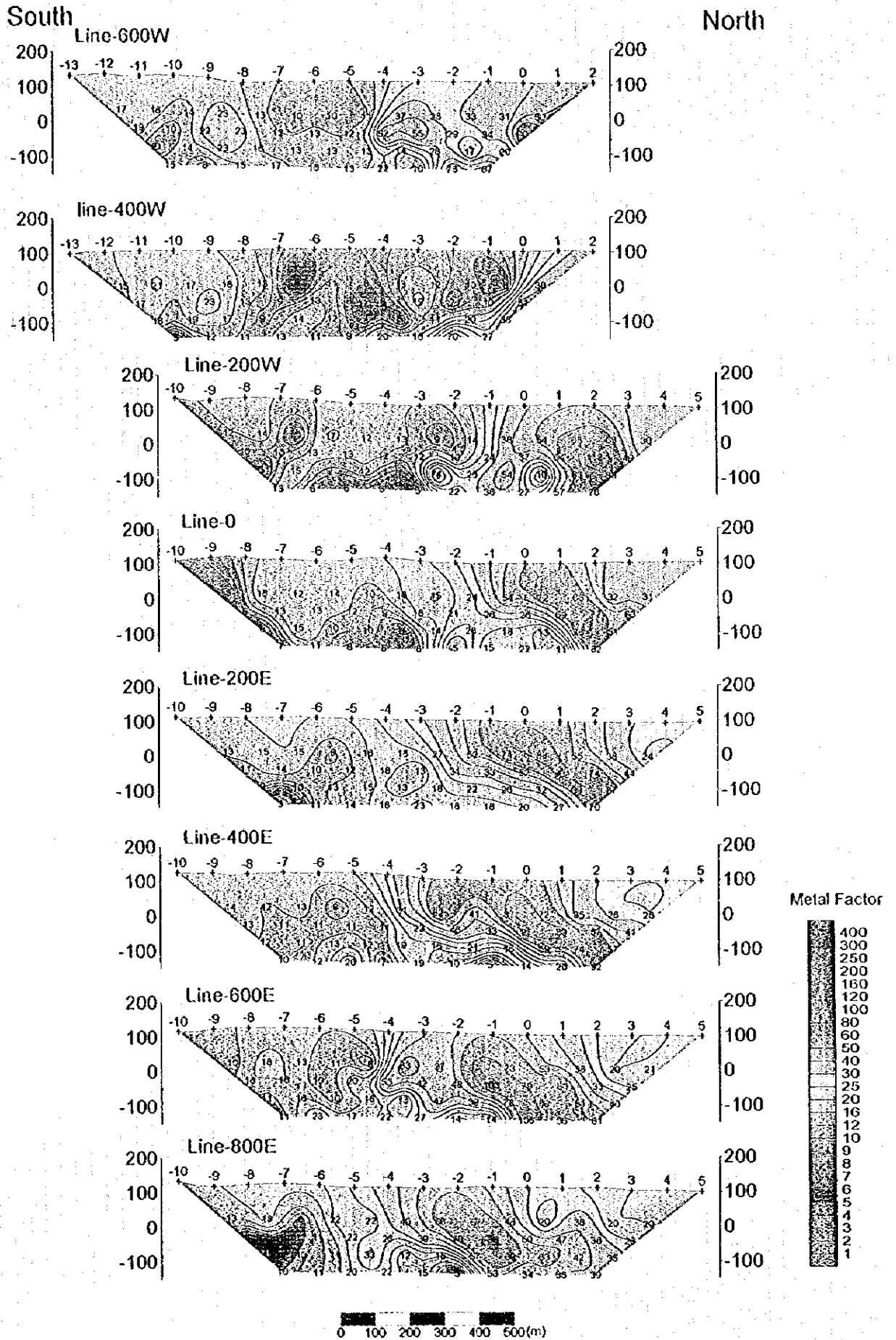


Fig.II-2-7 Metal factor pseudo-sections in Fardah area

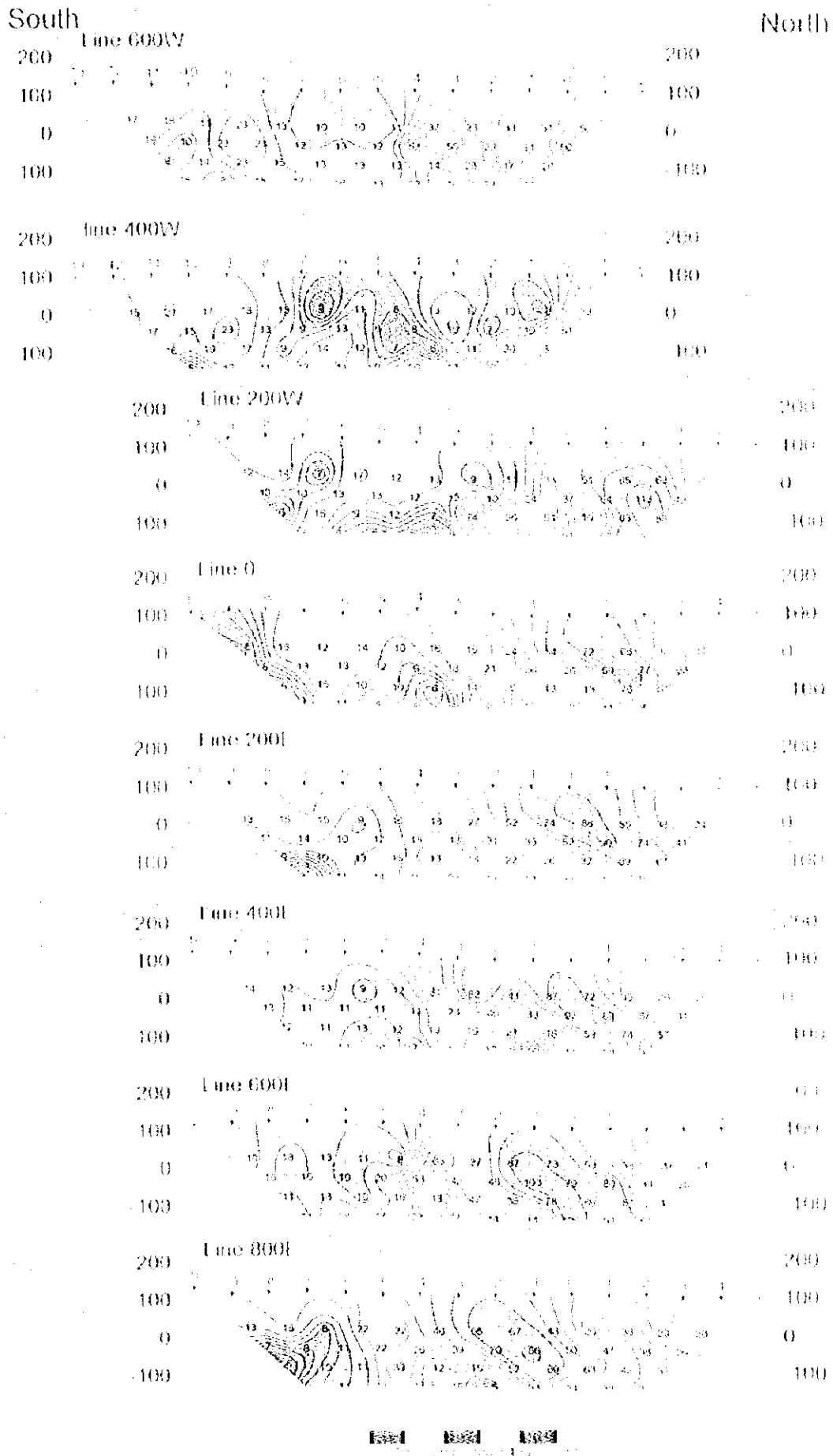
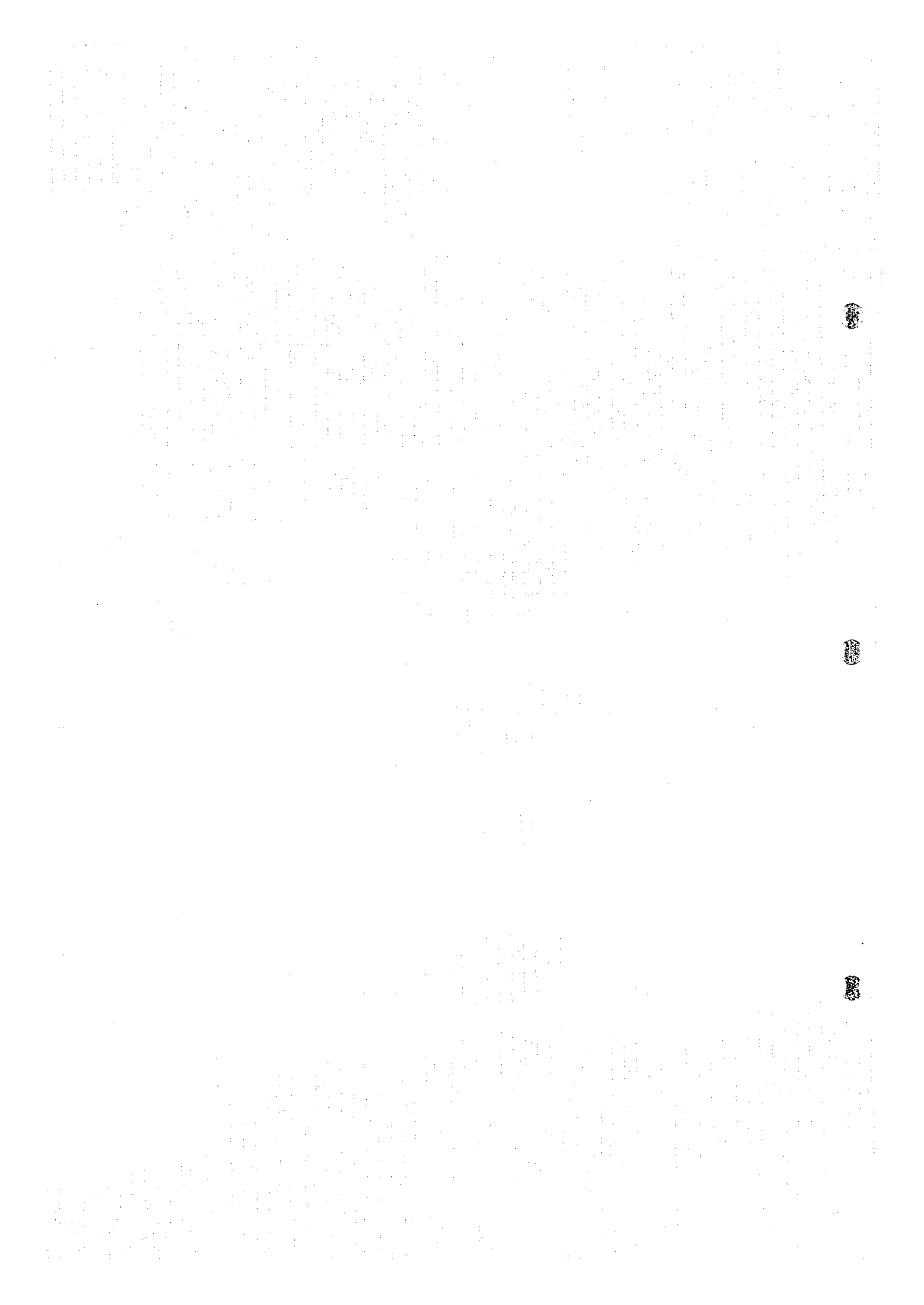
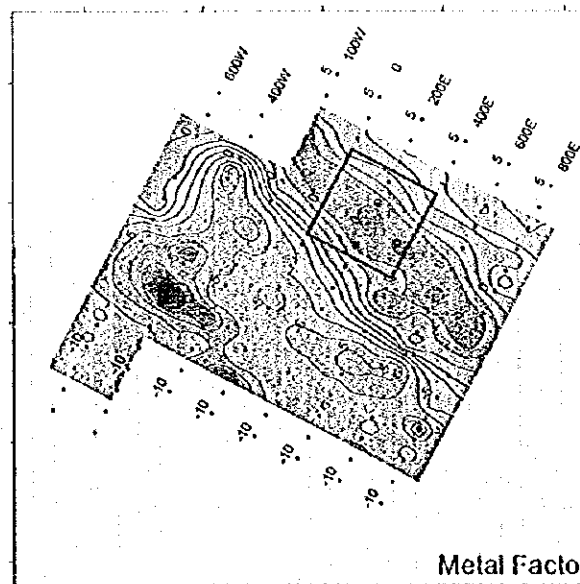
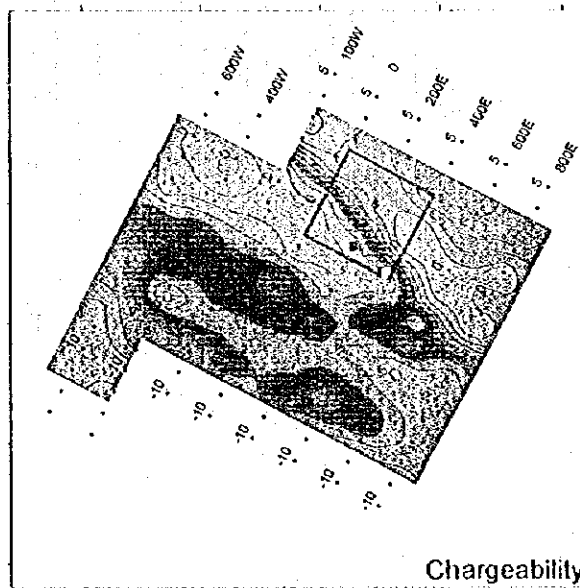
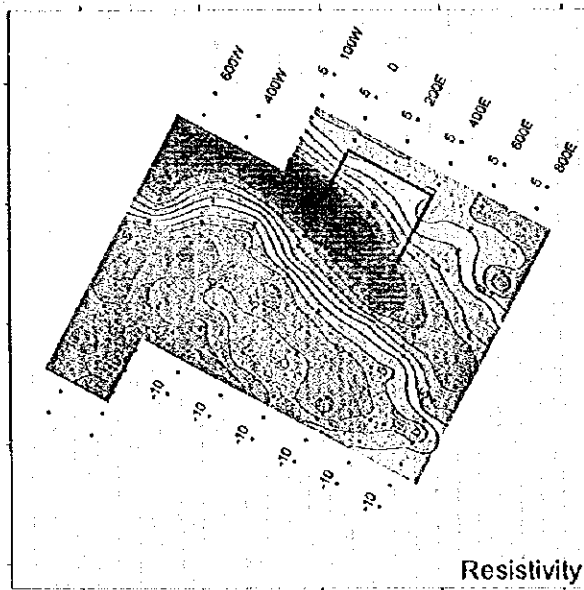


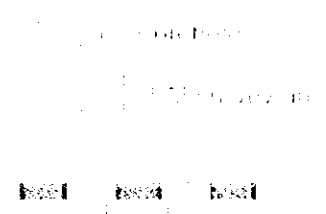
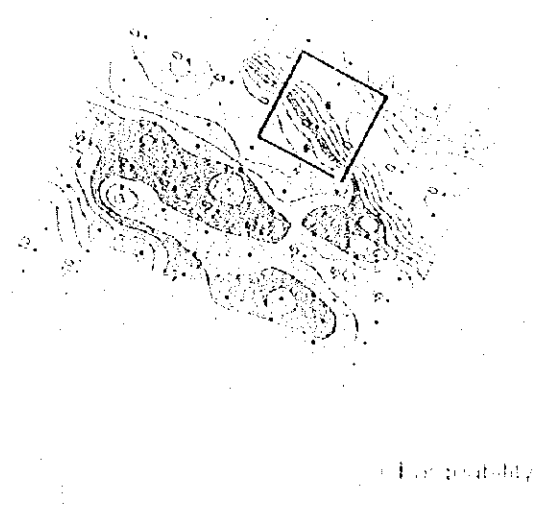
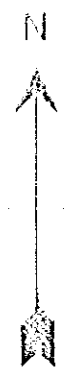
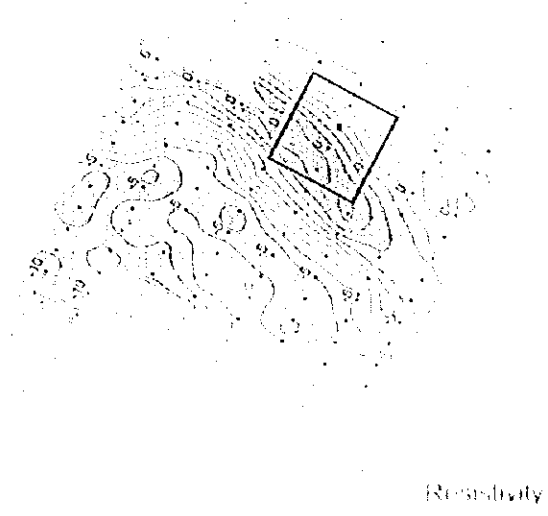
Fig. 11. Meridional temperature profiles as in Fig. 10.





Fardah Area  
TDIP Survey  
N=1

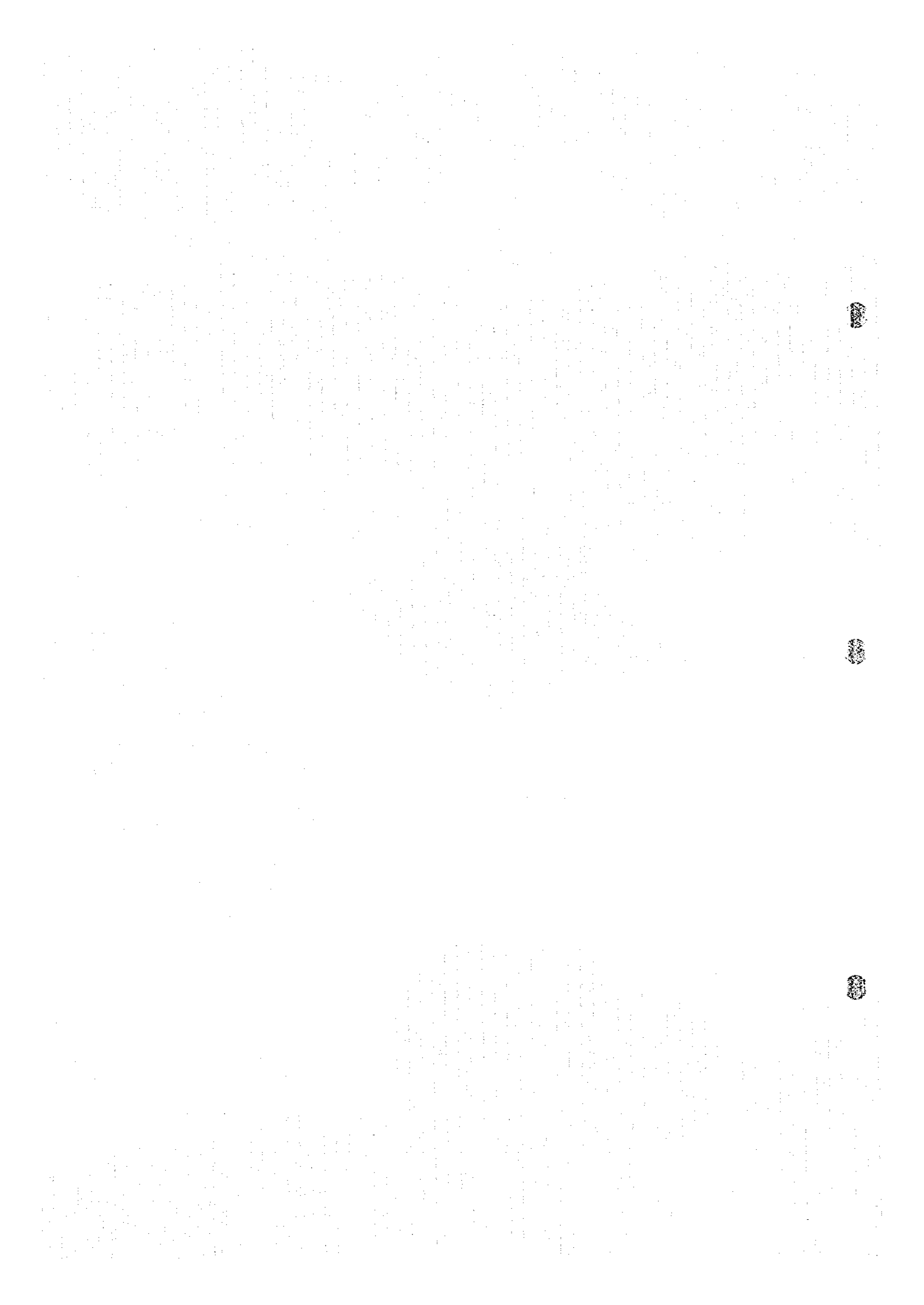
Fig.II-2-8 IP plane map of  $n=1$  in Farda area



Fardah Area  
EDIP Survey  
N-1

Fig. 1. Resistivity, Porosity, and Depth Factor





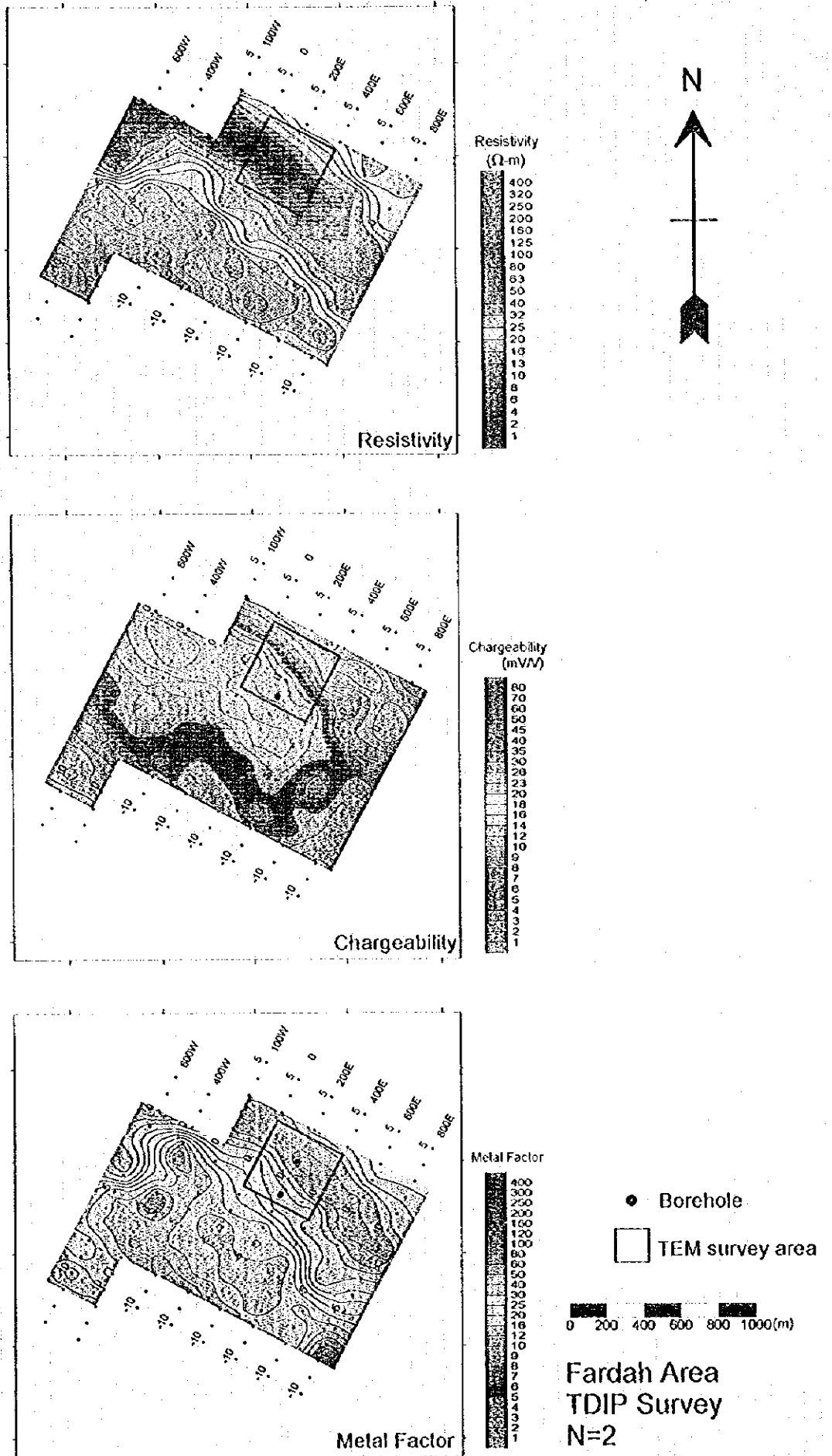
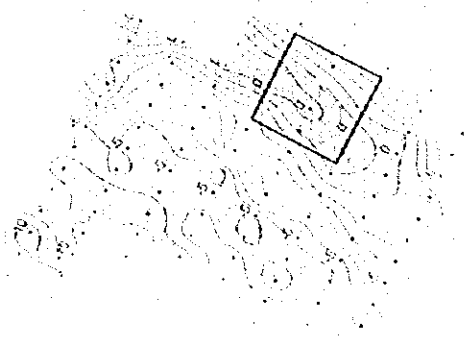
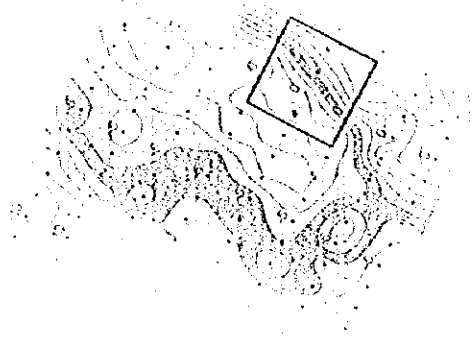


Fig. II-2-9 IP plane map of  $n=2$  in Farda area



Contour



Feasibility



Detail Factor

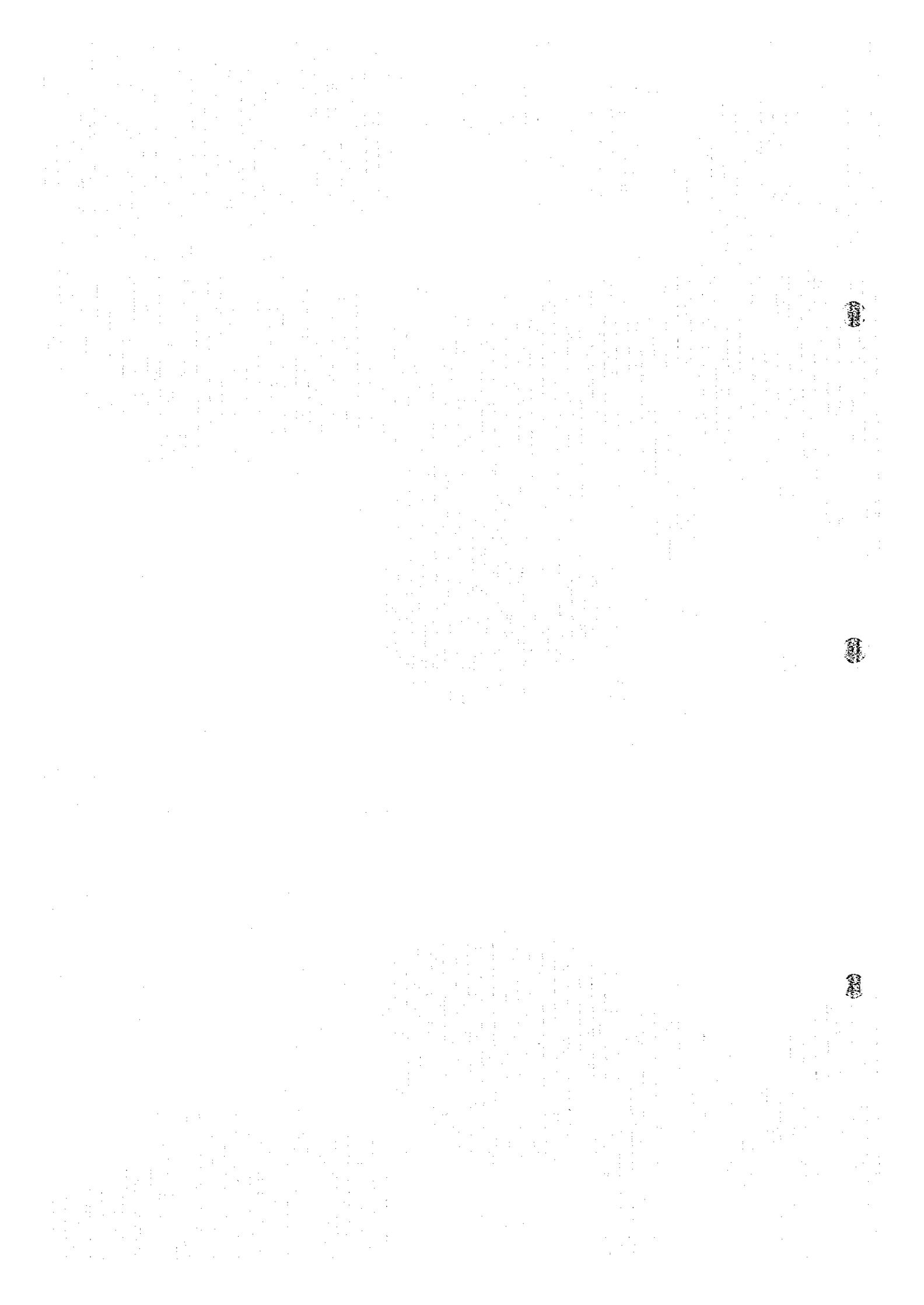
Legend

Contour

Feasibility

Detail Factor

Fardah Area  
 TDIP Survey  
 N-2



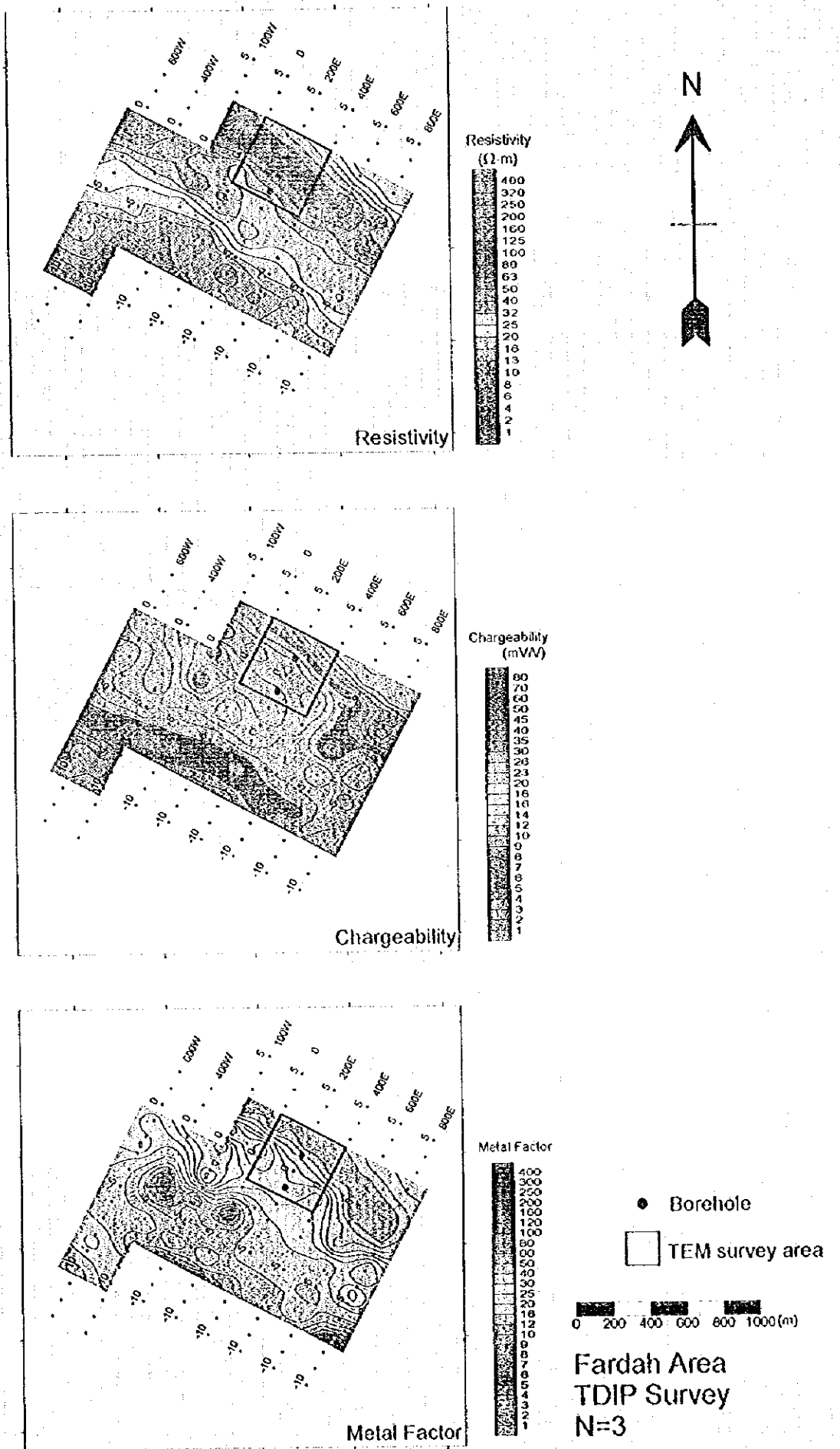


Fig.II-2-10 IP plane map of  $n=3$  in Fardah area

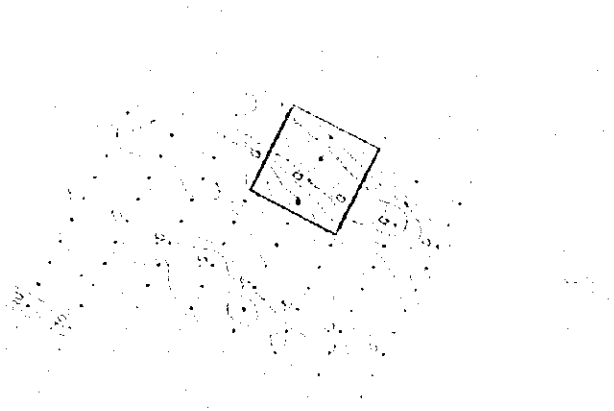


Figure 1

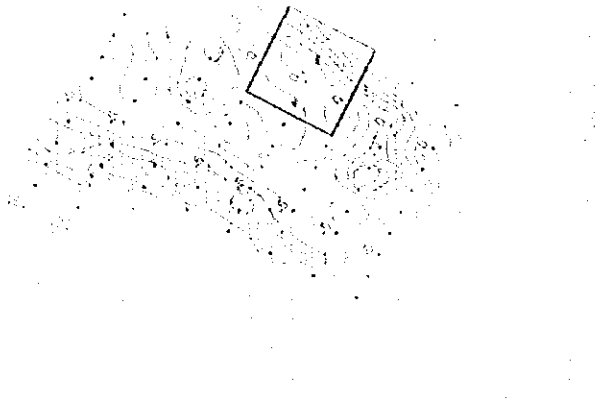


Figure 2

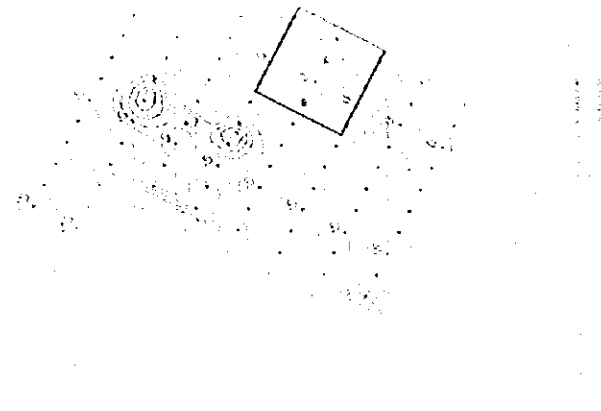
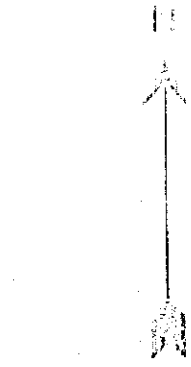


Figure 3



Scale 1:50,000  
 1:50,000  
 1:50,000

East East East

Eardah Area  
 TDP Survey  
 N 3



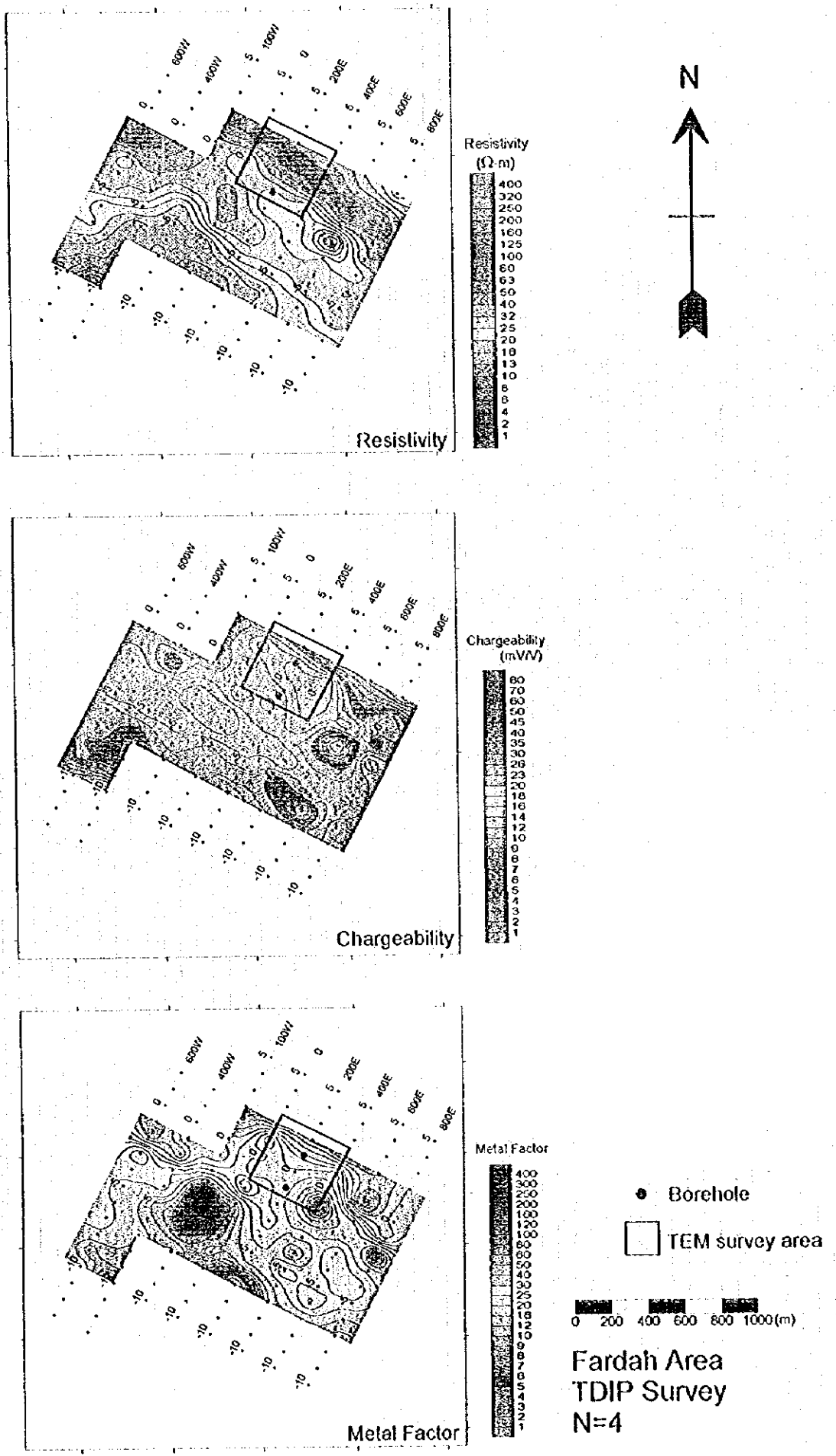


Fig.H-2-11 IP plane map of n=4 in Farda area





Chargeability values of about 10mV/V are seen as medium chargeability zones distributed in the same way as the zone of low resistivity values previously mentioned but displaced toward the north. This chargeability zone of medium values is also seen displaced towards the NE in such a way that for  $n=4$  this chargeability zone looks like is out of the range of the area under study. In the SW corner of the area under study, medium values chargeability distributions are seen with values above 10mV/V. In relation to the metal factor, the zone of low resistivity and the zone of medium chargeability values with values higher than 60 are seen also extended in a similar way as a low resistivity zone along the NW-SE direction.

### 2-6-3 2-D Analysis

For this area, the line 200E was selected for 2 dimensional analysis purposes. Fig. II-2-12 shows the results of 2-D analysis.

The resistivity section shows a distribution centered around station No -1 with values less than 10  $\Omega$ m and a width of about 200m. This distribution seems oriented about 60° inclined towards the north.

By observing the chargeability section, it is possible to delineate from station No. 1 and northwards, a shallow medium chargeability distribution of above 9 mV/V.

The metal factor section shows around the Station No. 0, a shallow distribution of above 60. This distribution trends northwards and presents similar patterns as the resistivity distribution mentioned above.

## 2-7 Sanah Area

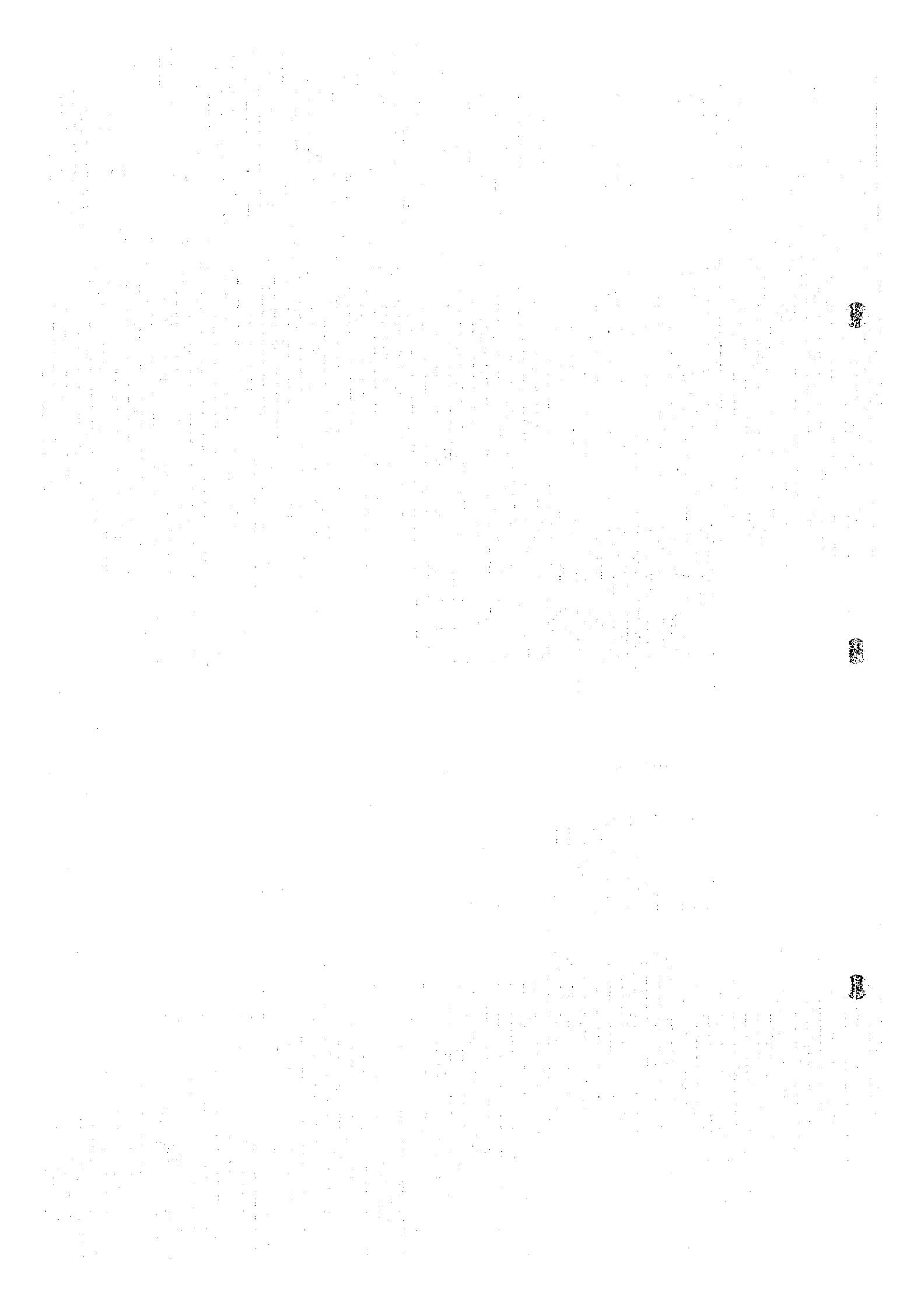
### 2-7-1 Lines location

Within the area under study, seven IP lines of 1.5 km each were located along N28°E. To the north of the area, the line 400E were displaced 100m towards the south to avoid houses located in the north margin. The location of the lines are indicated in Fig. II-2-13.

### 2-7-2 Results

The apparent resistivity, chargeability and metal factor pseudo-sections are indicated in Figs. II-2-14, II-2-15 and II-2-16, respectively. Figs. II-2-17, II-2-18, II-2-19 and II-2-20 show the resistivity, chargeability and metal factor maps for  $n=1$  to  $n=4$ , respectively.

The apparent resistivity and chargeability distributions found in this area present very similar patterns



# Line 200E

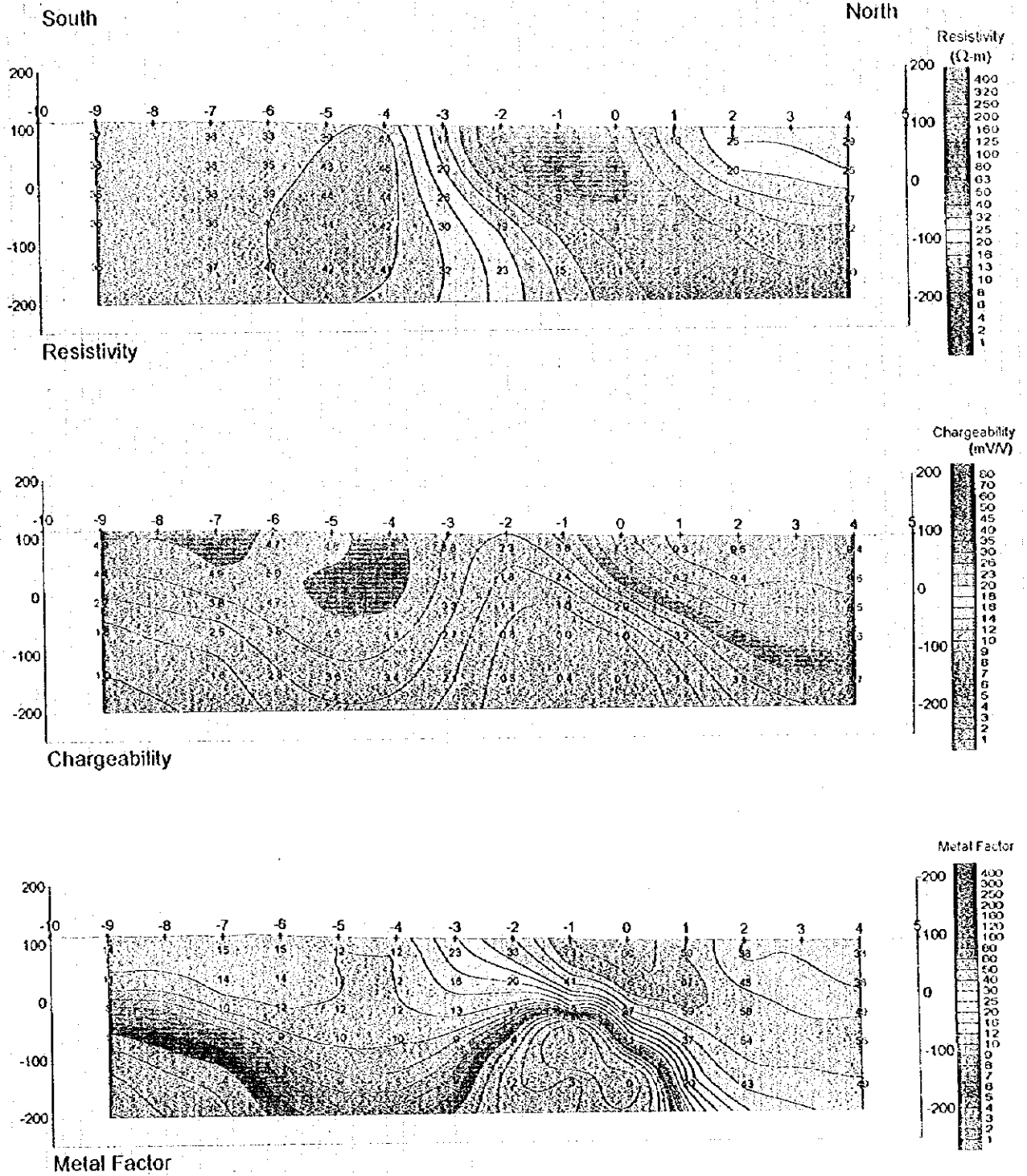
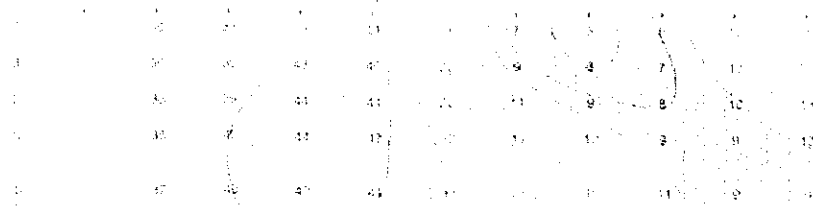


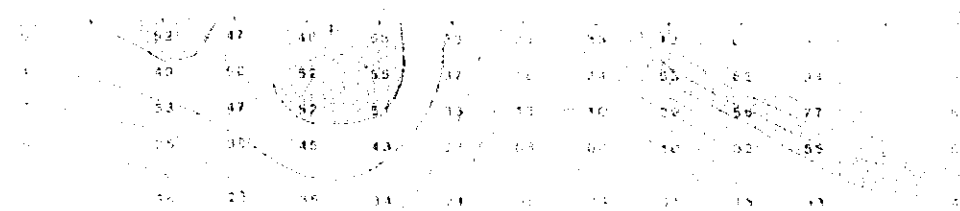
Fig.II-2-12 Results of model simulation on Line 200E in Fardah area

# Line 200E

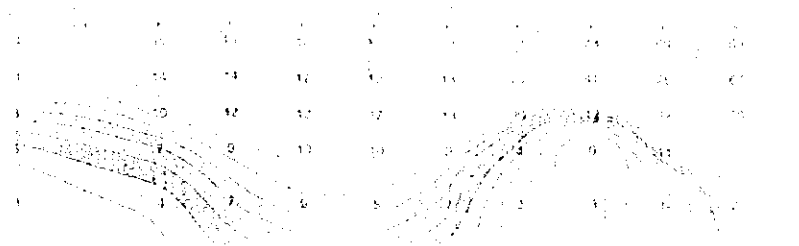
Results



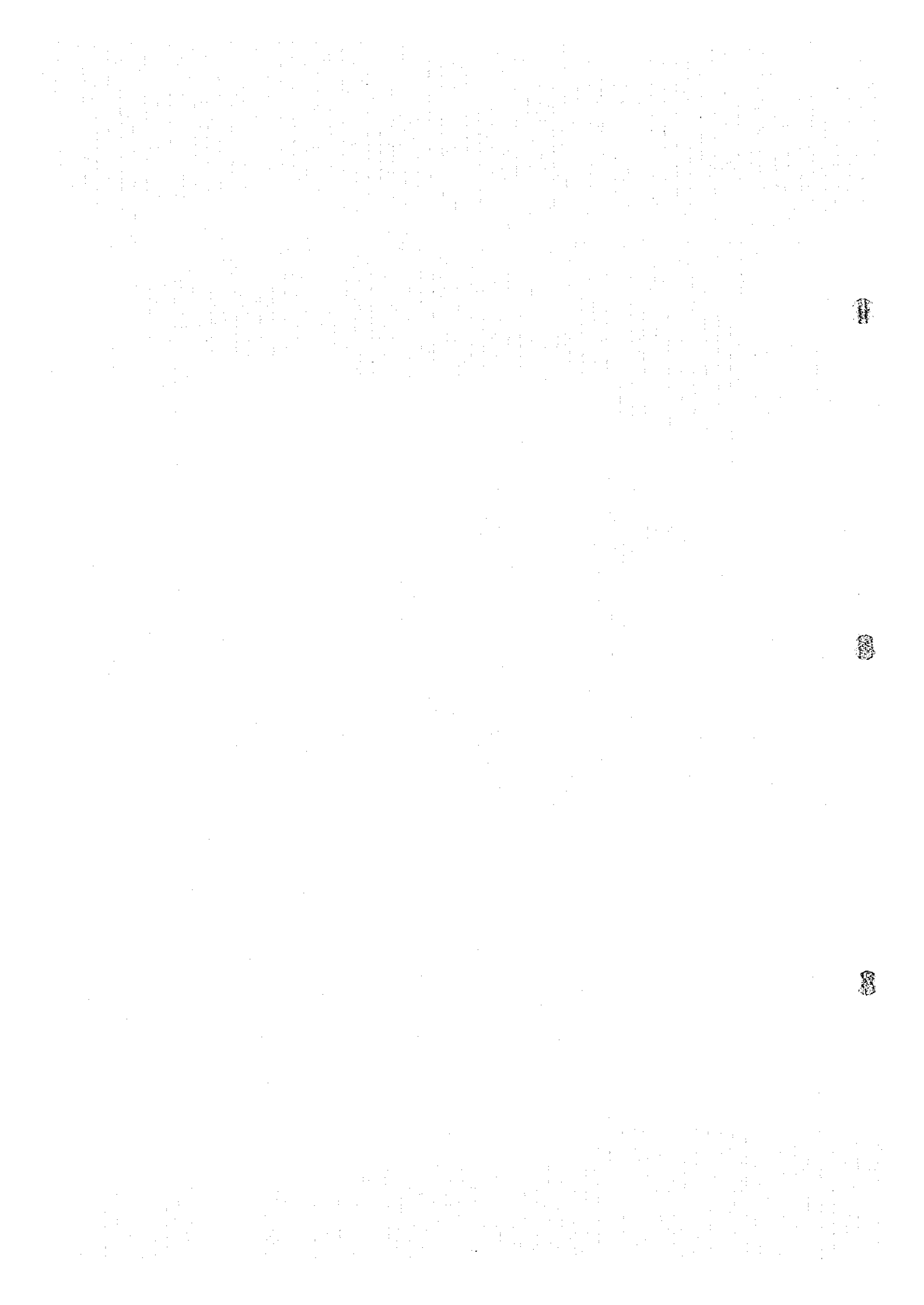
Residuals



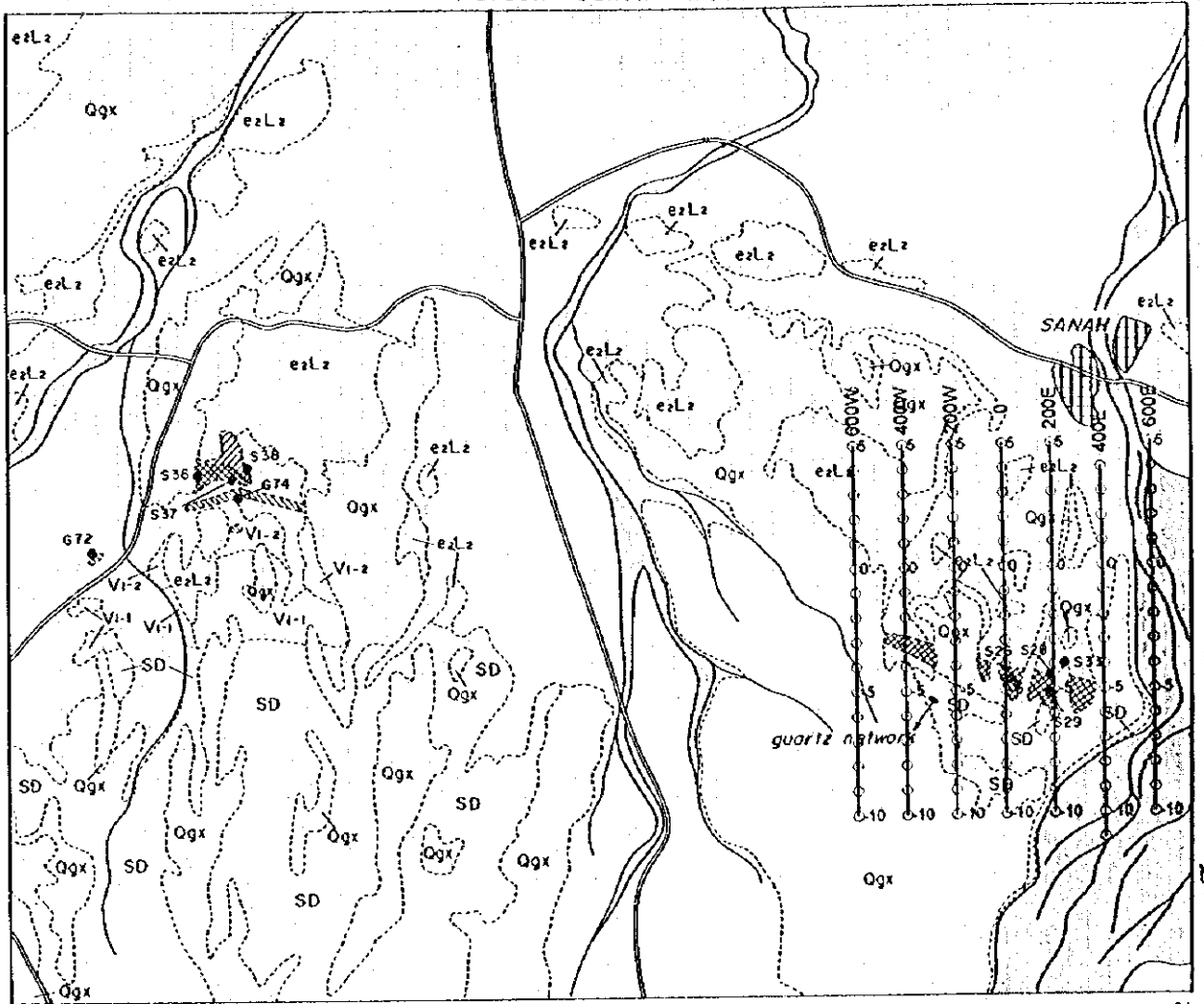
Line 200E



Line 200E



Fardoh - Sanah Area



LITHOLOGY

- QUATERNARY**
- Wadi sediments and Sub-recent alluvial fans; terraces
  - Qgx Ancient alluvial fans; terraces
- TERTIARY**
- ezL<sub>2</sub> Upper nodular limestone
- SANAIL OPHIOLITE**  
Sanail Volcanic Rocks
- Vi-2 Lower extrusives 2
  - Vi-1 Lower extrusives 1
- Sheeted-dyke complex**
- SD Sheeted dykes; dolerite

MINERALIZATION

- Gossan
- Argillized zone
- Gossanized metalliferous sediments

Other symbols

- S36 Sample location
- Road
- Wadi

○—○—○ YDIP Survey Lines

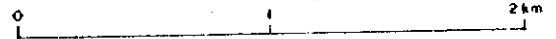
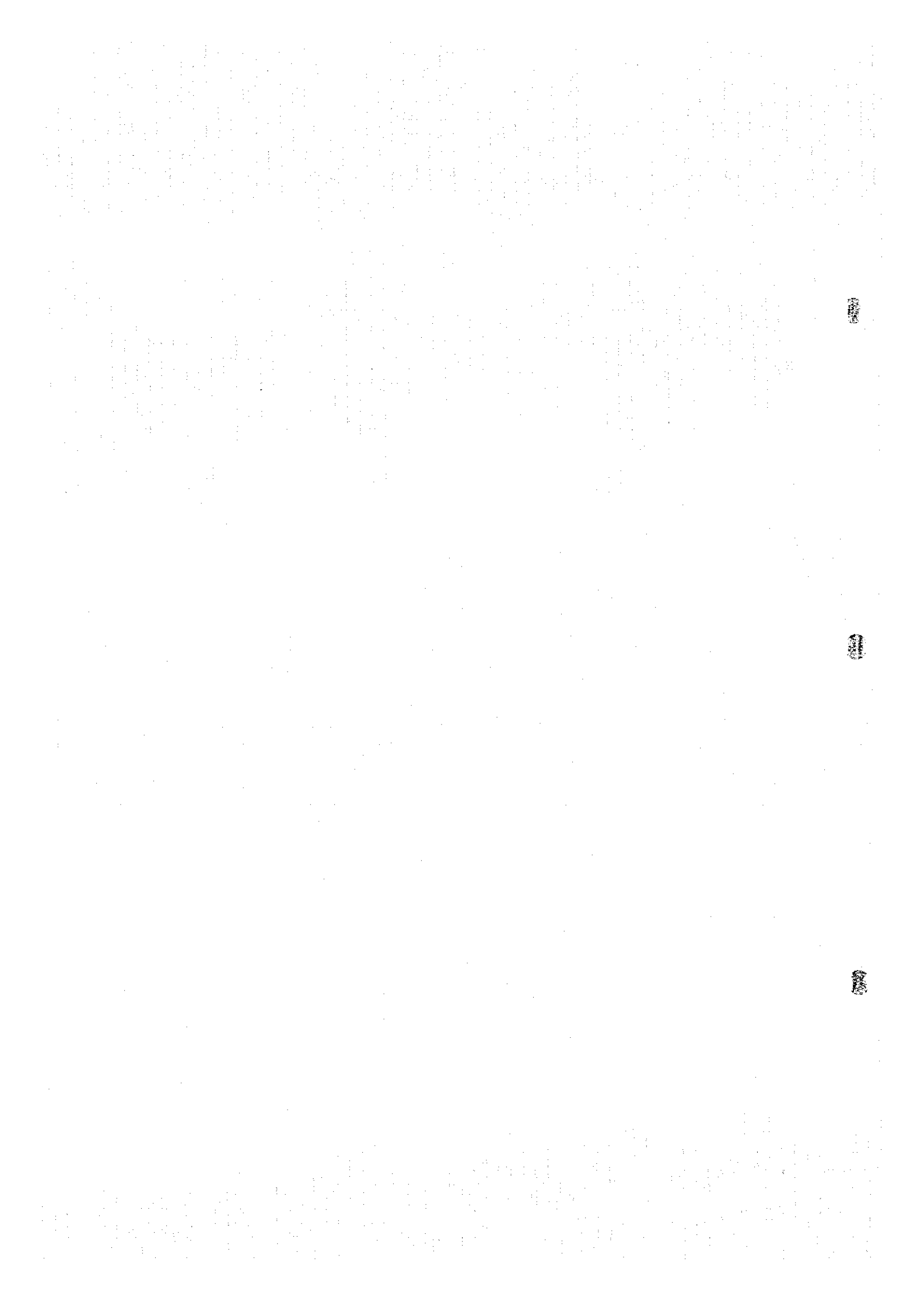


Fig.II-2-13 IP line locations in Sanah area





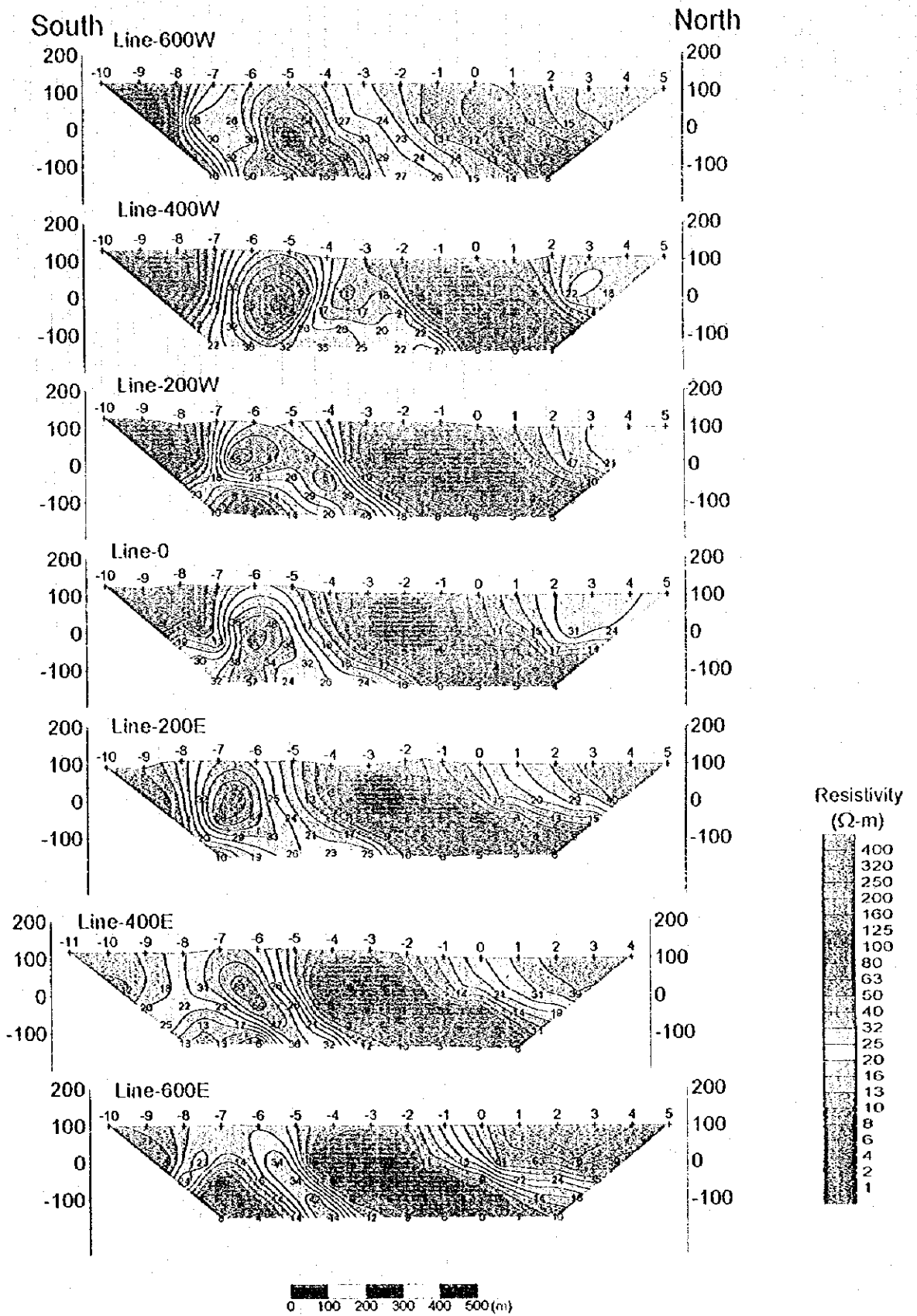
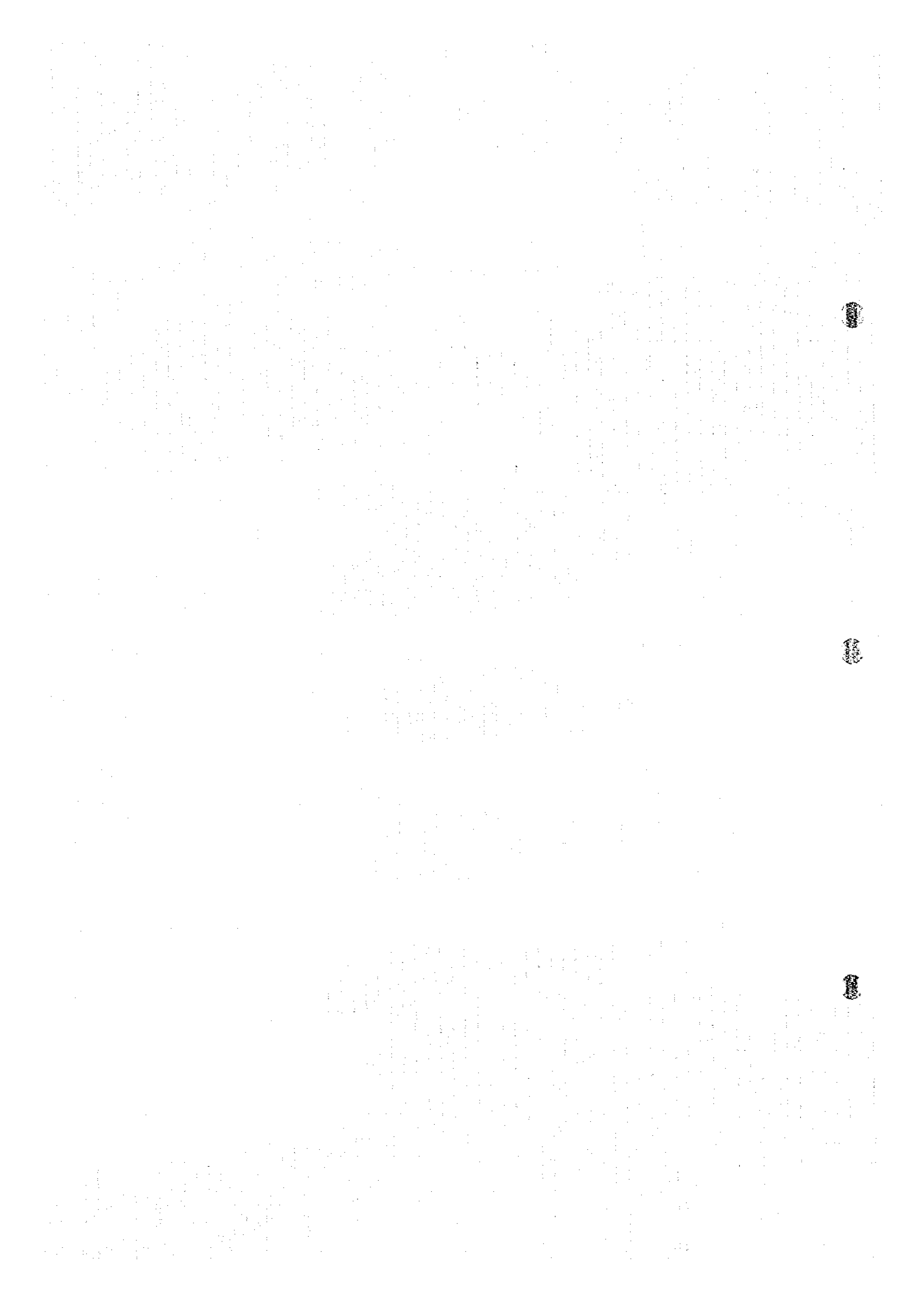


Fig.II-2-14 Apparent resistivity pseudo-sections in Sanah area





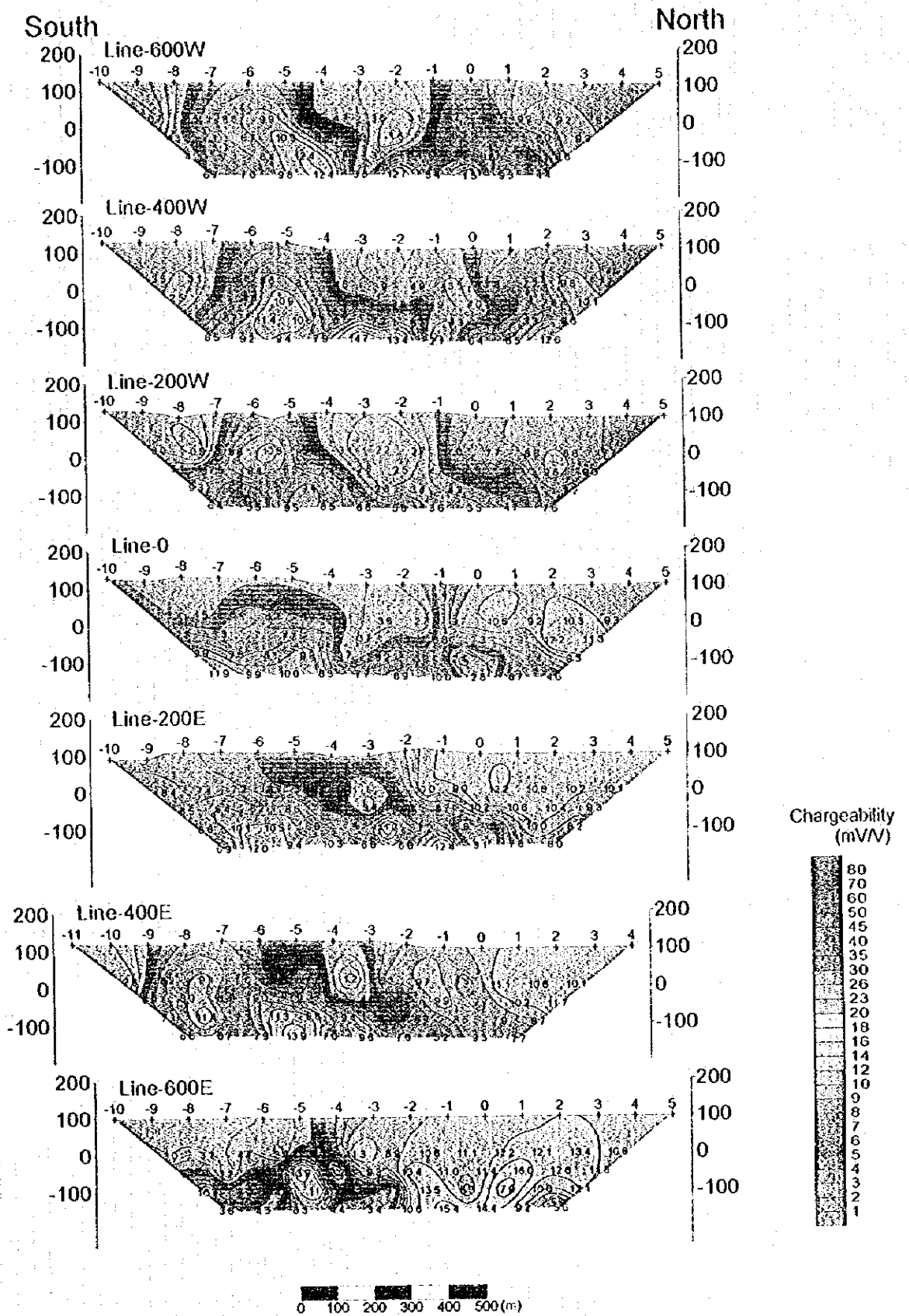


Fig.H-2-15 Chargeability pseudo-sections in Sanah area

South

North

200 Line 60007

100

0

100

200 Line 40007

100

0

100

200 Line 20007

100

0

100

200 Line 0

100

0

100

200 Line 2000

100

0

100

200 Line 4000

100

0

100

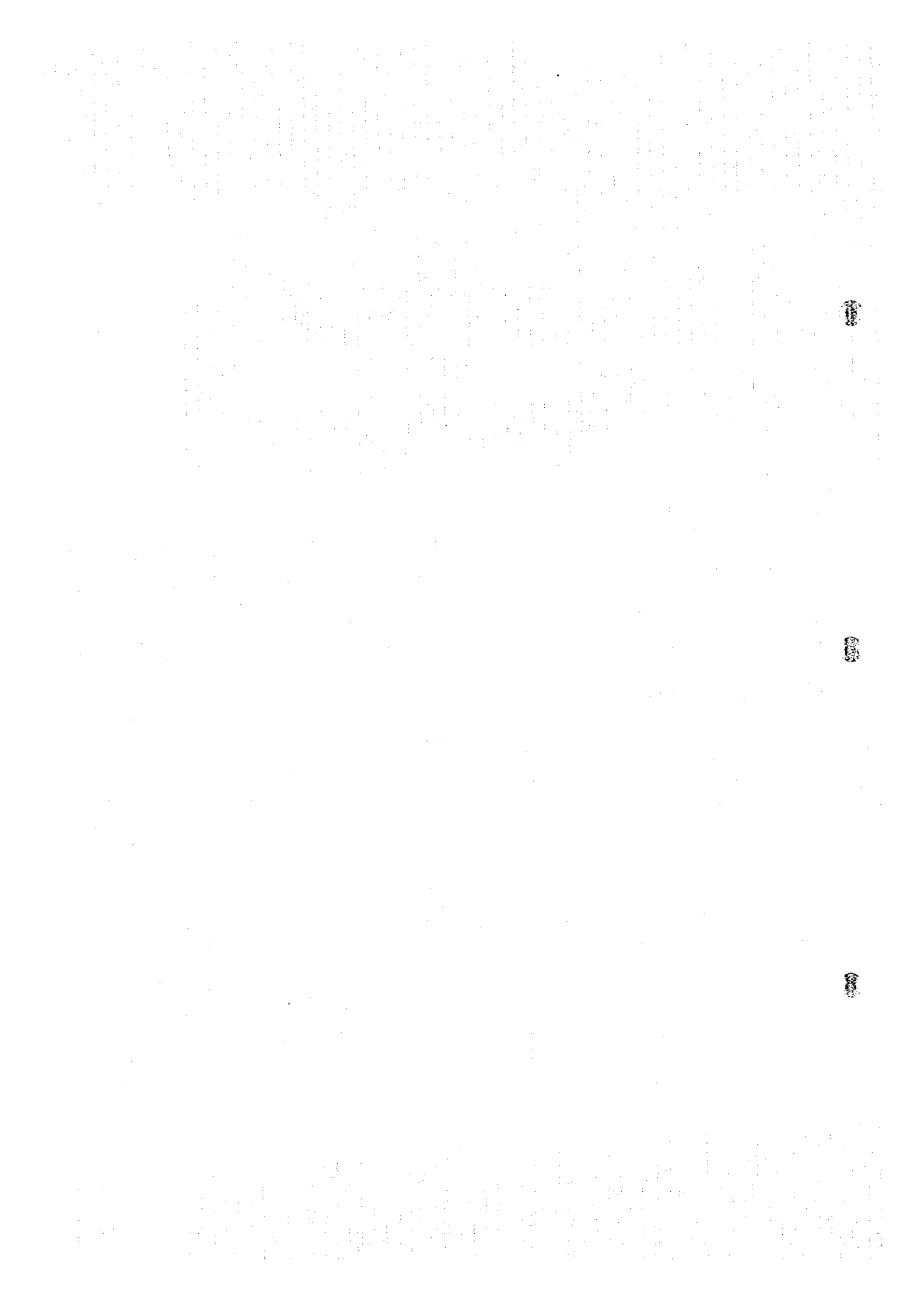
200 Line 6000

100

0

100

Scale 1:5000



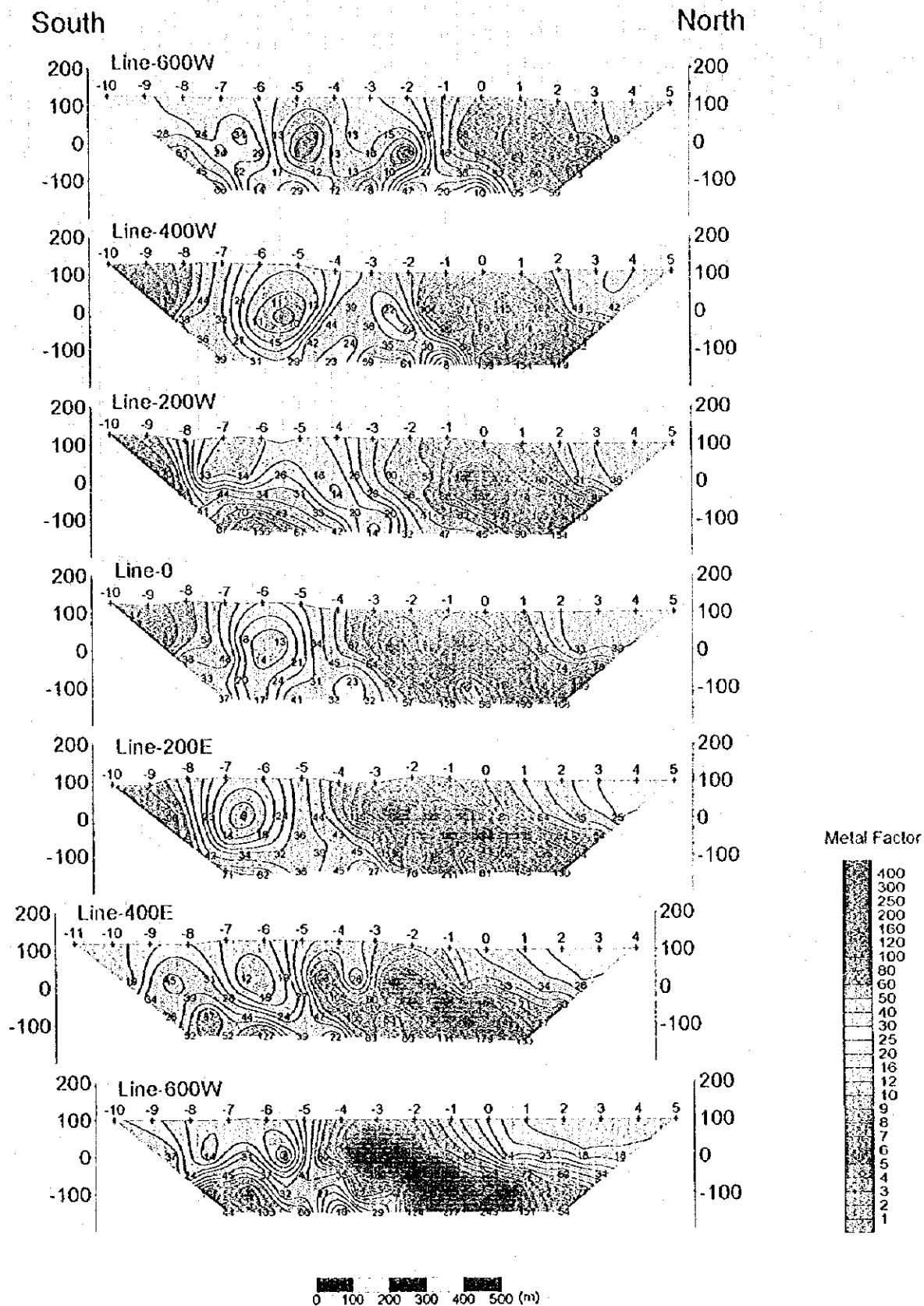
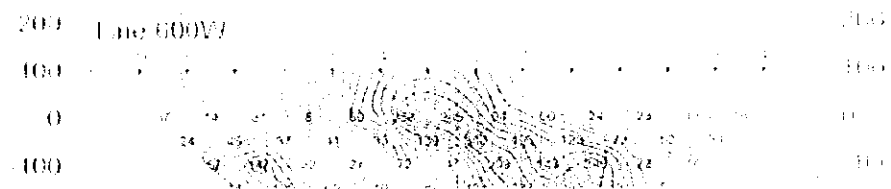
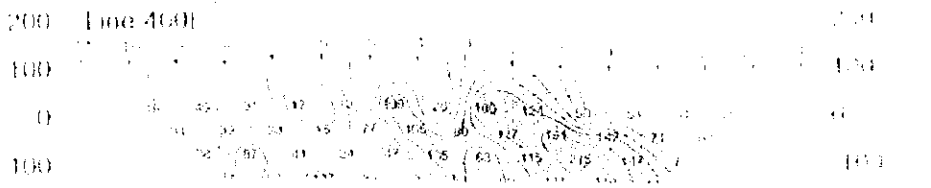
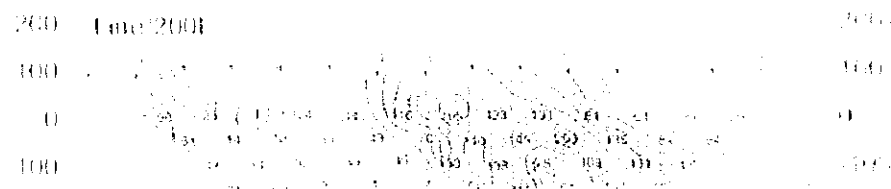
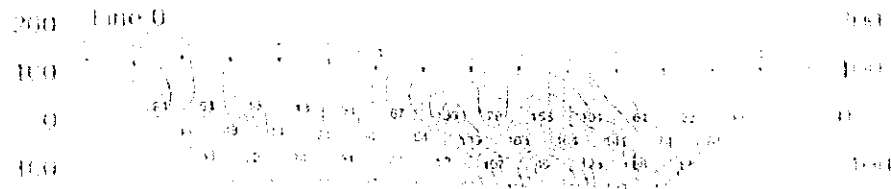
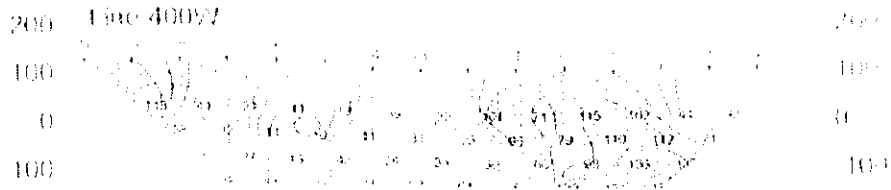
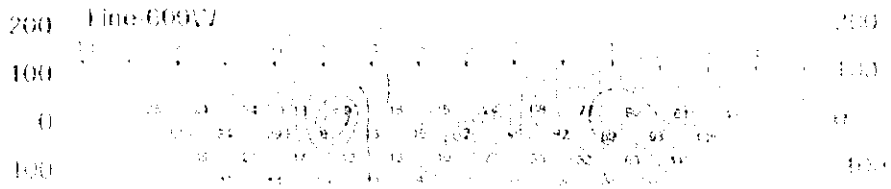


Fig. II-2-16 Metal factor pseudo-sections in Sanah area

South

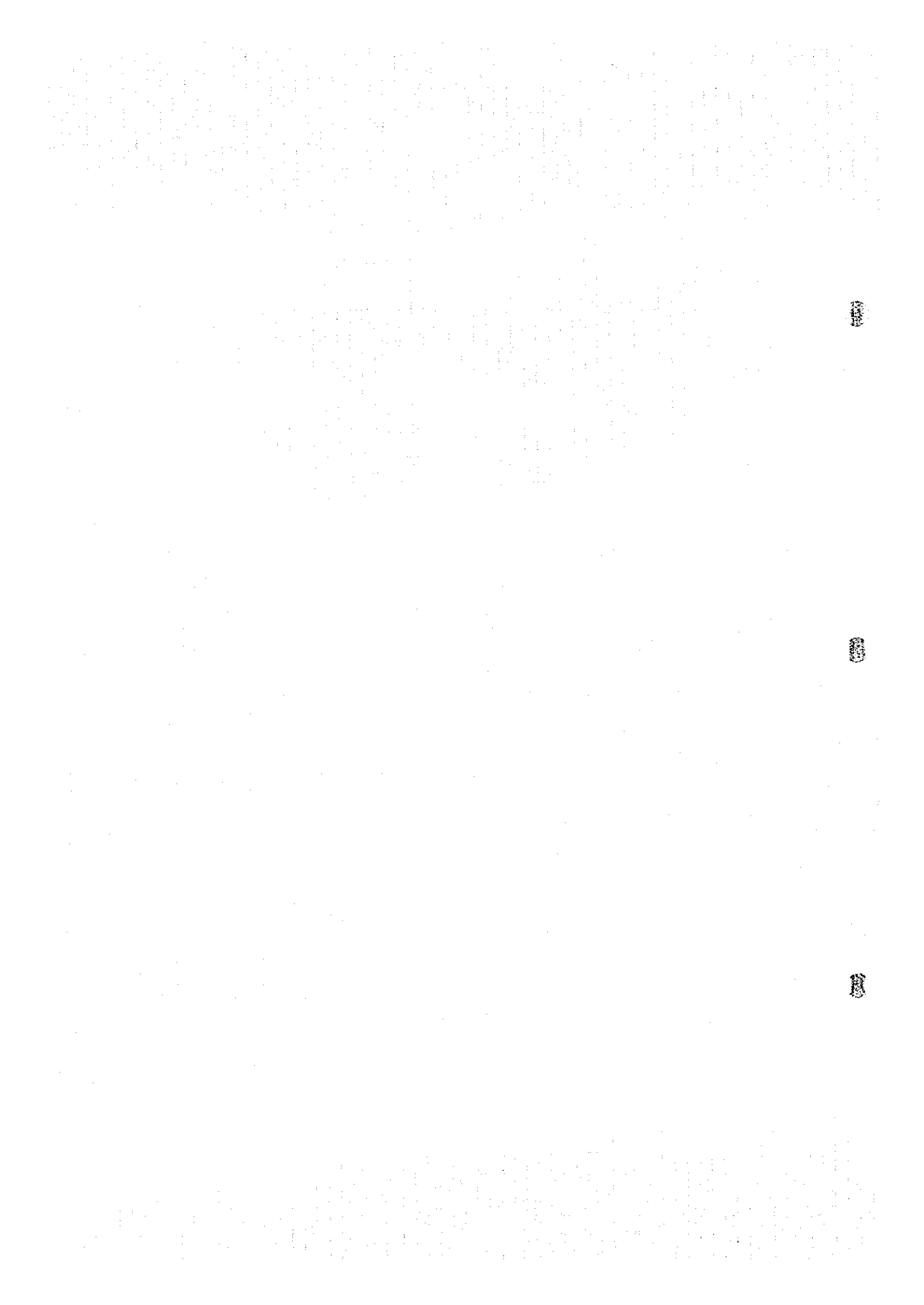
North



1:250 1:500 1:1000

Figure 16. Model topographic contours and data points.





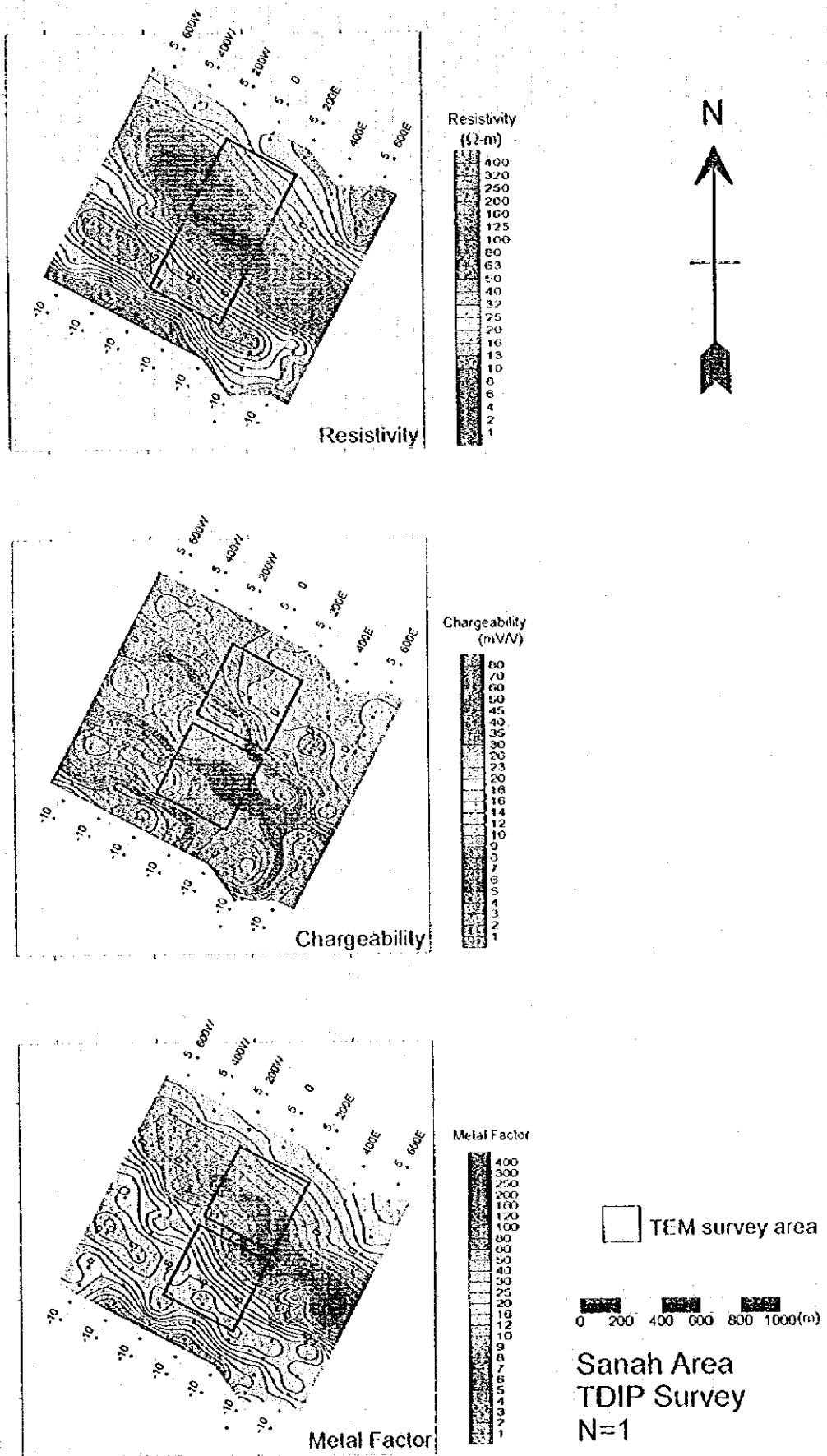
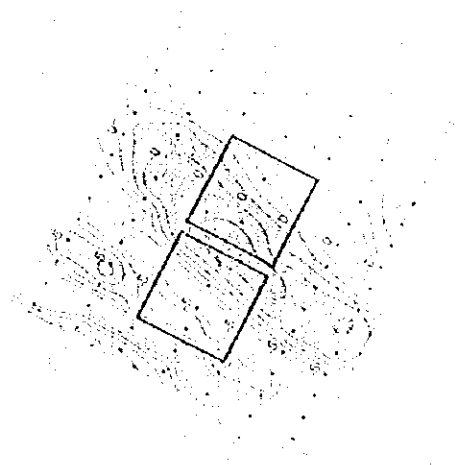
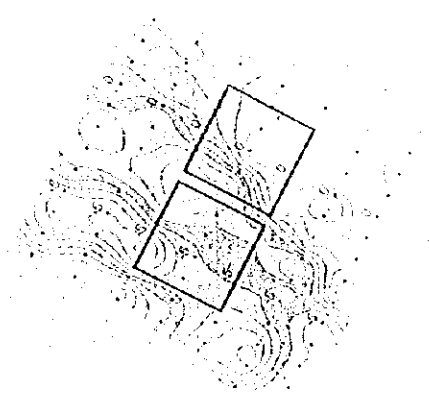


Fig.II-2-17 IP plane map of  $n=1$  in Sanah area



Resistivity



Permeability

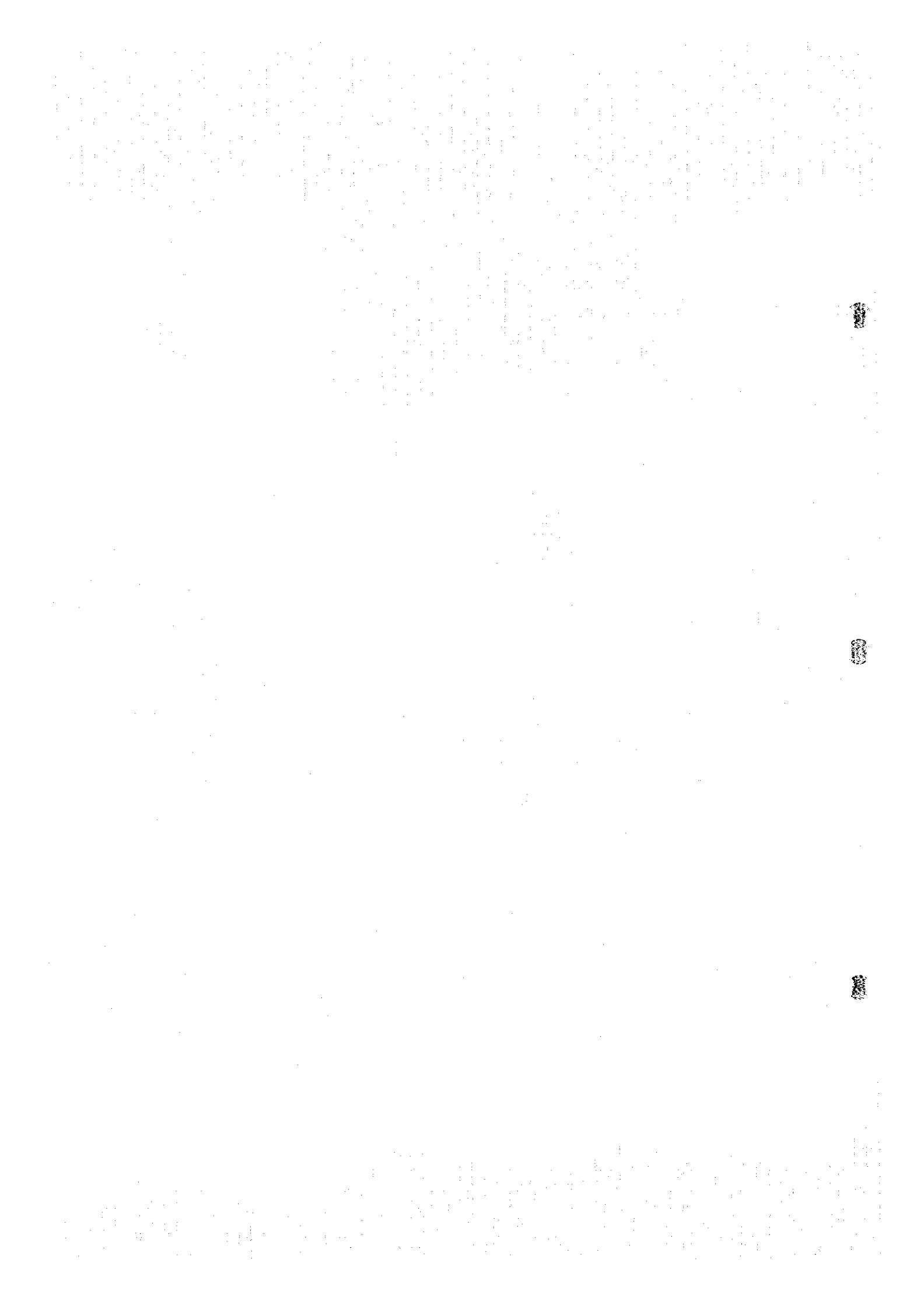


Total Thickness

Scale 1:5000

Legend

Sanah Area  
 TDIP Survey  
 N-1



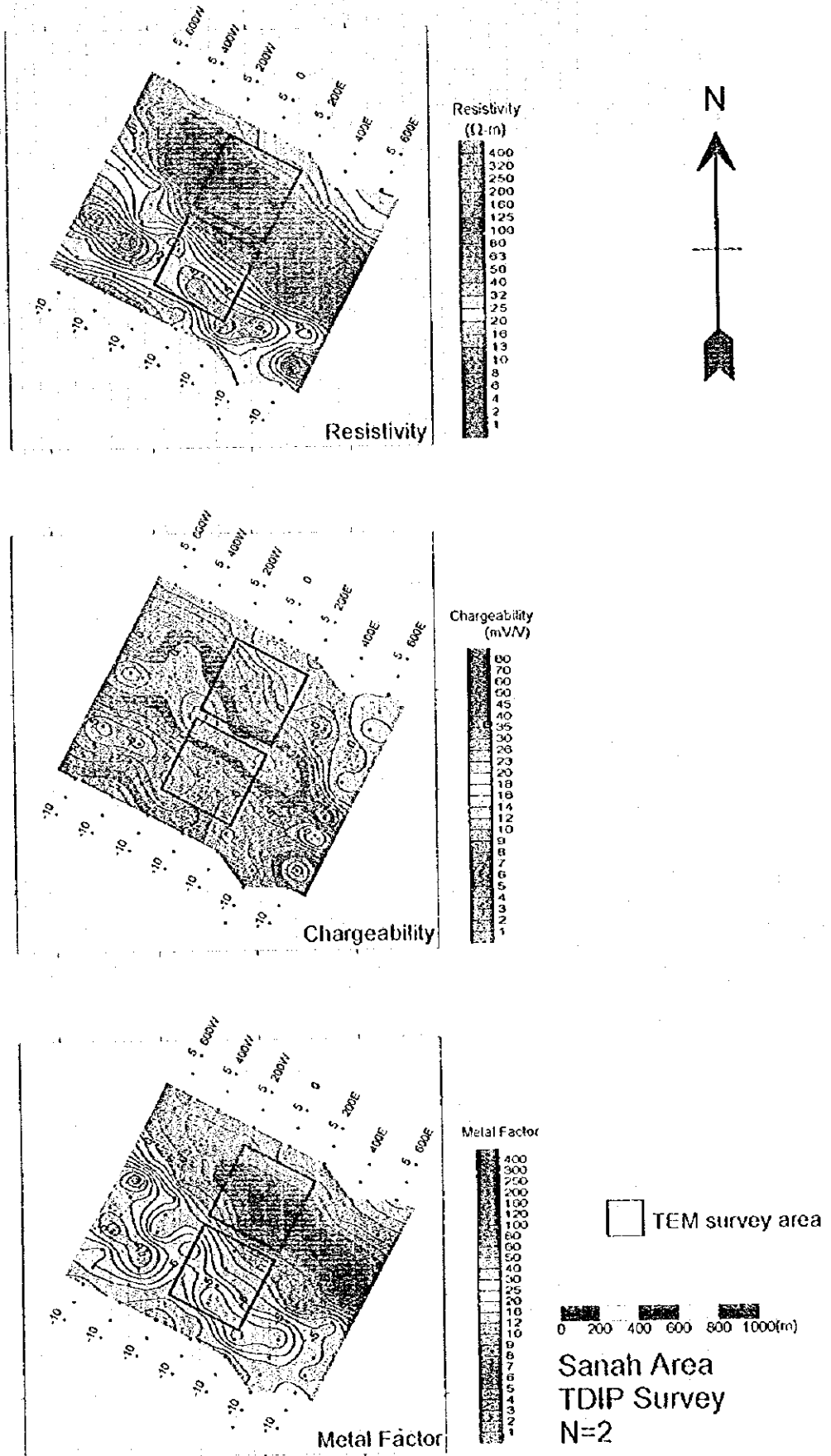
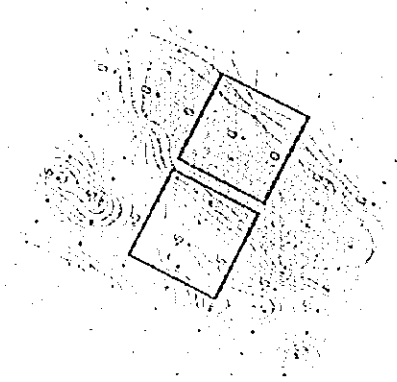
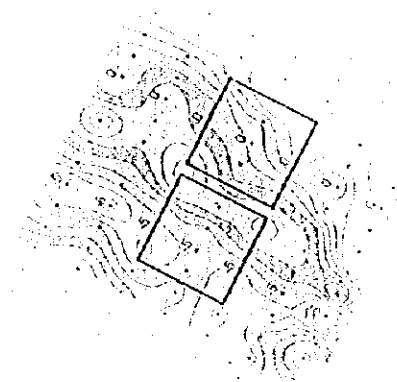


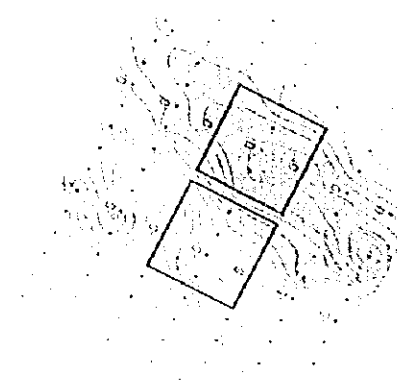
Fig.H-2-18 IP plane map of n=2 in Sanah area



Resistivity



Chargeability

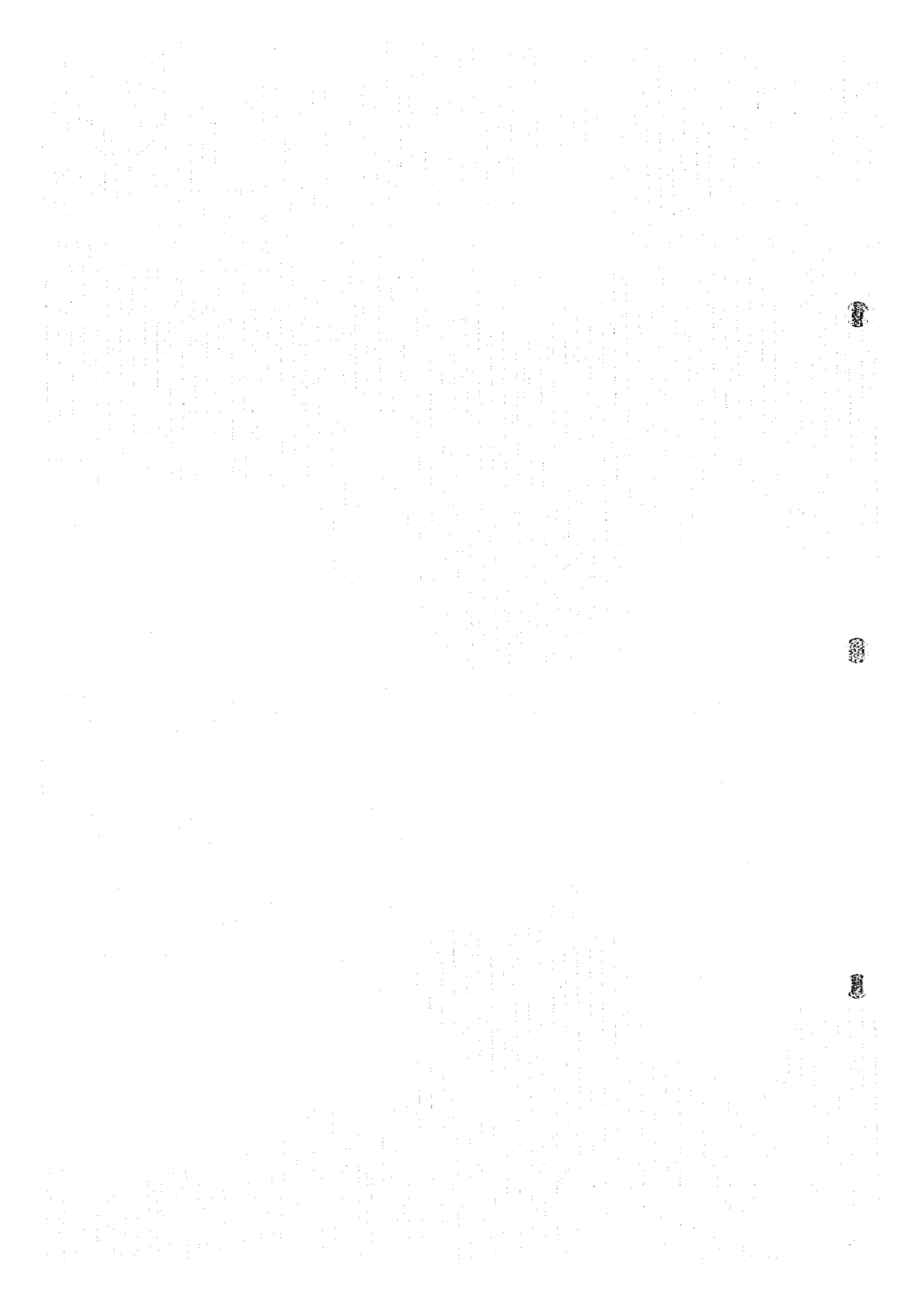


Detail Factor

0.1 0.2 0.3 0.4 0.5 0.6 0.7 0.8 0.9 1.0 1.1 1.2 1.3 1.4 1.5 1.6 1.7 1.8 1.9 2.0 2.1 2.2 2.3 2.4 2.5 2.6 2.7 2.8 2.9 3.0 3.1 3.2 3.3 3.4 3.5 3.6 3.7 3.8 3.9 4.0 4.1 4.2 4.3 4.4 4.5 4.6 4.7 4.8 4.9 5.0 5.1 5.2 5.3 5.4 5.5 5.6 5.7 5.8 5.9 6.0 6.1 6.2 6.3 6.4 6.5 6.6 6.7 6.8 6.9 7.0 7.1 7.2 7.3 7.4 7.5 7.6 7.7 7.8 7.9 8.0 8.1 8.2 8.3 8.4 8.5 8.6 8.7 8.8 8.9 9.0 9.1 9.2 9.3 9.4 9.5 9.6 9.7 9.8 9.9 10.0

1000 2000 3000 4000 5000 6000 7000 8000 9000 10000

Sanah Area  
TDIP Survey  
N. 2



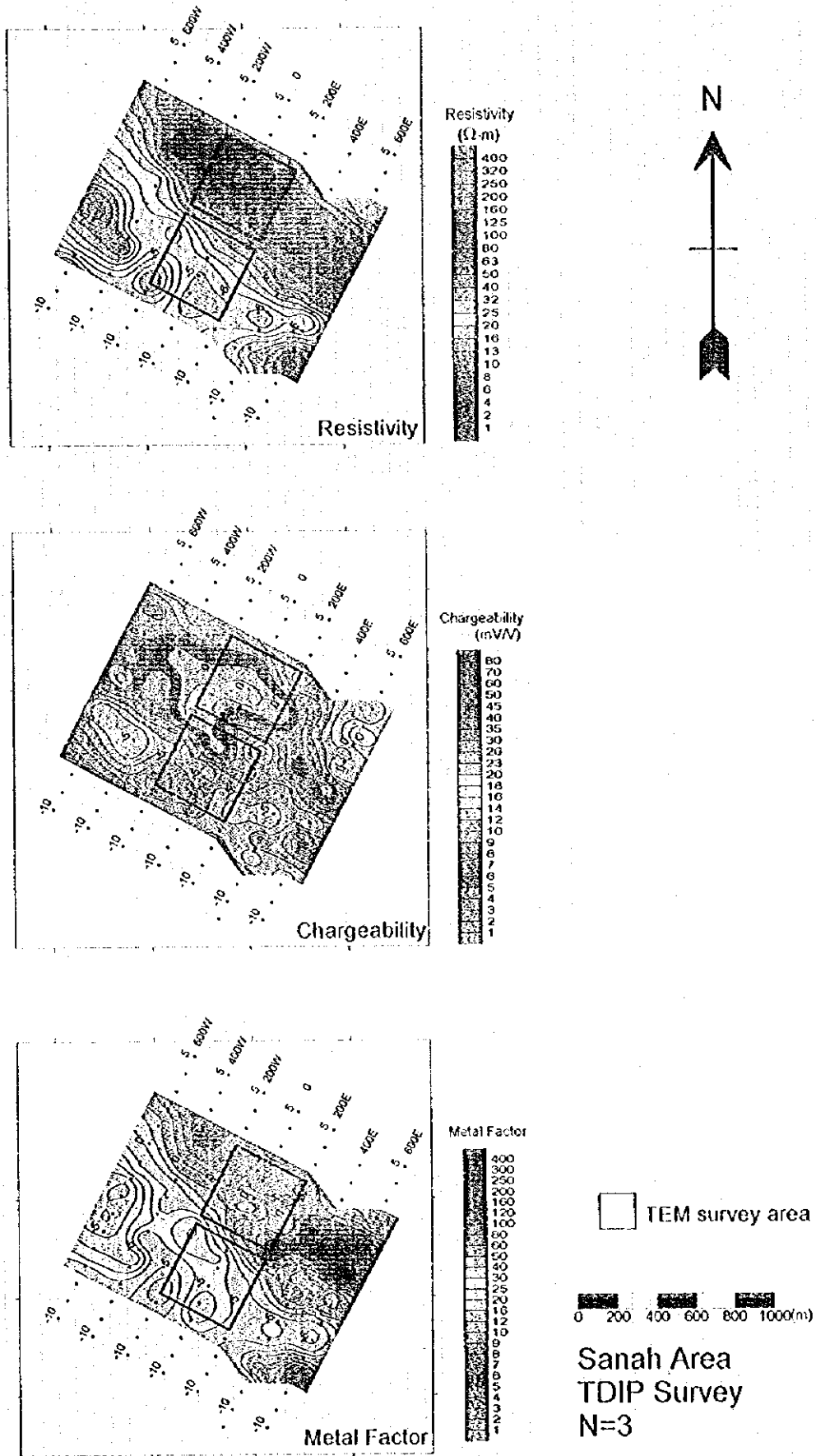
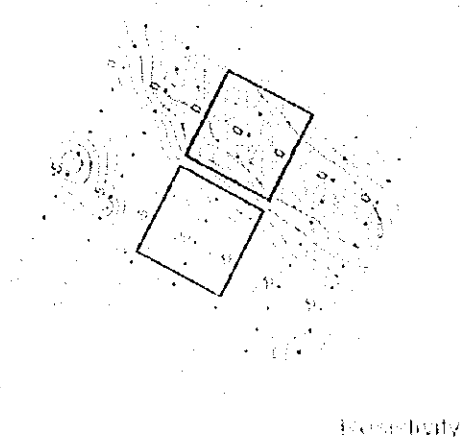
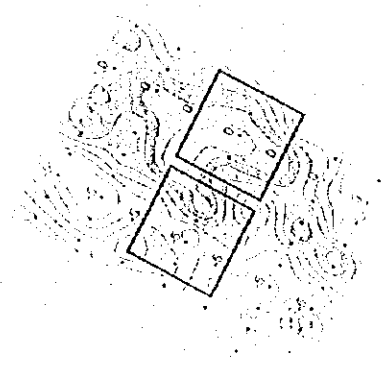


Fig.H-2-19 IP plane map of n=3 in Sanah area

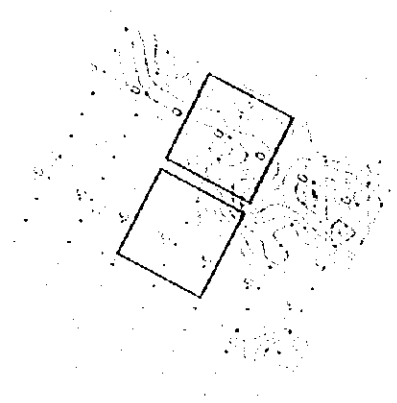




Isochividy



Isohypathy



Isochividy

1:5000

Sanah Area  
 IDIP Survey  
 N-3

Fig. 1. IDIP plots for the Sanah Area



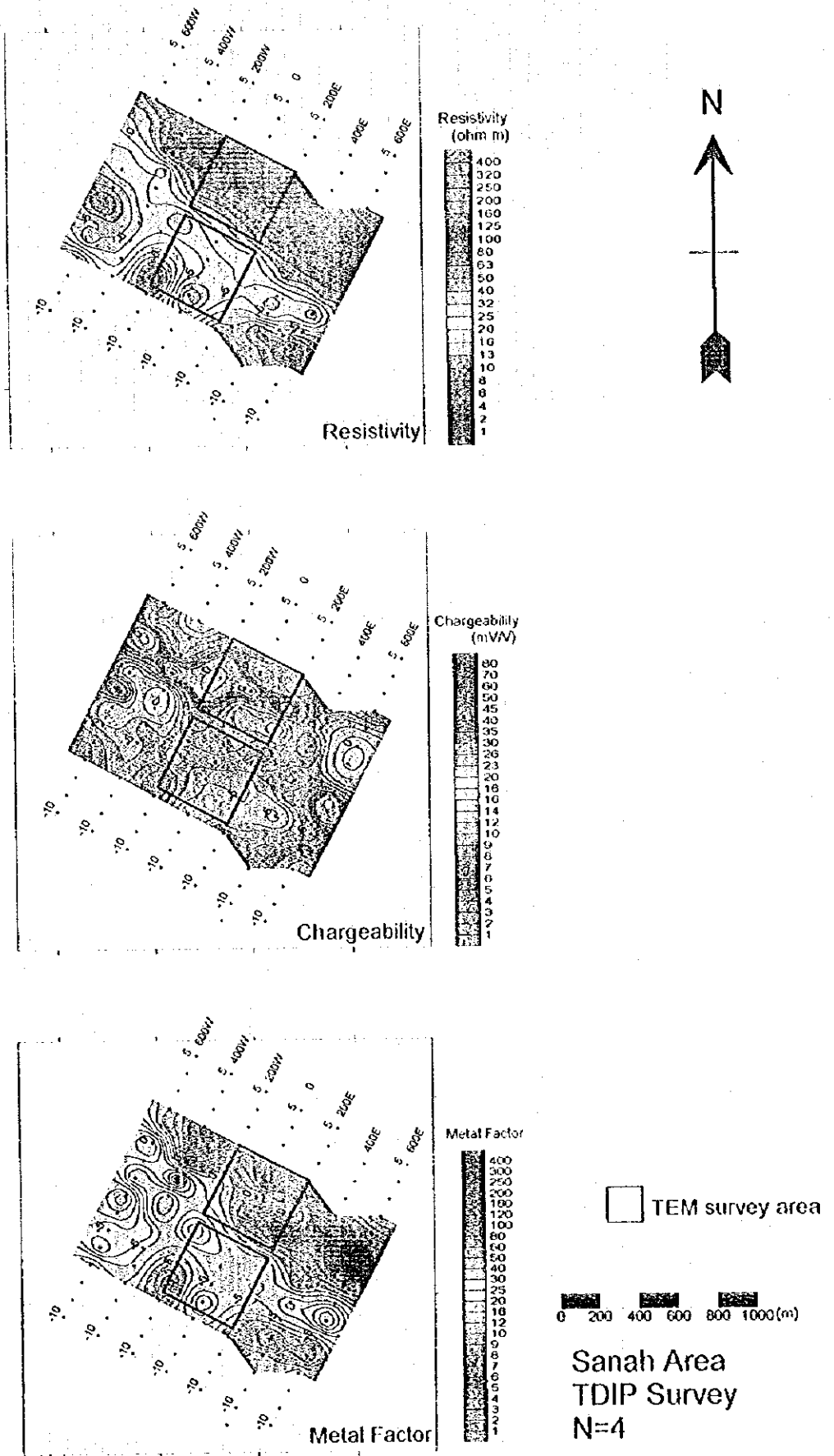
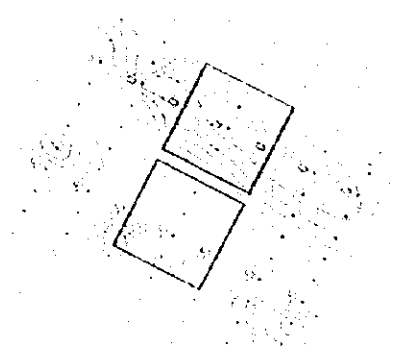
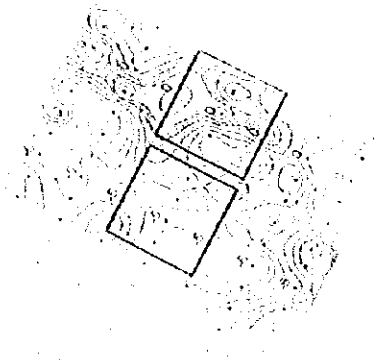


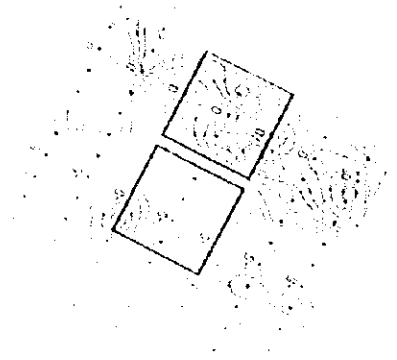
Fig. II-2-20 IP plane map of n=4 in Sanah area



Existing



Change study



Detail study

Scale 1:500

2004 2004 2004

Sanah Area  
TDIP Survey  
N 4

Fig. 1. TDIP plan view, study area



as the ones found in Fardah area.

In relation to the apparent resistivity, the results show values between 3 to 134  $\Omega\text{m}$ , however, it is observed that more than 90% of the results show in general values of less than 50  $\Omega\text{m}$ . To the north side of the gossanized area, which is distributed along NW-SE, it is seen a low resistivity zone of about 300m distributed also along NW-SE. This low resistivity distribution is seen at shallow depth of line No.0 with station No. -2 as the center and displaced at depth towards NE. This low resistivity distribution runs parallel to another low resistivity distributed in the south part of the area where resistivities of less than 10  $\Omega\text{m}$  were confirmed in some places.

In relation to the chargeability, it can be seen in general low values, however, a somewhat medium chargeability zone of about 10 mV/V is seen adjacent to the north of the above mentioned low resistivity zone along the NW-SE direction.

Metal factor values above 100 can be also seen about 150m to the north of the low resistivity distribution and nearly similar to the chargeability distribution pattern.

### 2-7-3 2-D analysis

The data obtained from the line No 0 were interpreted by a 2 dimensional analysis. The results of simulation are indicated in the Fig. II-2-21.

According to the results, a low resistivity distribution of less than 10  $\Omega\text{m}$  and a width of about 200m is seen dipping northwards from the surroundings of station No. -2.

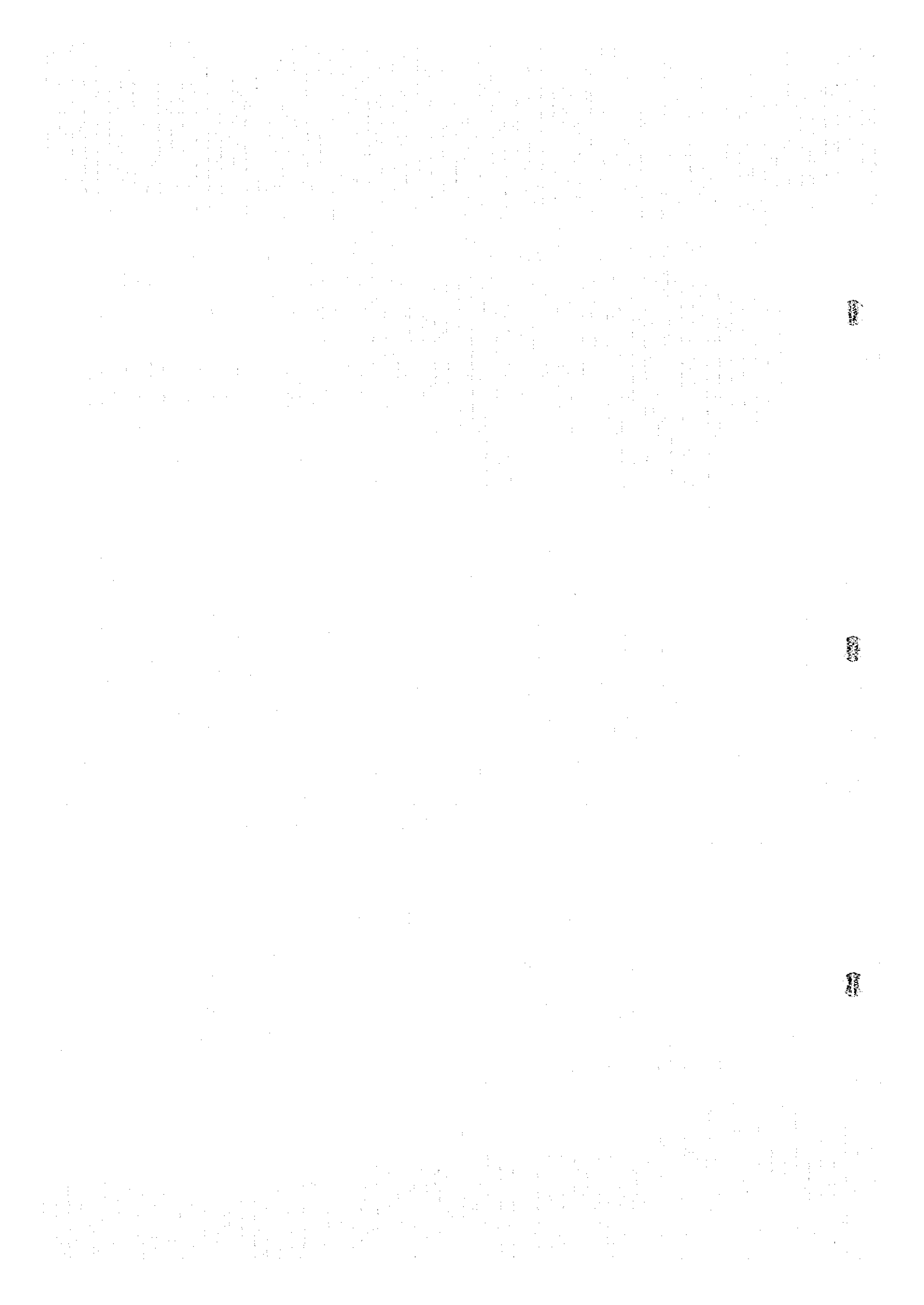
According to the chargeability results, two medium chargeability distributions of more than 9 mV/V are seen, one of them is distributed above a depth of less than 100m of station No. 0 extended towards the north and, another is seen below a depth of about 100m of station No. -2 extended southwards.

The metal factor section shows a distribution of above 100 at shallow depth around station No. 0. and dipping northwards in the same way as the low resistivity distribution mentioned above.

## 2-8 Ghuzayn Village North Area

### 2-8-1 Lines Location

On this area, two lines were set along the direction  $N27^\circ E$  and a third line perpendicular to the above two lines. As indicated in the Fig. II-2-22, the line 000N has a length of 1.5km, the line 180S has a length of 1.4 km and the line 000E has a length of 800m.



# Line 0

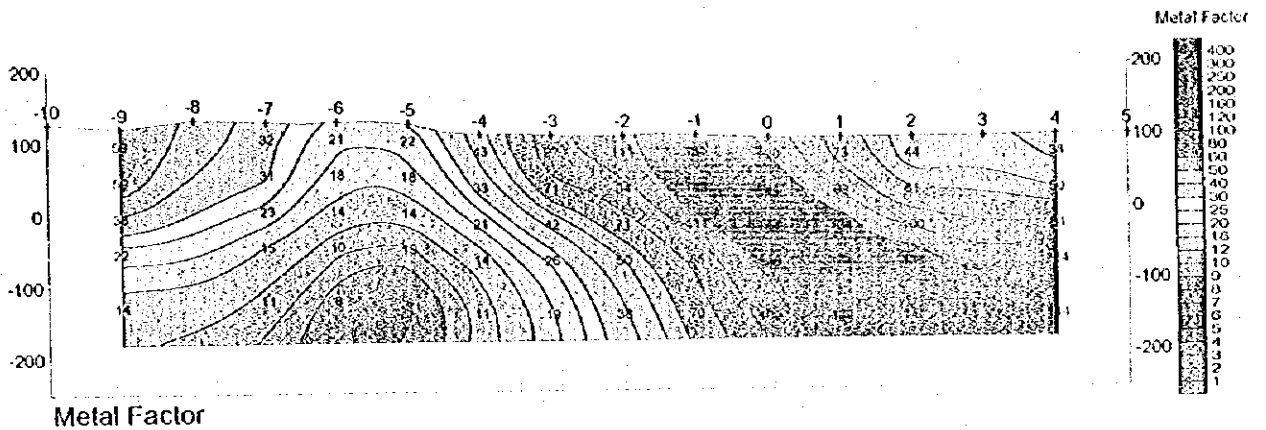
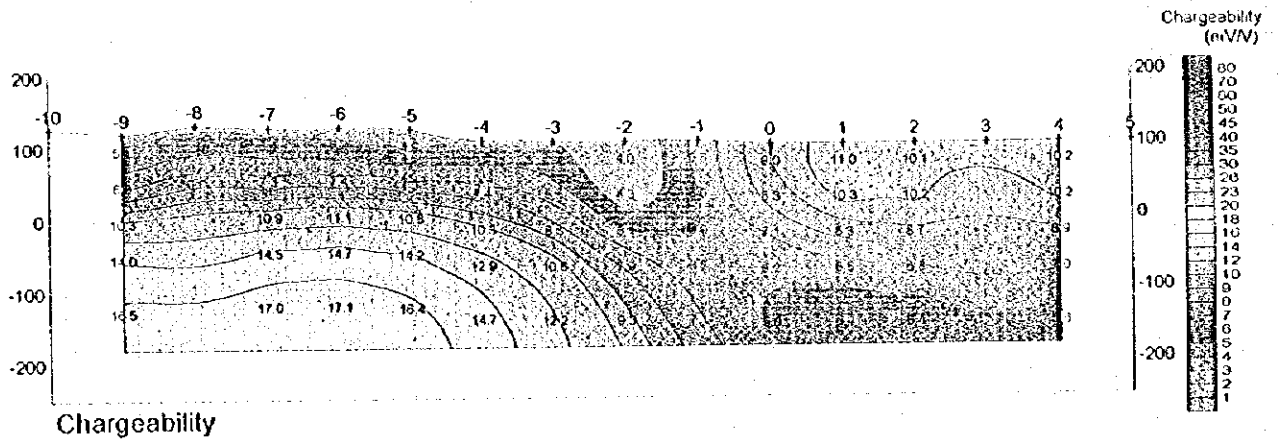
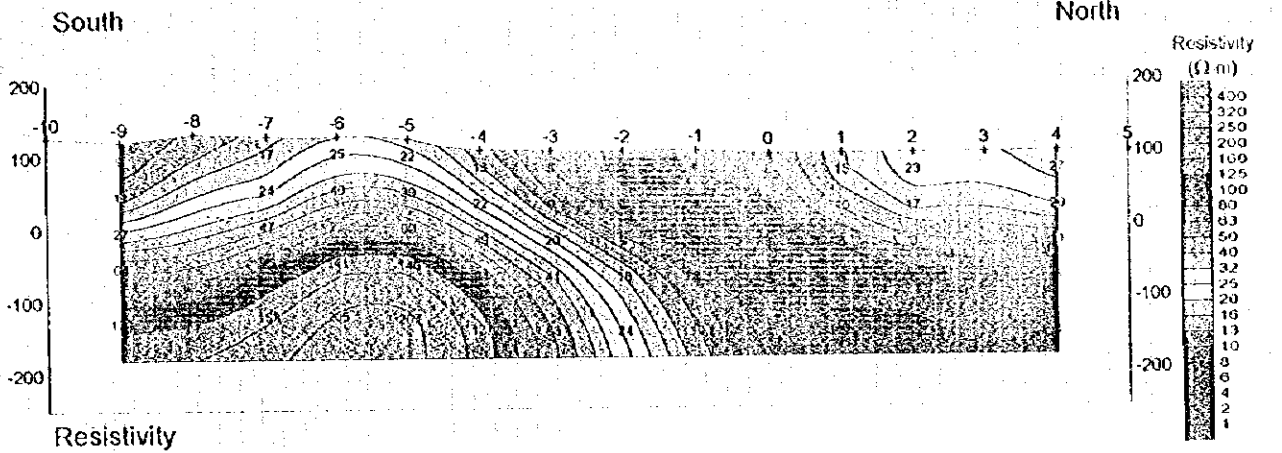
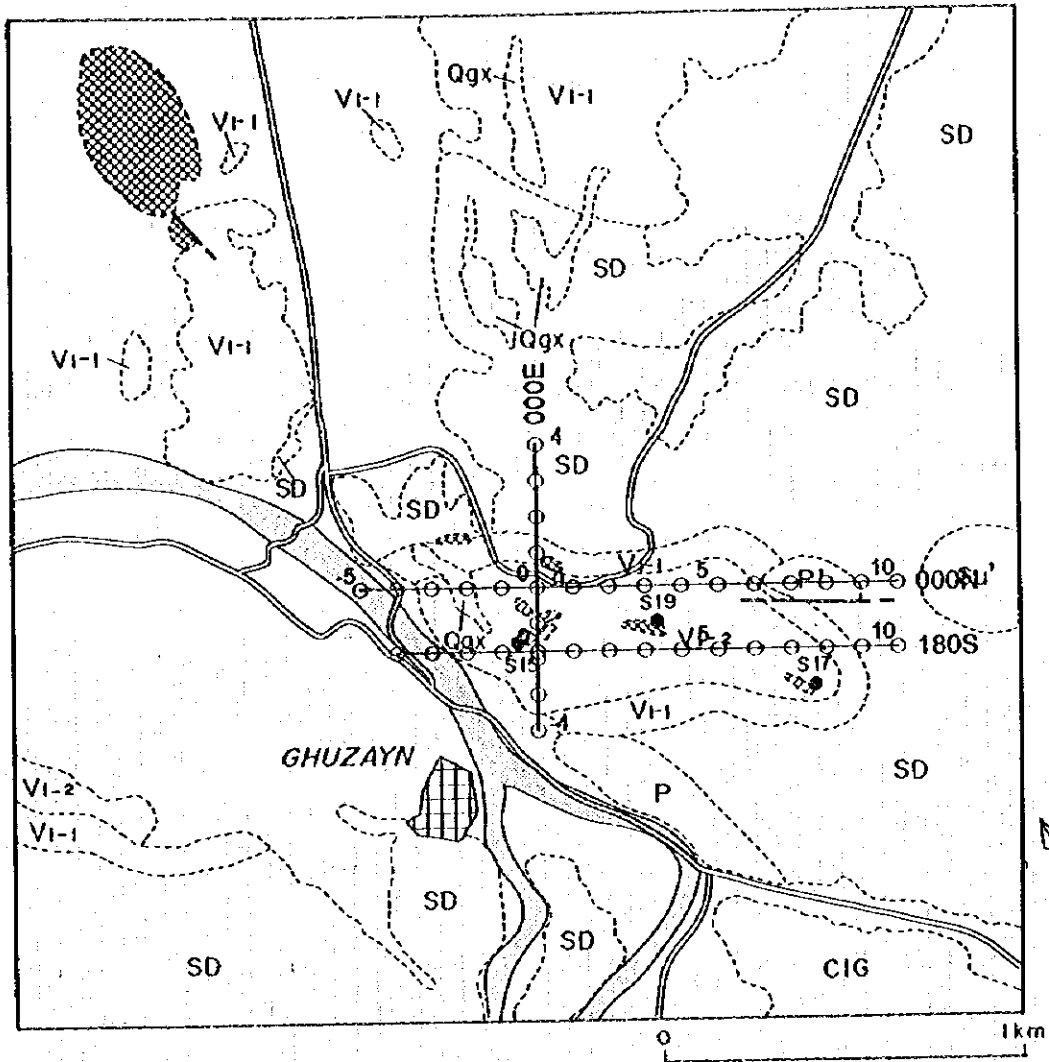


Fig.II-2-21 Results of model simulation on Line 00013 in Sanah area





# Ghuzayn Village North Area



## LITHOLOGY

**QUATERNARY**  
 Wadi sediments and Sub-recent alluvial fans; terraces

Qgx Ancient alluvial fans; terraces

## SAMAII OPHIOLITE

Samail Volcanic Rocks

Vi-2 Lower extrusives 2

Vi-1 Lower extrusives 1

## Sheeted-dyke complex

SD Sheeted dykes; dolerite

## Cumulate Sequence

CIG Cumulate layered gabbro

## Intrusives

Gu' Uralitic Gabbro

P' Peridotite

## MINERALIZATION

Gossan

Silicified or argillized zone

## Other symbols

● S15 Sample location

Ghuzayn village

Road

Wadi

○-○-○ TDIP Survey Lines

Fig.II-2-22 IP line locations in Ghuzayn north area

## 2-8-2 Results

The apparent resistivity, chargeability and metal factor pseudo-sections are indicated in the Figs. II-2-23, II-2-24 and II-2-25, respectively. The Figs. II-2-26, II-2-27, II-2-28 and II-2-29 show the resistivity, chargeability and metal factor maps for  $n=1$  to  $n=4$ , respectively.

Although the measured apparent resistivity values range from 50 to 1440  $\Omega\text{m}$ , most of the values are within 100 to 250  $\Omega\text{m}$ , which indicates that in general, the area presents rather high apparent resistivity values. Only a relatively low resistivity distribution is seen on the line 000N but limited to the area surrounding the station No. -2.

In relation to chargeability and at shallow depth ( $n=1$ ), it is seen medium chargeability values in the extension north of the line 000E as well as in the intersection of this line with the line 180S towards the station No.-2 of the last mentioned line. At higher depths ( $n=2$  to 4), the north part of the line 000E as well of the east part of line 000N, indicate relatively high chargeability values above 10 mV/V.

Metal factor values above 10 are seen on the line 000N at the shallow depths ( $n=1,2$ ) of the surroundings of the station No. -1.

## 2-8-3 2-D Analysis

Fig. II-2-30 presents the calculated simulation results on line 000N. The calculations showed in all the depth, resistivity values of several hundreds  $\Omega\text{m}$  in the east part of this line but decreasing towards 100  $\Omega\text{m}$  as it is approaching the surface. On station No. -2 and close to the surface, values around 50  $\Omega\text{m}$  are seen.

The simulation of chargeability shows in general, relatively high values, and specially the east part indicates values above 30 mV/V below 100m depth. Below station No. 1, chargeability values are seen also to be increasing towards depth.

Relatively medium metal factor values of above 10 are seen only at shallow depths below stations Nos. -1, -2 and surroundings.

## 2-9 Doqal Area

### 2-9-1 Line Locations

A total of 7 IP lines were set on the survey area. The lines were oriented along the EW direction and with a length of 1.5 km. The locations of the IP survey lines are indicated in Fig. II-2-31.

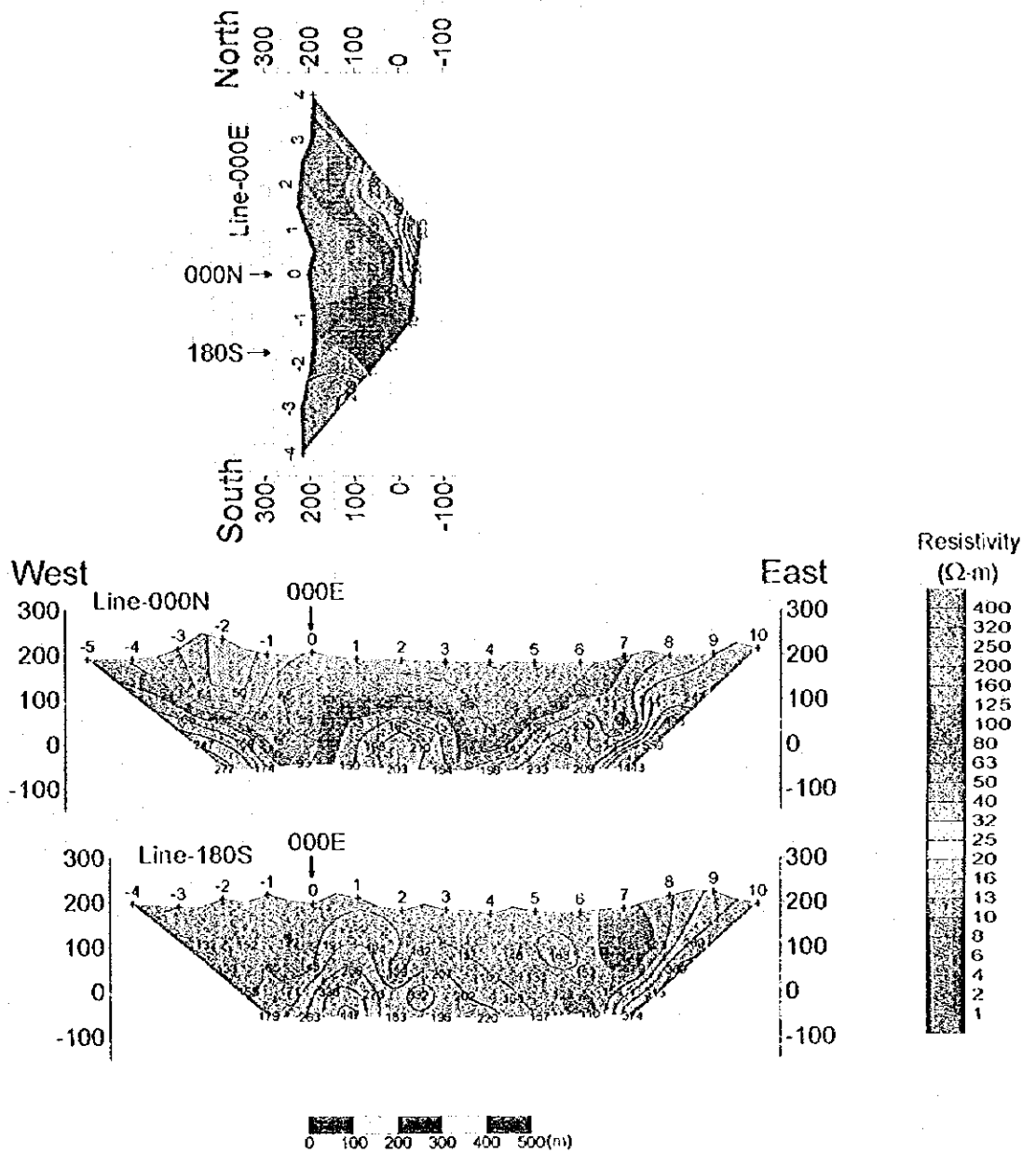
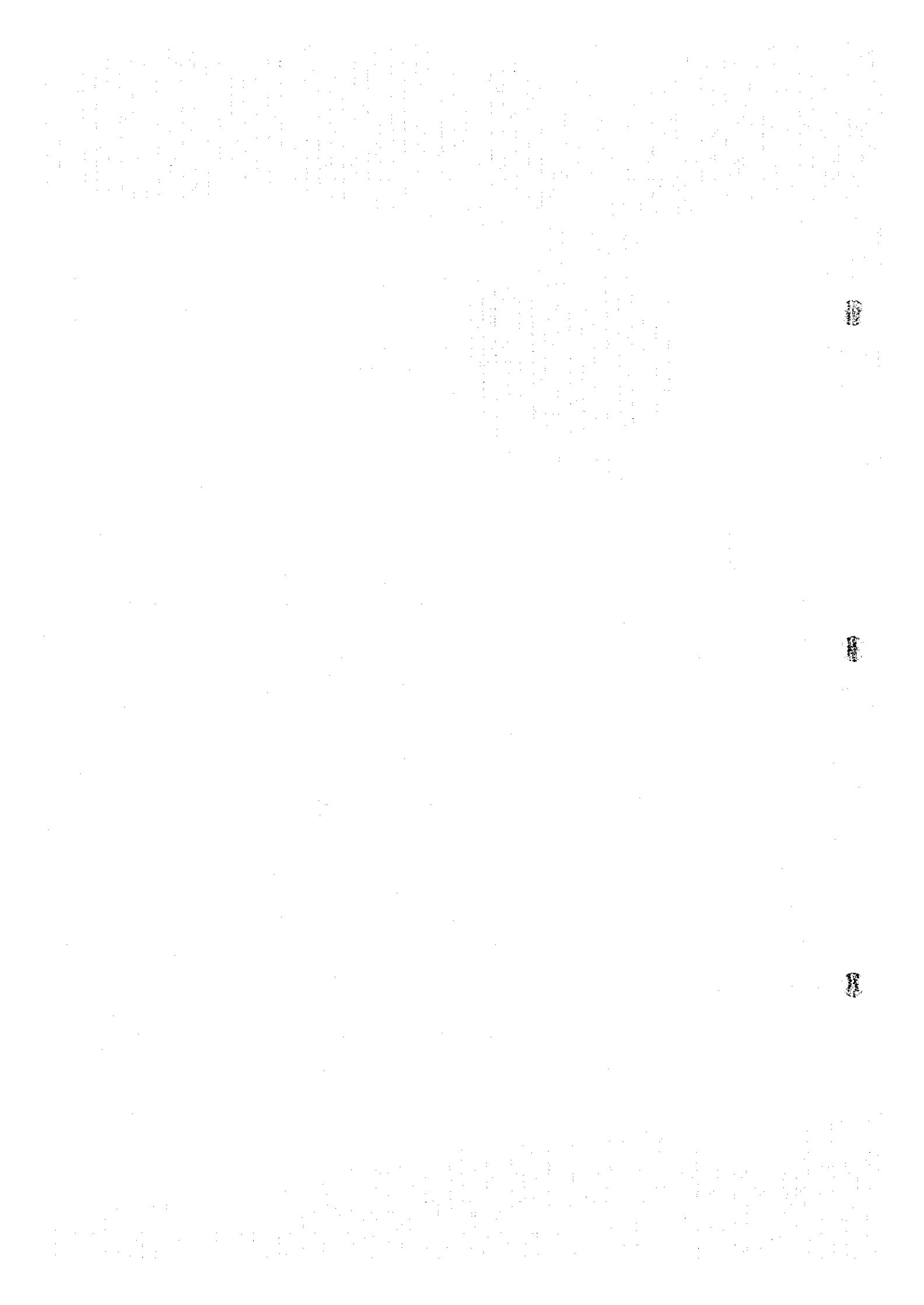


Fig.H-2-23 Apparent resistivity pseudo-sections in Ghuzayn north area



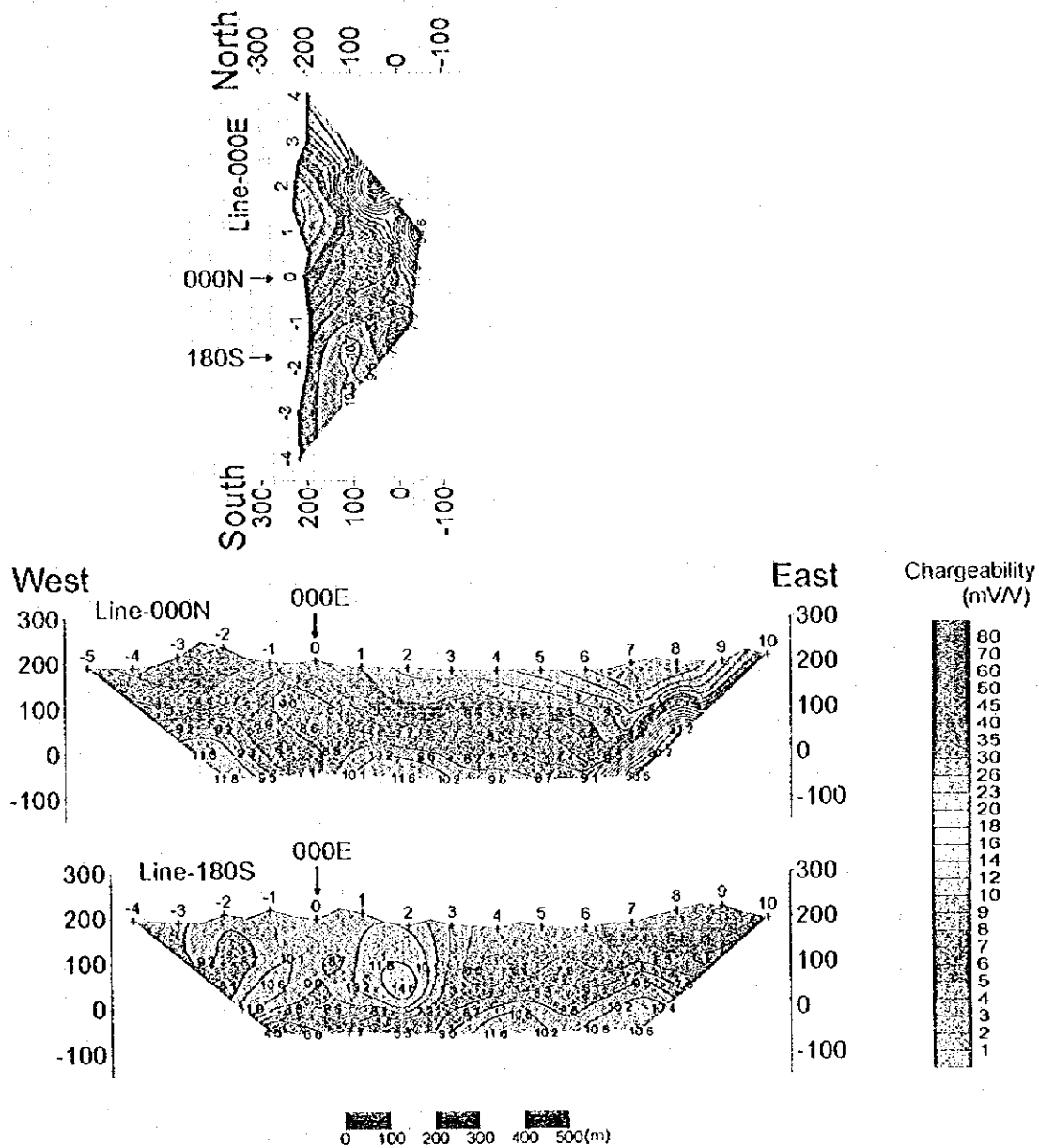
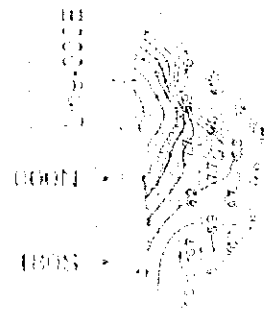


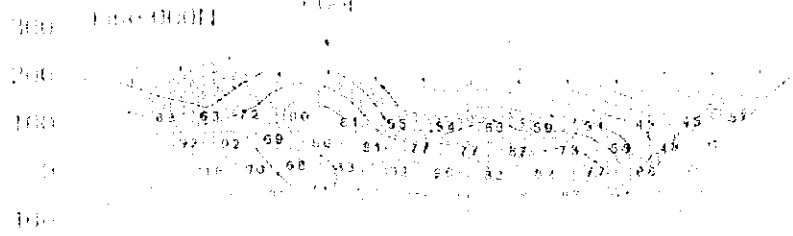
Fig.II-2-24 Chargeability pseudo-sections in Ghuzayn north area

0  
 0  
 0  
 0  
 0

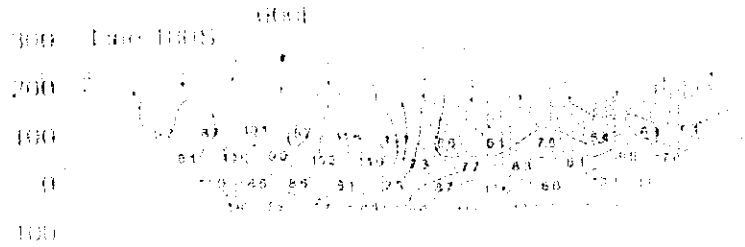


0  
 0  
 0  
 0  
 0

West

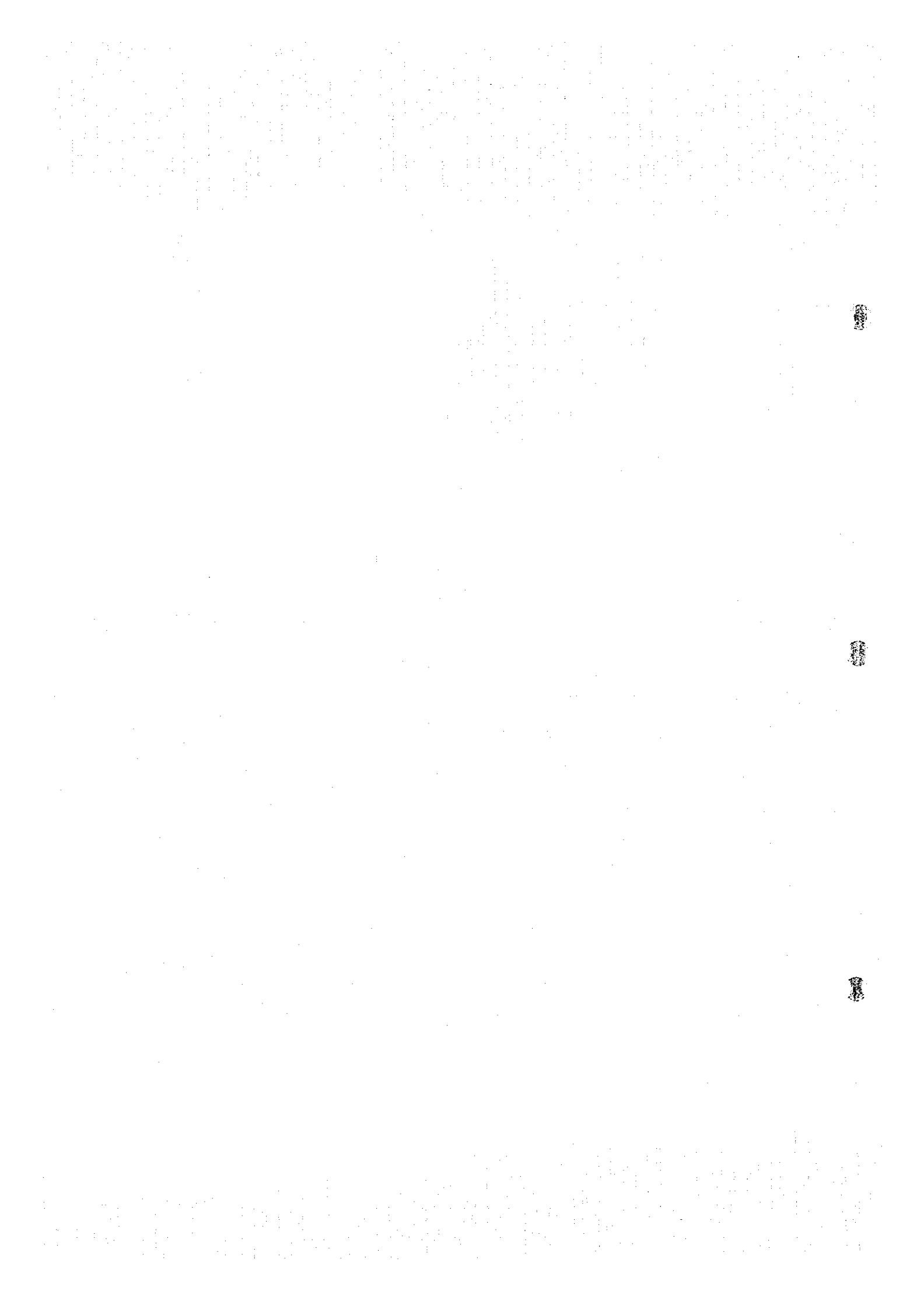


East



1000 1005 1010

1000 1005 1010 1015 1020 1025 1030 1035 1040 1045 1050 1055 1060 1065 1070 1075 1080 1085 1090 1095 1100 1105 1110 1115 1120 1125 1130 1135 1140 1145 1150 1155 1160 1165 1170 1175 1180 1185 1190 1195 1200 1205 1210 1215 1220 1225 1230 1235 1240 1245 1250 1255 1260 1265 1270 1275 1280 1285 1290 1295 1300 1305 1310 1315 1320 1325 1330 1335 1340 1345 1350 1355 1360 1365 1370 1375 1380 1385 1390 1395 1400 1405 1410 1415 1420 1425 1430 1435 1440 1445 1450 1455 1460 1465 1470 1475 1480 1485 1490 1495 1500 1505 1510 1515 1520 1525 1530 1535 1540 1545 1550 1555 1560 1565 1570 1575 1580 1585 1590 1595 1600 1605 1610 1615 1620 1625 1630 1635 1640 1645 1650 1655 1660 1665 1670 1675 1680 1685 1690 1695 1700 1705 1710 1715 1720 1725 1730 1735 1740 1745 1750 1755 1760 1765 1770 1775 1780 1785 1790 1795 1800 1805 1810 1815 1820 1825 1830 1835 1840 1845 1850 1855 1860 1865 1870 1875 1880 1885 1890 1895 1900 1905 1910 1915 1920 1925 1930 1935 1940 1945 1950 1955 1960 1965 1970 1975 1980 1985 1990 1995 2000





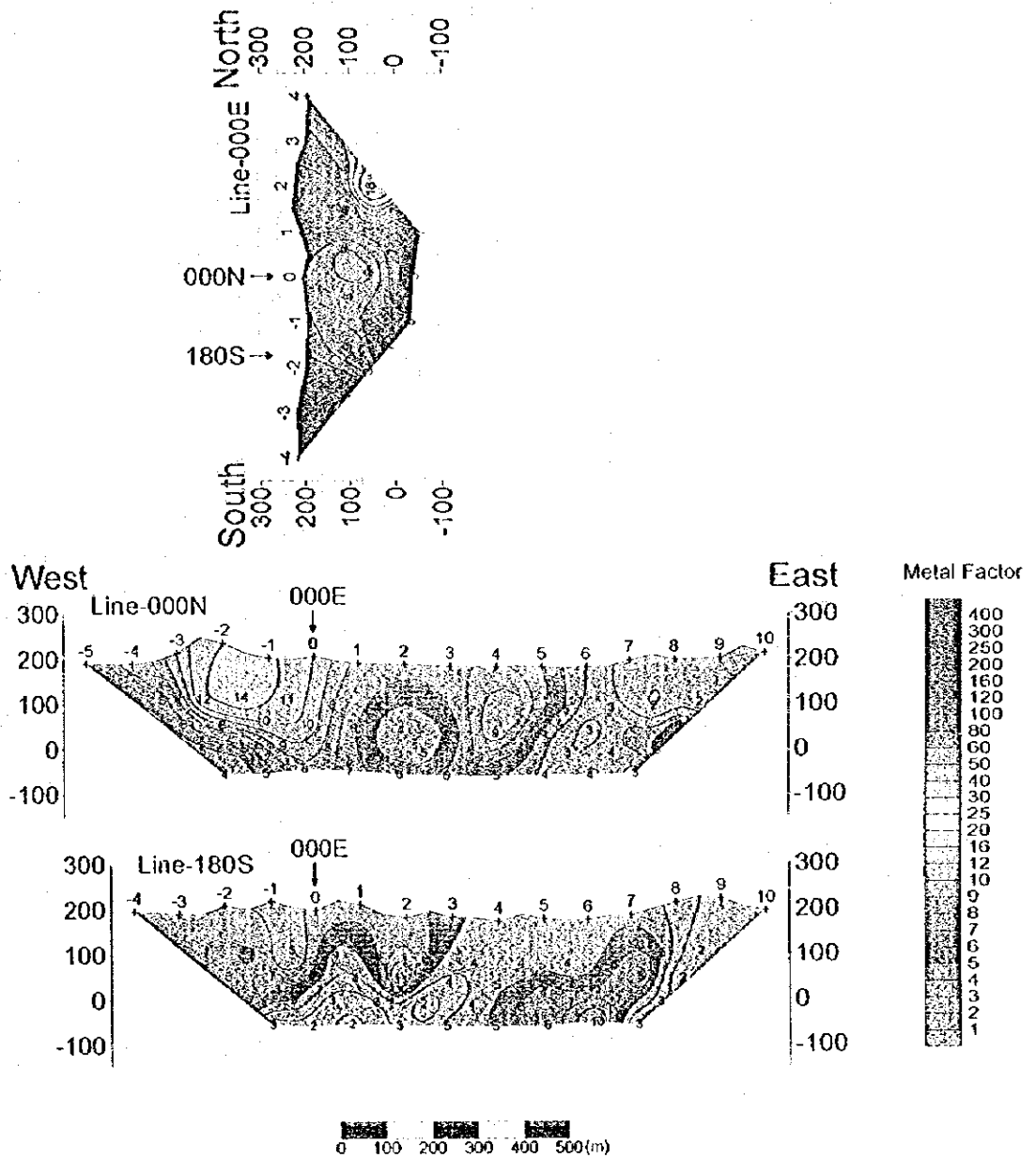


Fig.II-2-25 Metal factor pseudo-sections in Ghuzayn north area

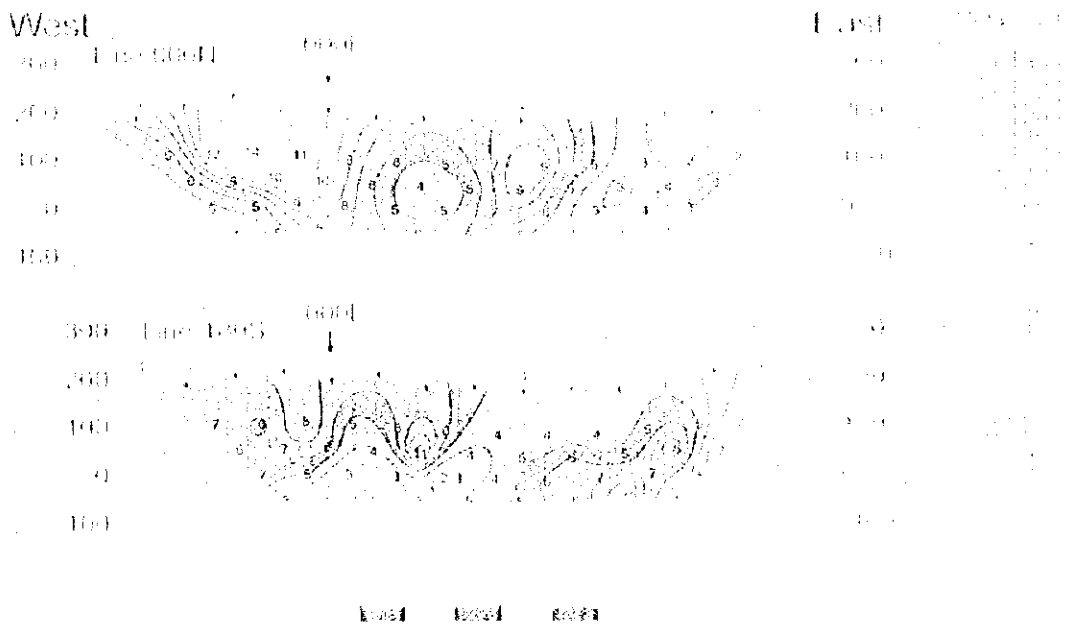


FIG. 10. Topographic map of the mountain range.



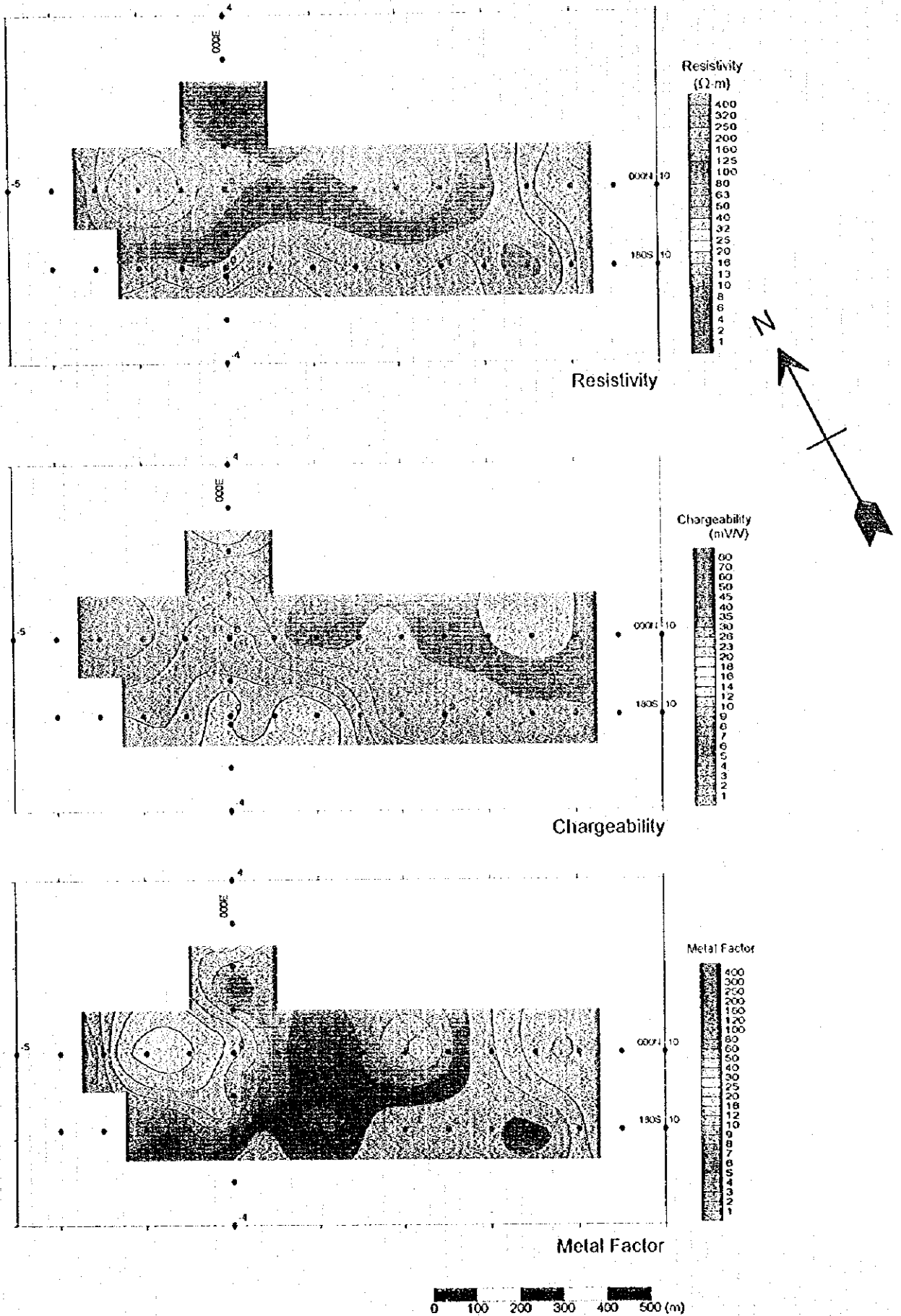
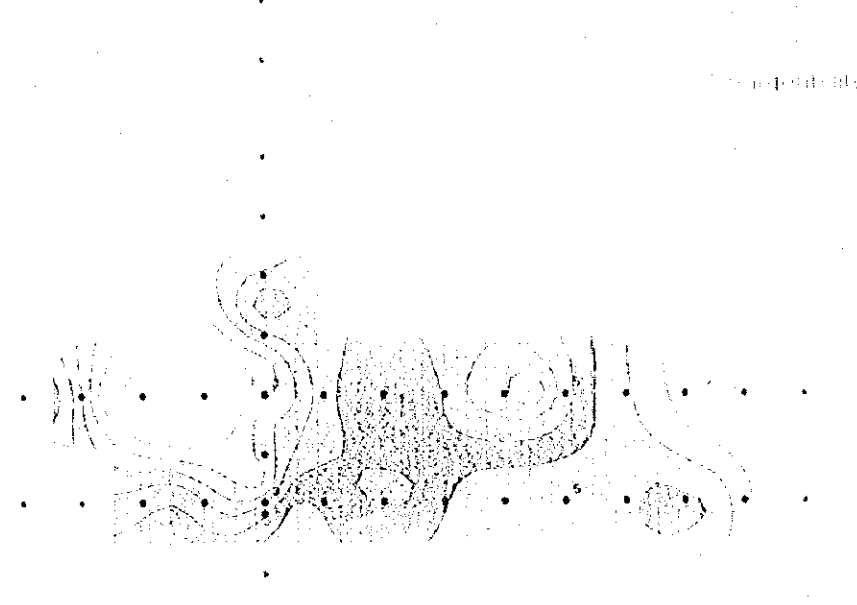
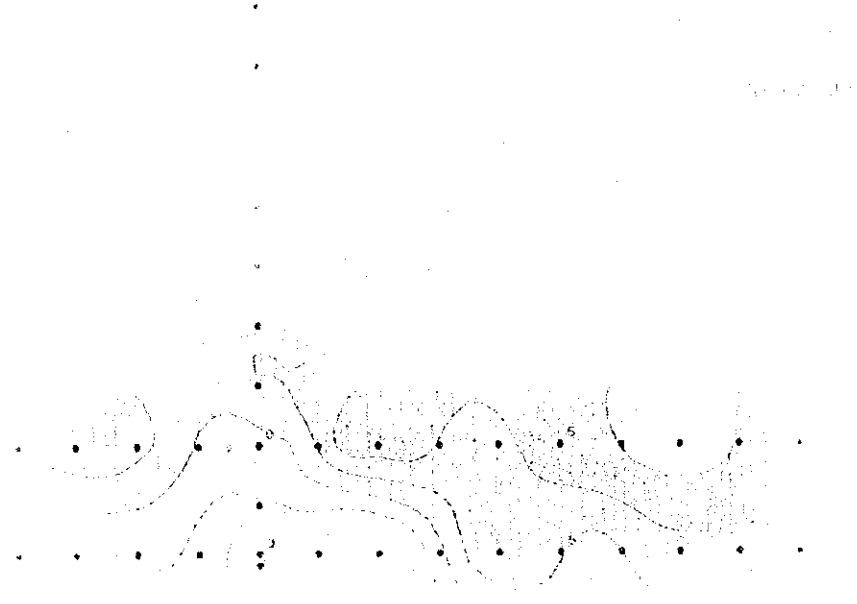
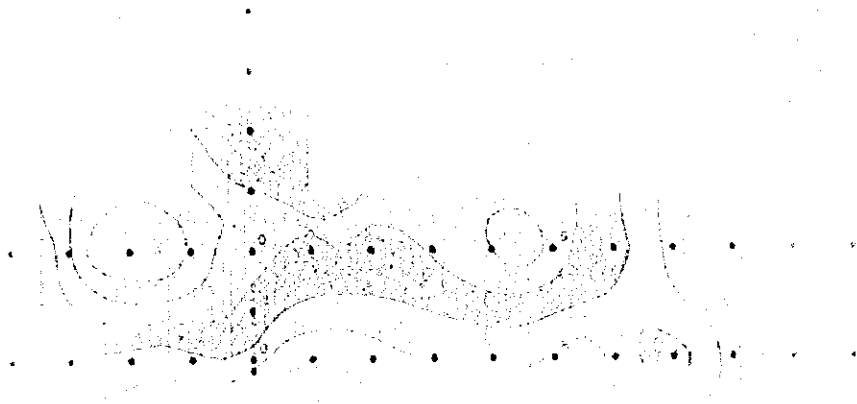


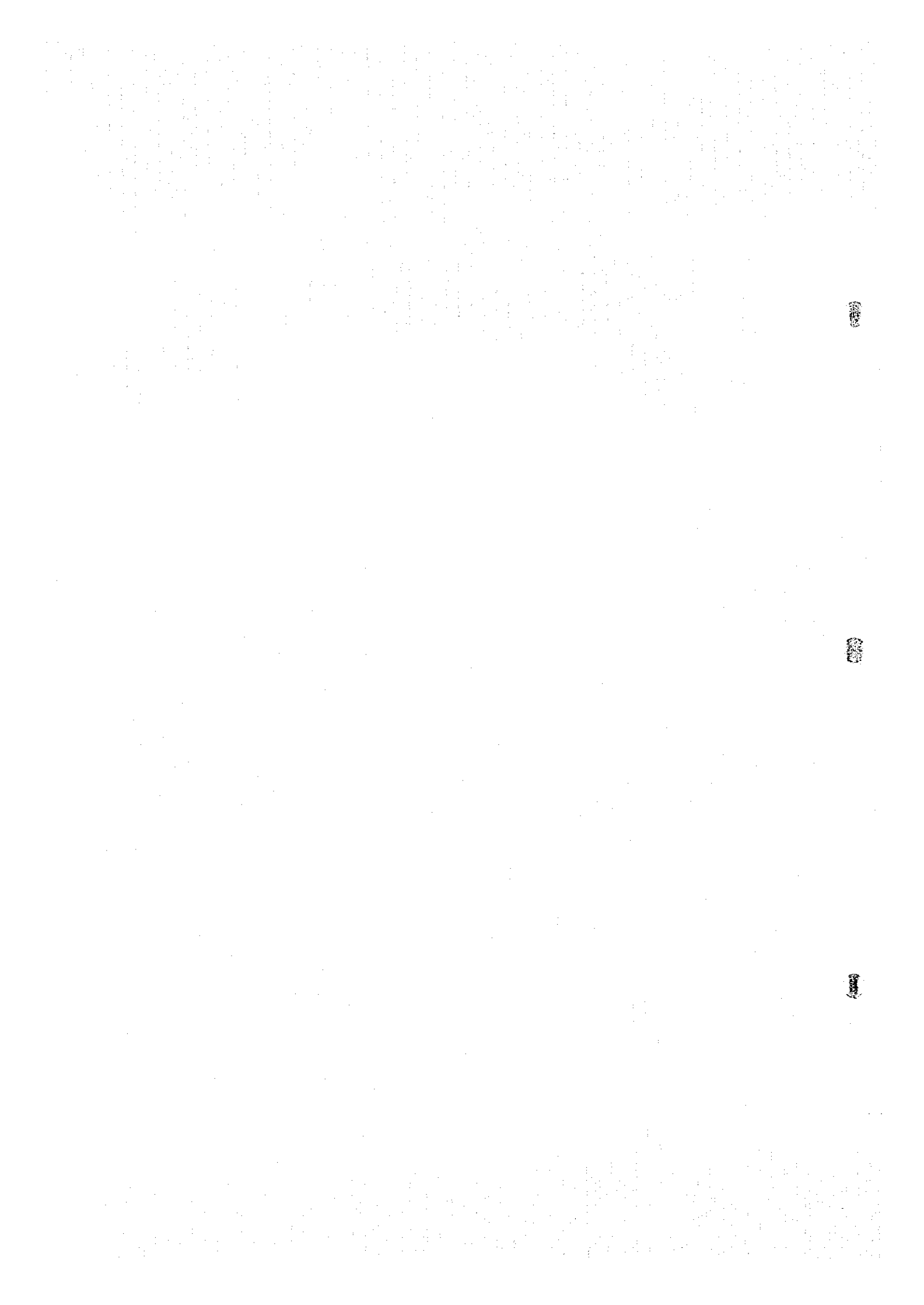
Fig.II-2-26 IP plane map of n=1 in Ghuzayn north area

Ghuzayn North Area TDIP Survey N=1



Legend:   
 [shaded box] shaded   
 [contour line] contour

Figure 1: Three contour plots illustrating the distribution of a variable across different conditions. The shaded regions represent the central area of the distribution, and the contour lines represent the level of the variable.



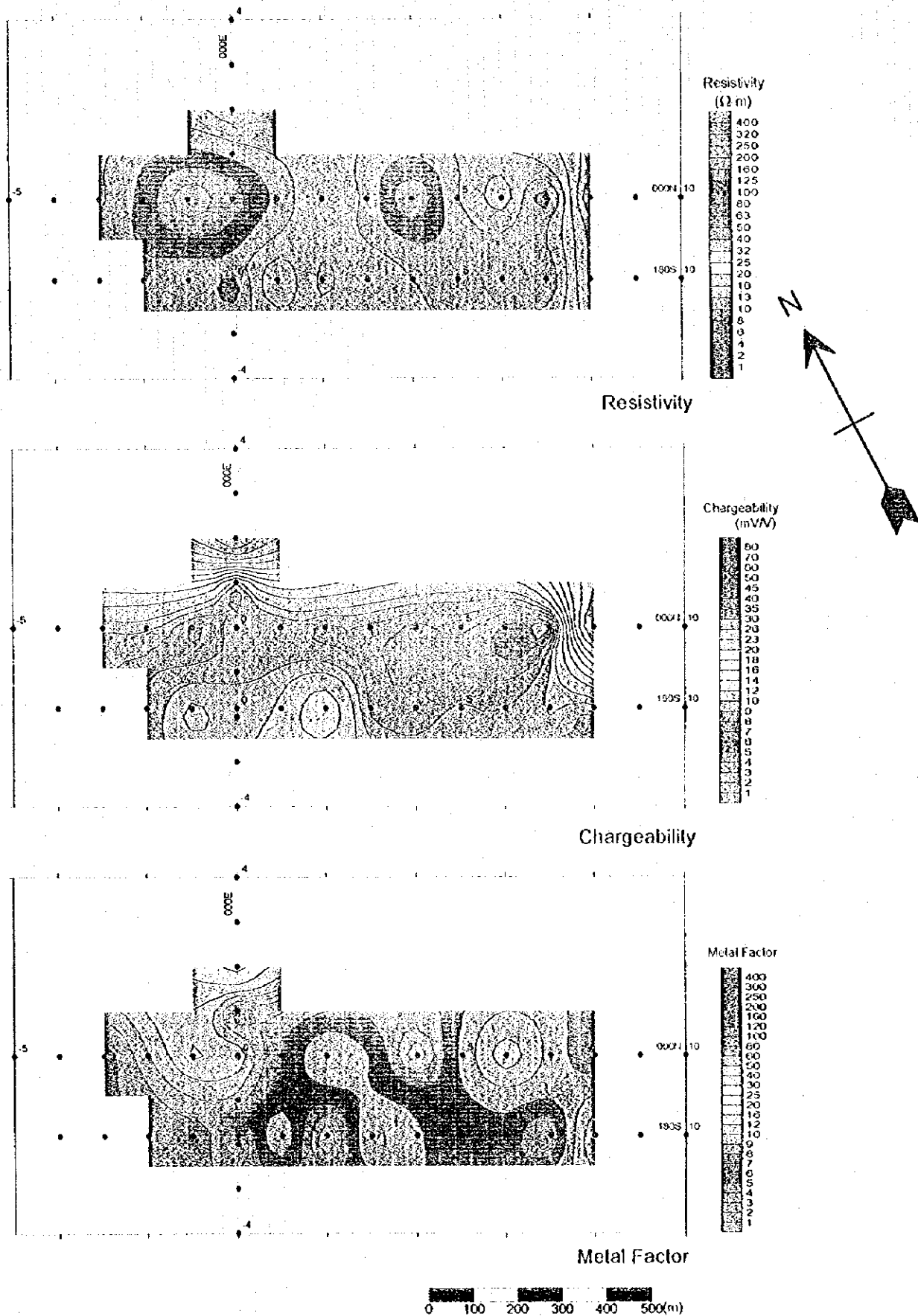
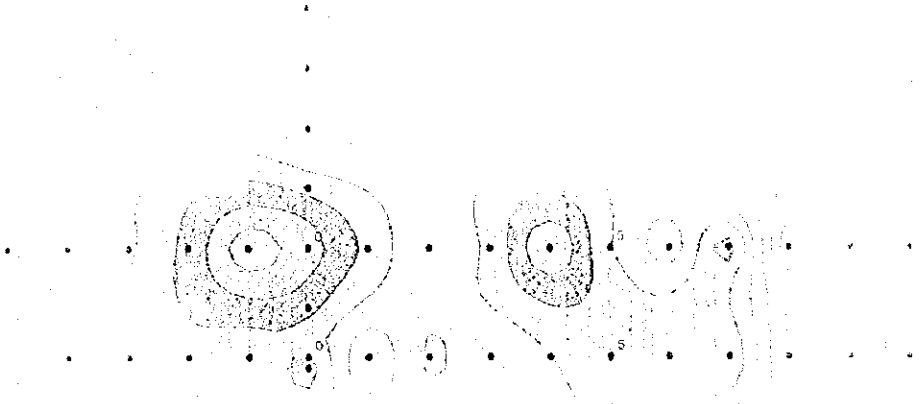
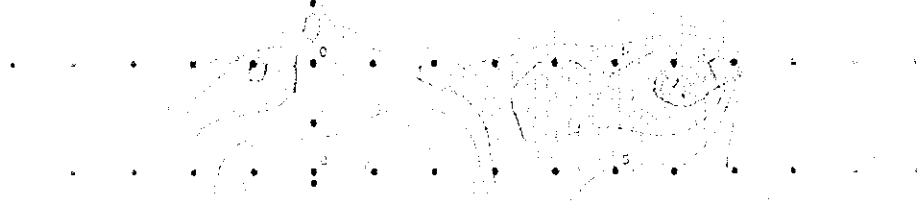


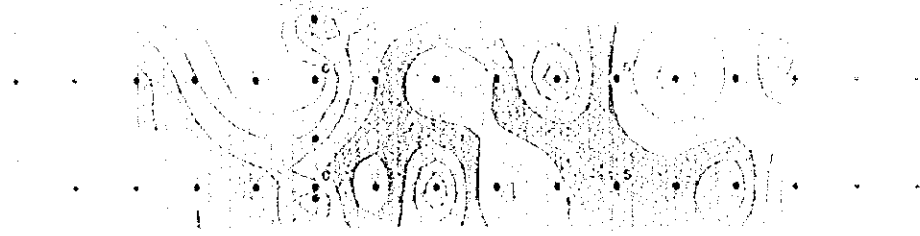
Fig.II-2-27 IP plane map of n=2 in Ghuzayn north area



100x



100x



100x

100x 100x 100x

100x 100x 100x





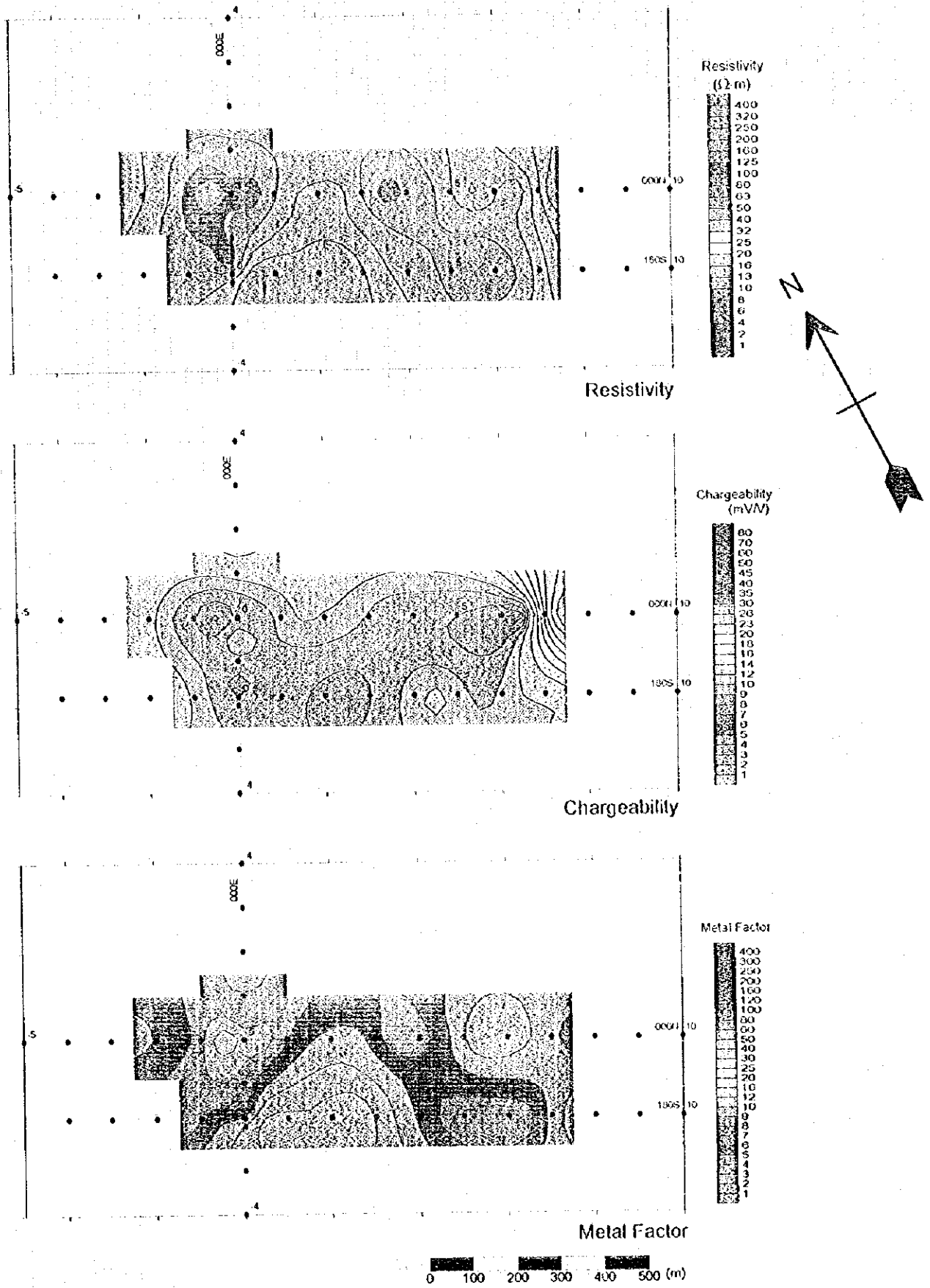


Fig.H-2-28 IP plane map of n=3 in Ghuzayn north area

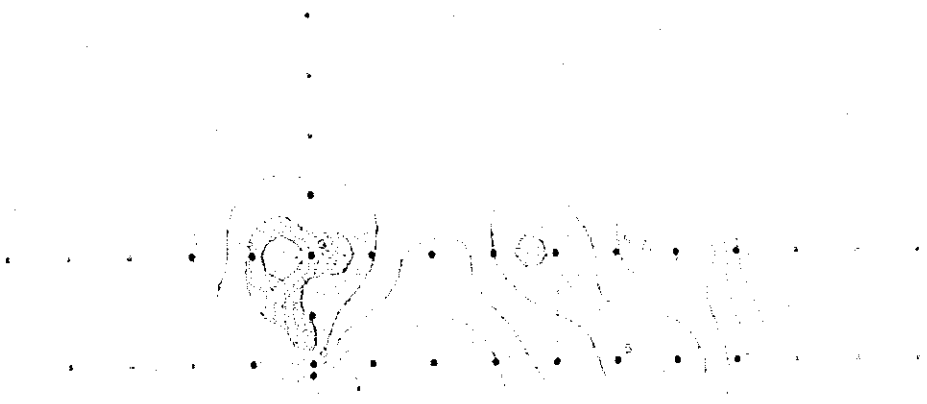


Figure 1

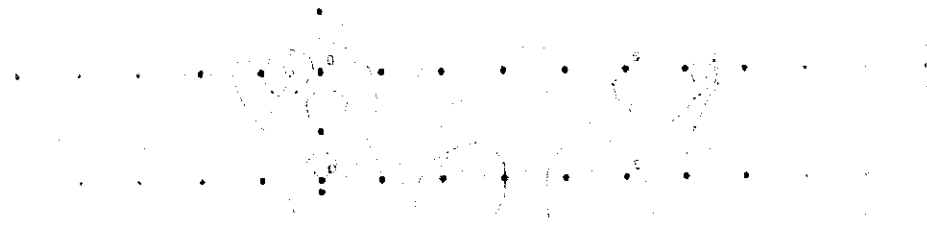


Figure 2

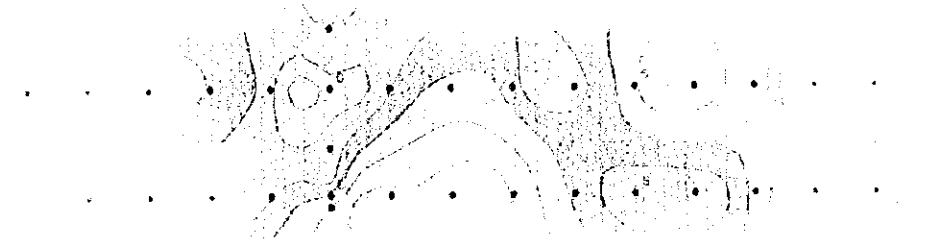
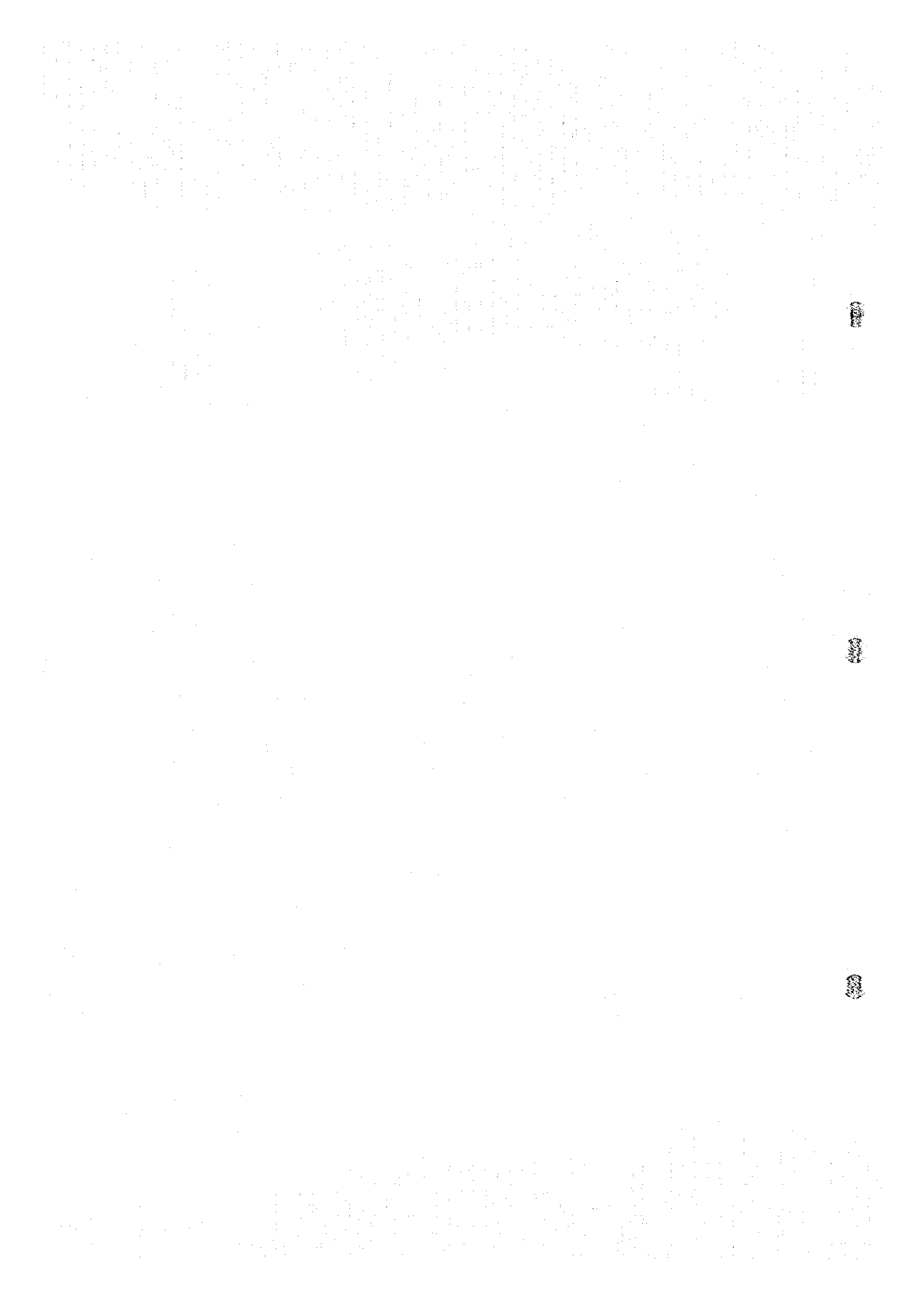


Figure 3

Figure 4

Figure 5





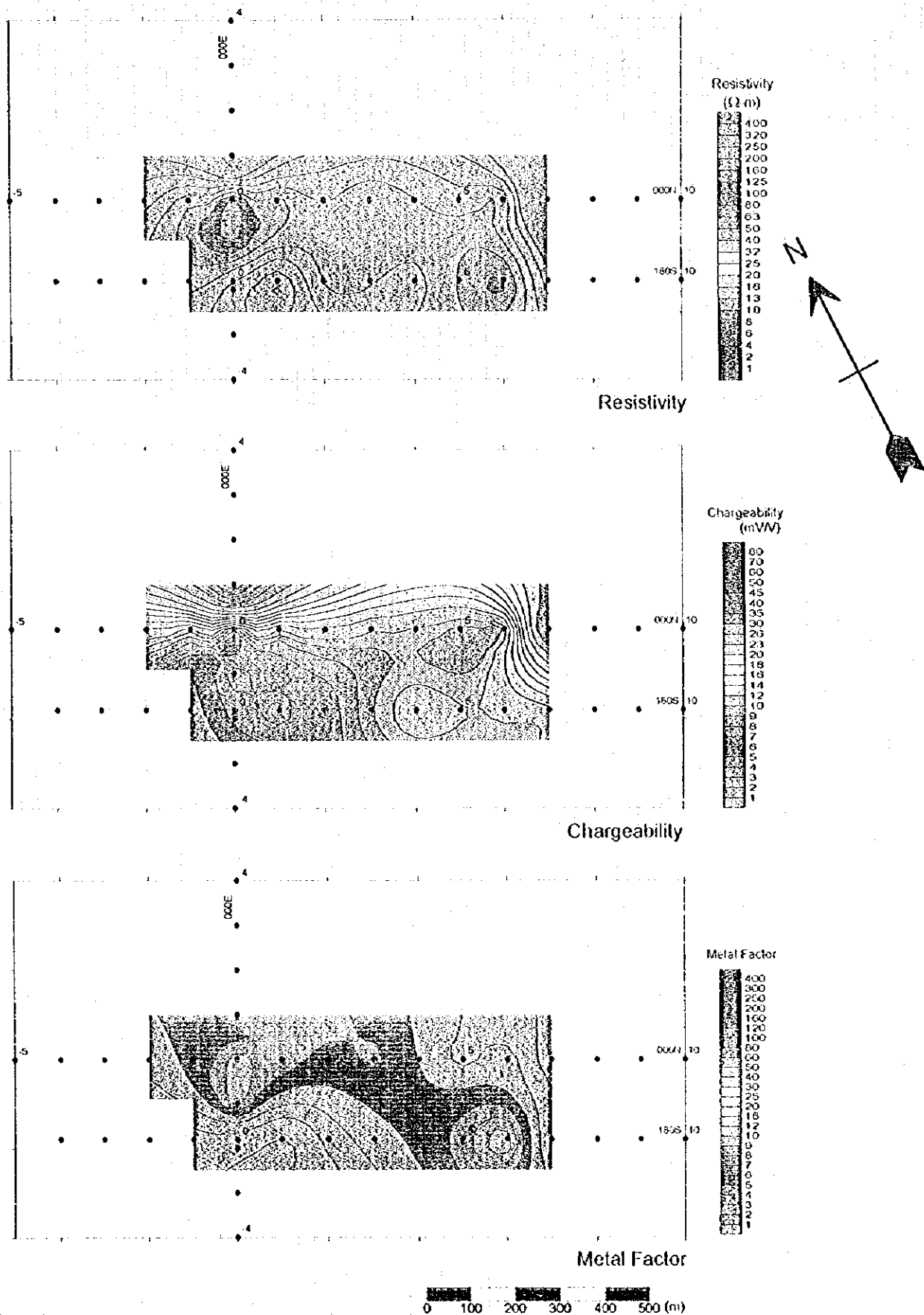
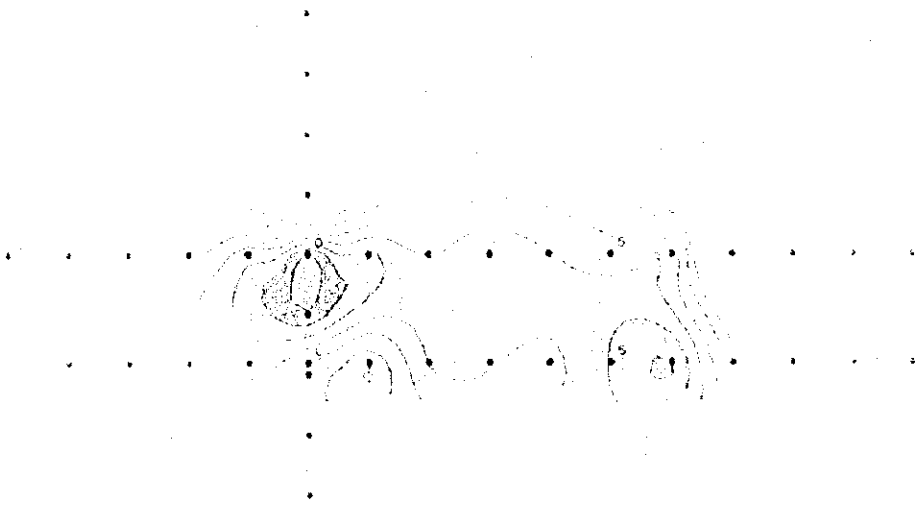
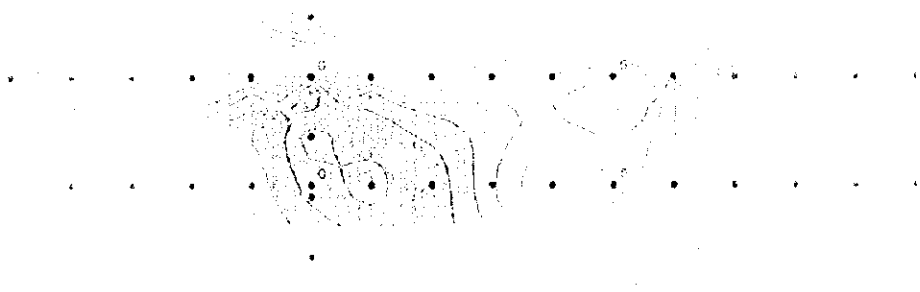


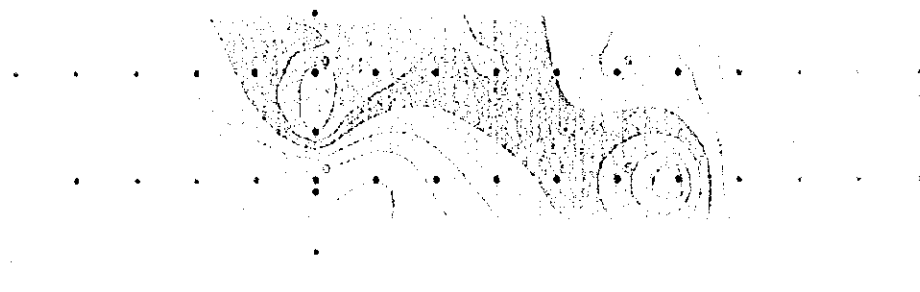
Fig II-2-29 IP plane map of n=4 in Ghuzayn north area



Positive



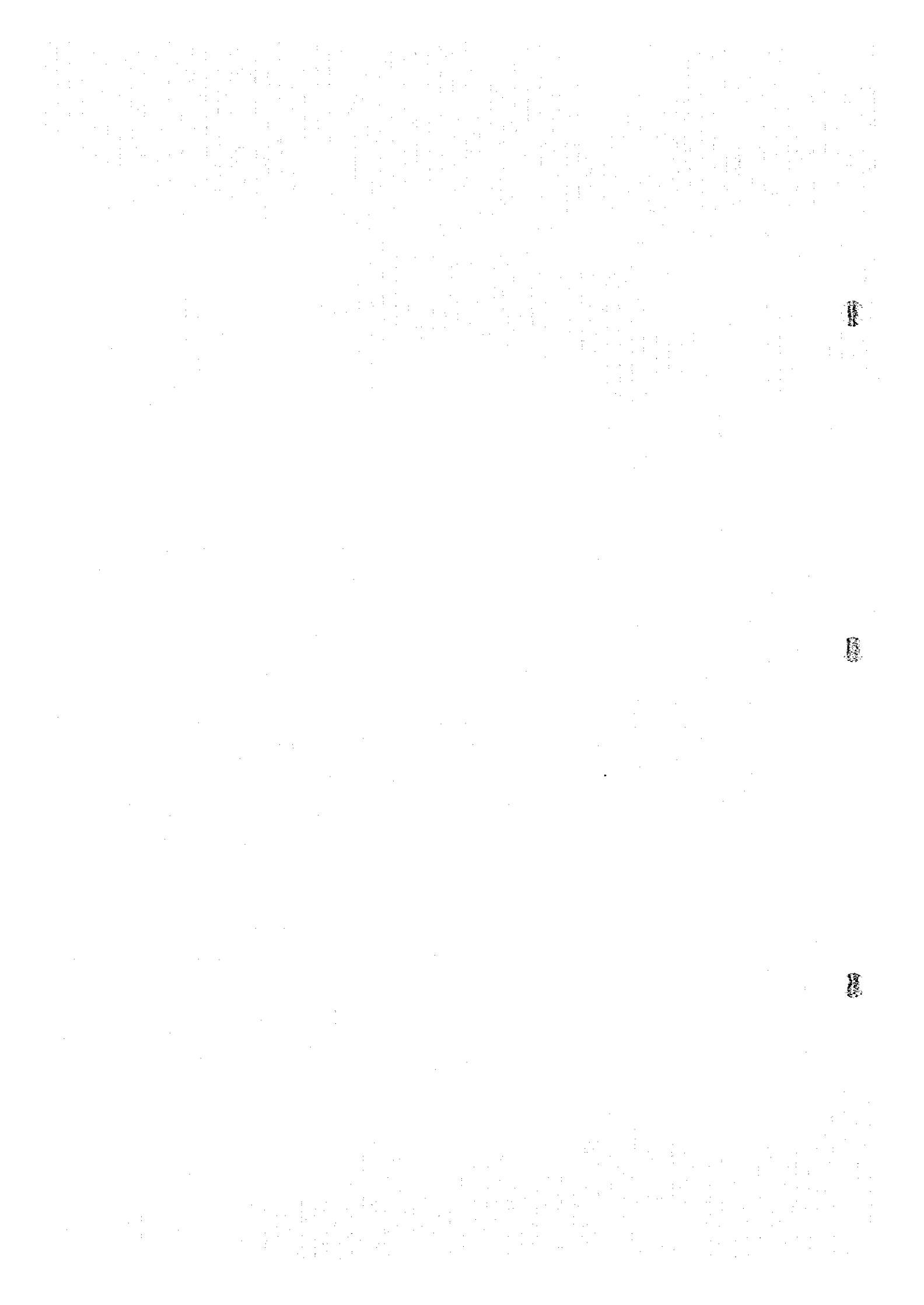
Grouped



Distal

Legend

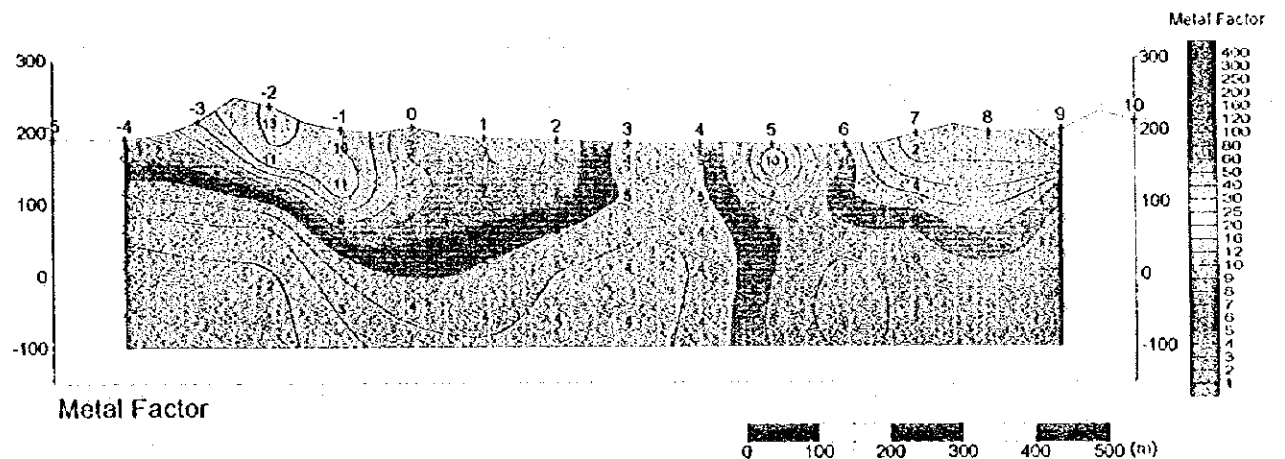
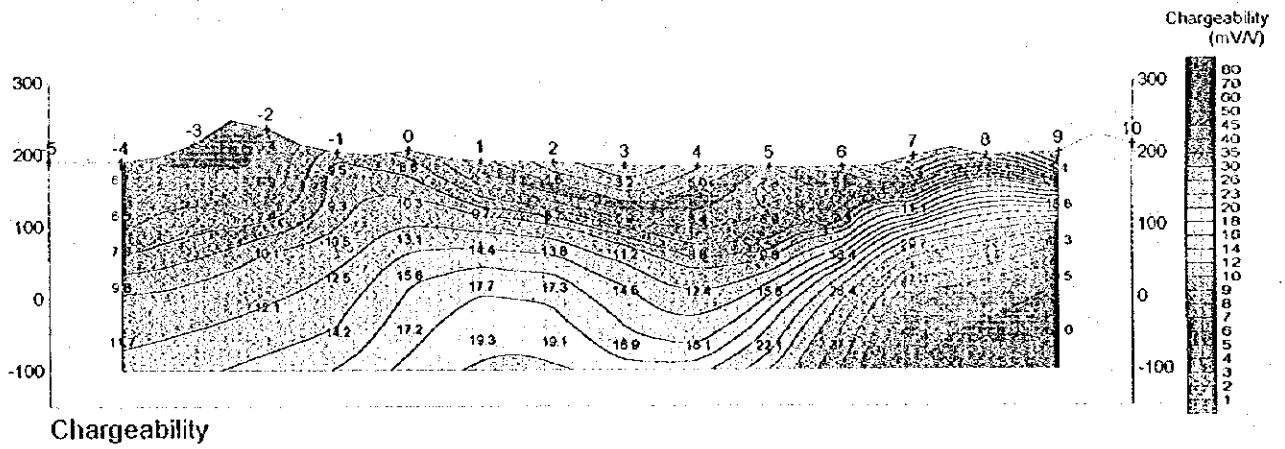
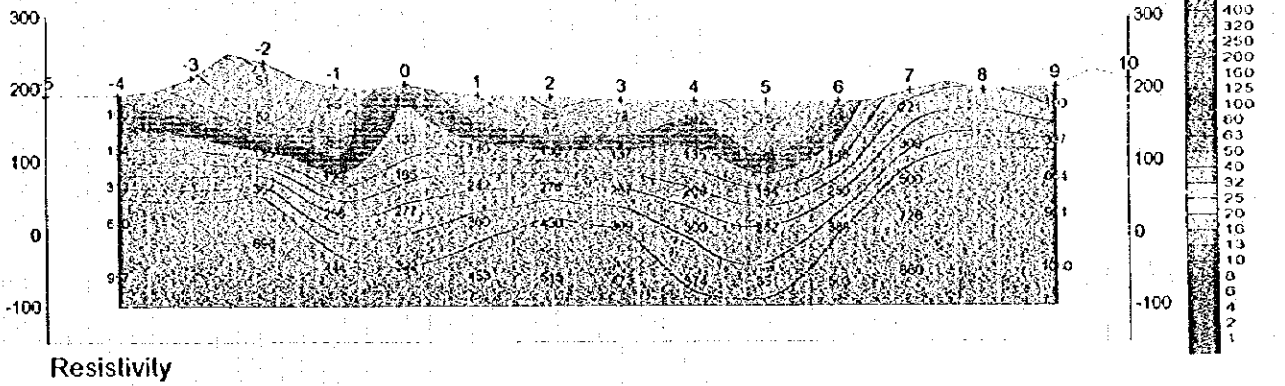
Figure 1: Contour plots showing the distribution of data points across three different stages or conditions.



# Line 000N

West

East



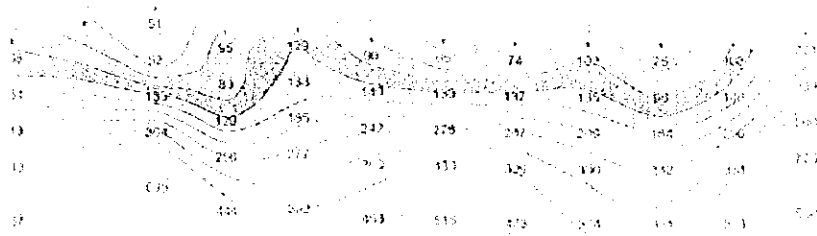
0 100 200 300 400 500 (m)

Fig II-2-30 Results of model simulation on Line 000N in Ghuzayn North area

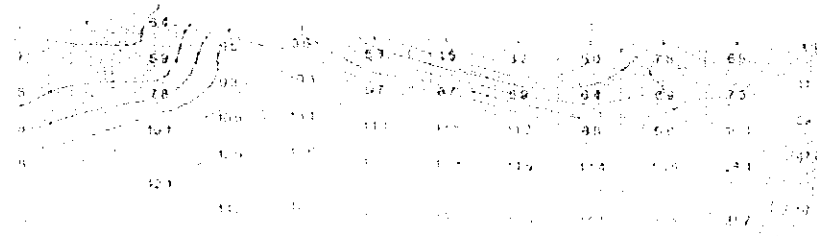


# Line 000N

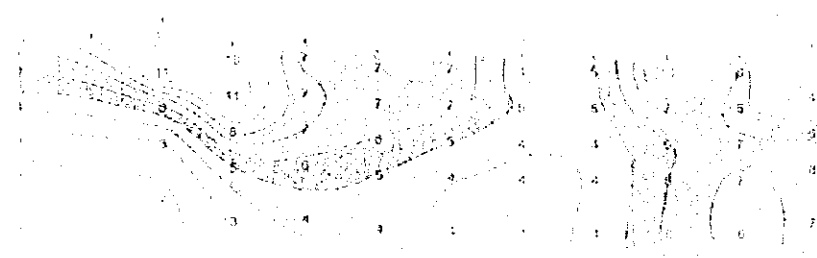
Sheet



## Resistivity

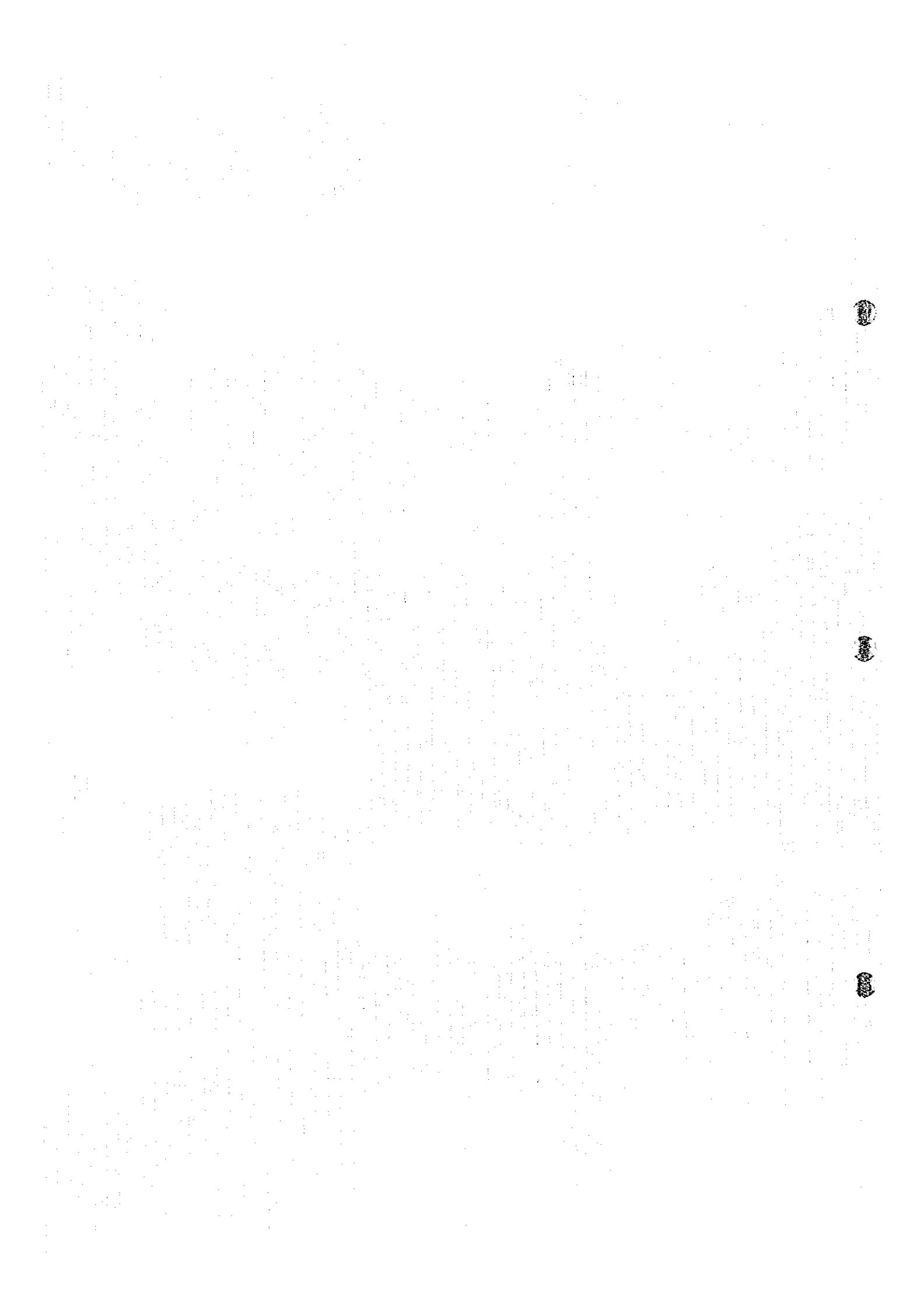


## Geological

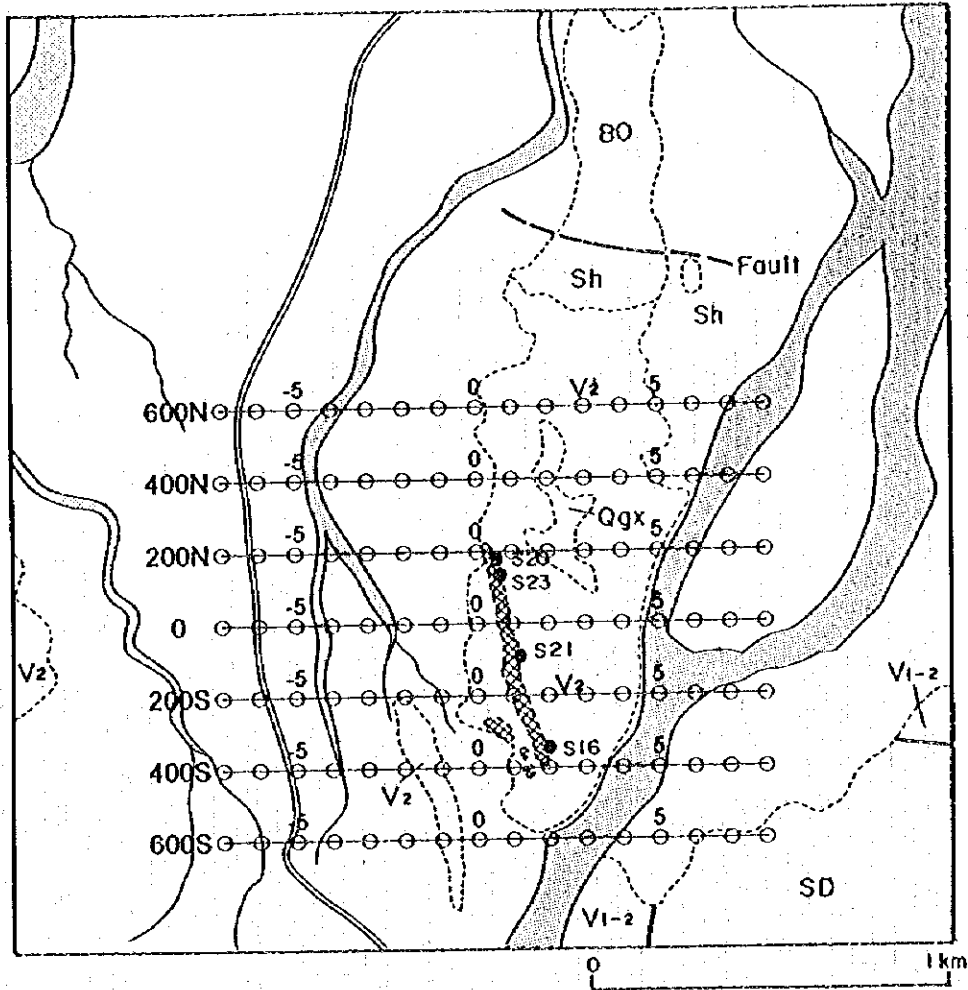


## Interpretation

Legend



# Doqal Area



### LITHOLOGY

- QUATERNARY**
- Wadi sediments and Sub-recent alluvial fans;terraces
  - Qgx Ancient alluvial fans;terraces
- SUPRA-OPHIOLITE SEDIMENTS**
- BO Batinah Olistostromes
- SMALL OPHIOLITE**  
Small Volcanic Rocks
- Sh Suhaylah Formation
  - V<sub>2</sub> Middle Volcanic Rocks
  - V<sub>1-2</sub> Lower Volcanic Rocks  
Lower extrusives 2
- Sheeted-dyke complex**
- SD Sheeted dykes;dolerite

### MINERALIZATION

- Gossan

### Other symbols

- S20 Sample location
- Road
- Wadi
- TDIP Survey Lines

Fig.II-2-31 IP line locations in Doqal area

### 2-9-2 Results

Apparent resistivity, chargeability and metal factor pseudo-sections are indicated in Figs. II-2-32, II-2-33 and II-2-34, respectively. Figs. II-2-35, II-2-36, II-2-37 and II-2-38 show the resistivity, chargeability and metal factor maps for  $n=1$  to  $n=4$ , respectively.

The apparent resistivity values range from 3 to 330  $\Omega\text{m}$ , distributed so that in general, low values are seen in the north part while increasing to higher values towards the south. Within this general tendency, partially relatively low resistivity distributions extend from the north along NS direction, one of them, can be seen in the central part of the survey area from the station No. 0 of the line 200N to the station No. 0 of the line 200S. Another distribution is seen extended from station No. 5 of the line 200N to the station No. -5 of the line 400S. The low resistivity distribution in the central part seems to coincide quite well with the NS direction of the gossanized mineralized zone. The low resistivity tendency located in the west part, coincides on the surface with the Wadi that elongates along NS direction.

In relation to the chargeability distribution, a comparatively high chargeability distribution of above 15 mV/V, is seen extended from the central part of the area towards the south. As same as in the case of the low resistivity distribution above mentioned, this high chargeability distribution coincides well with the gossanized zone, which at shallow depth ( $n=1$ ) reaches a maximum of about 25.5 mV/V around the stations 0 corresponding to the lines 200N and 000. At greater depth ( $n=4$ ), however, the high chargeability distribution seems to be splitted in two, one centered around the stations -1 of the lines 200N and 000 and the other around the station 1 of the line 200S. At shallow depths, it can also be added that the high chargeability distribution is seen at the northwest part of the area as a medium chargeability distribution of about 10 mV/V.

Regarding the metal factor, a distribution of above 15 seen in the central part which extends towards the north west part of the area becoming even wider. Within this distribution, prominent values can be seen around the station 0 of the lines 000N and 200N. Prominent values are also seen at shallow depths around the station -4 on the line 400N, and at greater depths, prominent values of more than 30 are seen around the stations -3 on the lines 000N and 200N.

### 2-9-3 2-D Analysis

The lines 400N, 200N, 0 and 200S underwent two dimensional analysis to match an assumed geo-electrical structure with the results obtained in the field. Simulation results of the above mentioned lines are indicated in Figs. II-2-39 to II-2-42.

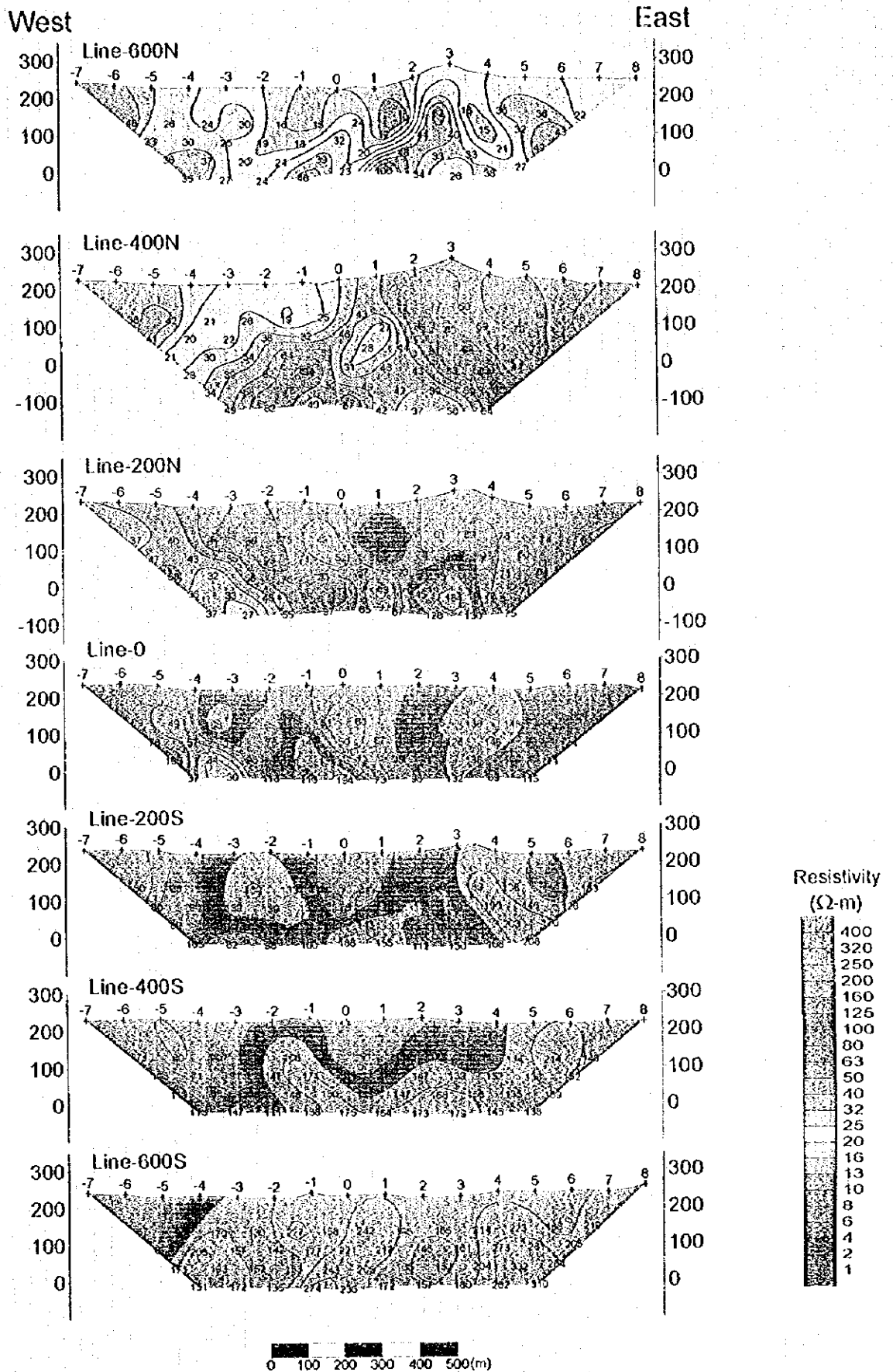


Fig. II-2-32 Apparent resistivity pseudo-sections in Doqal area

West

East

Line 03011

700

800

900

Line 13011

700

800

900

Line 20111

700

800

900

1000

1100

1200

Line 30111

700

800

900

Line 40111

700

800

900

Line 50111

700

800

900

1000 1100 1200



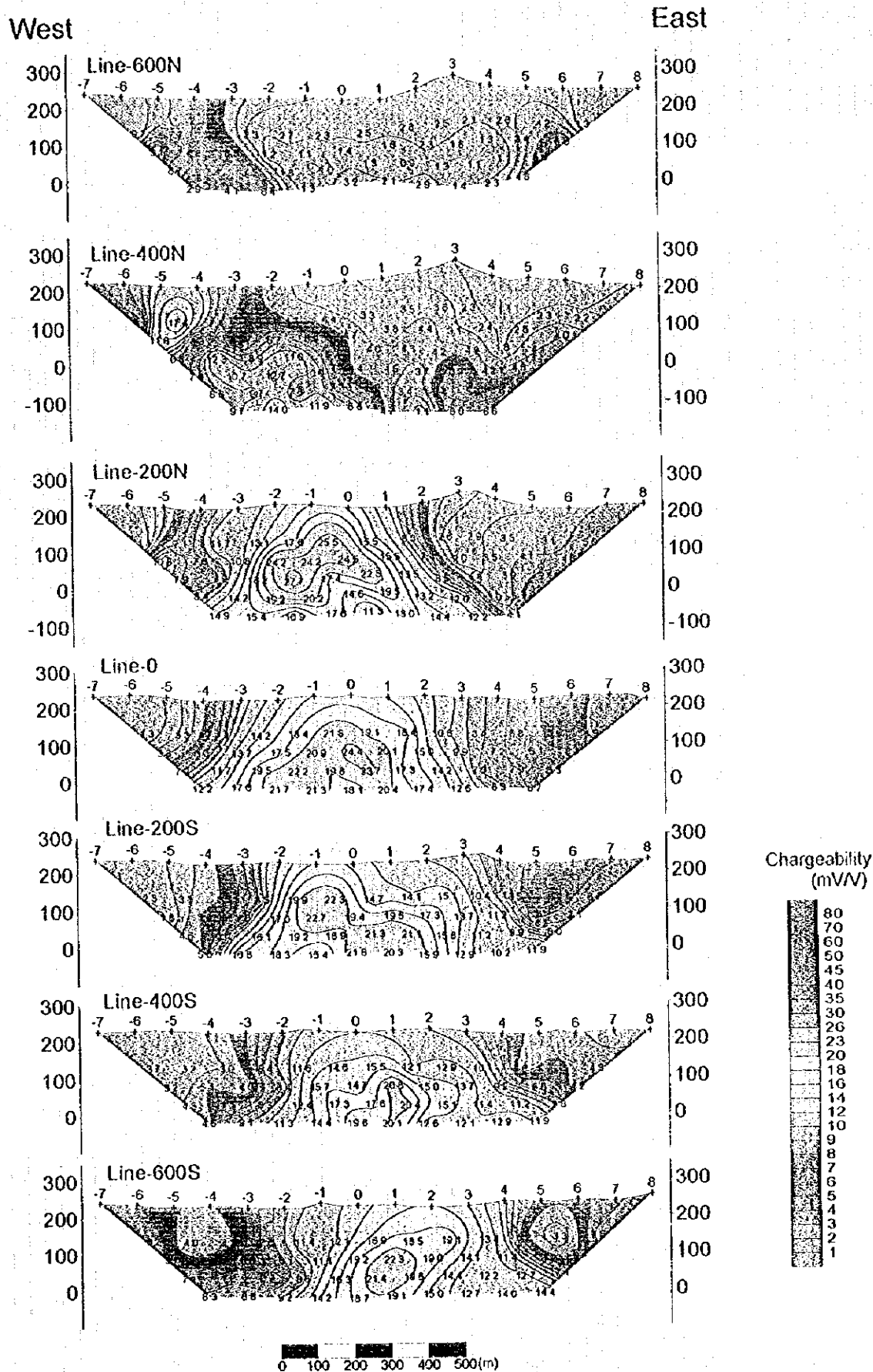


Fig. II-2-33 Chargeability pseudo-sections in Doqal area

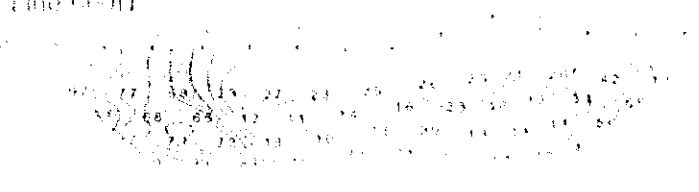


West

East

300 Time 00:00

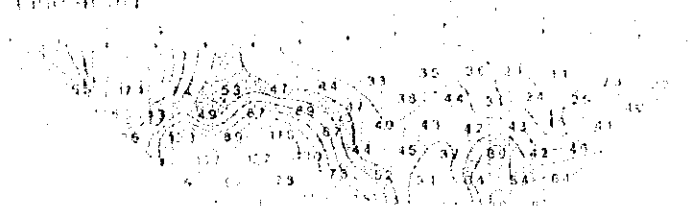
200  
100  
0



300  
200  
100  
0

300 Time 4:00

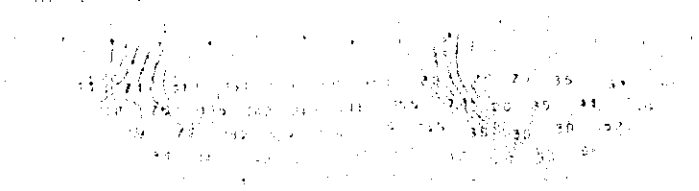
200  
100  
0



300  
200  
100  
0

300 Time 20:00

200  
100  
0



300  
200  
100  
0

300 Time 24:00

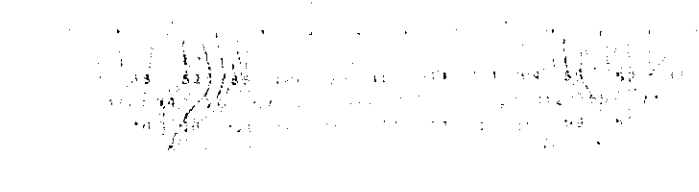
200  
100  
0



300  
200  
100  
0

300 Time 01:00

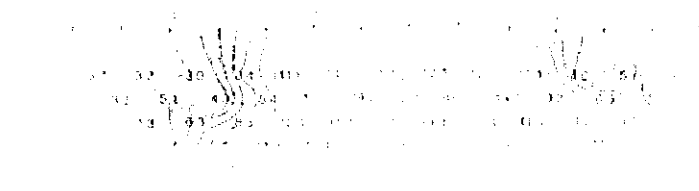
200  
100  
0



300  
200  
100  
0

300 Time 05:00

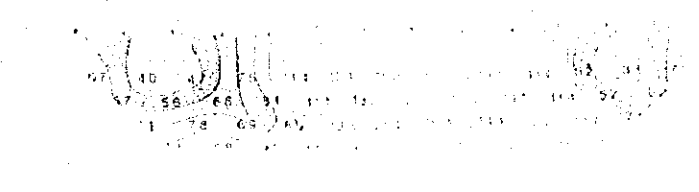
200  
100  
0



300  
200  
100  
0

300 Time 09:00

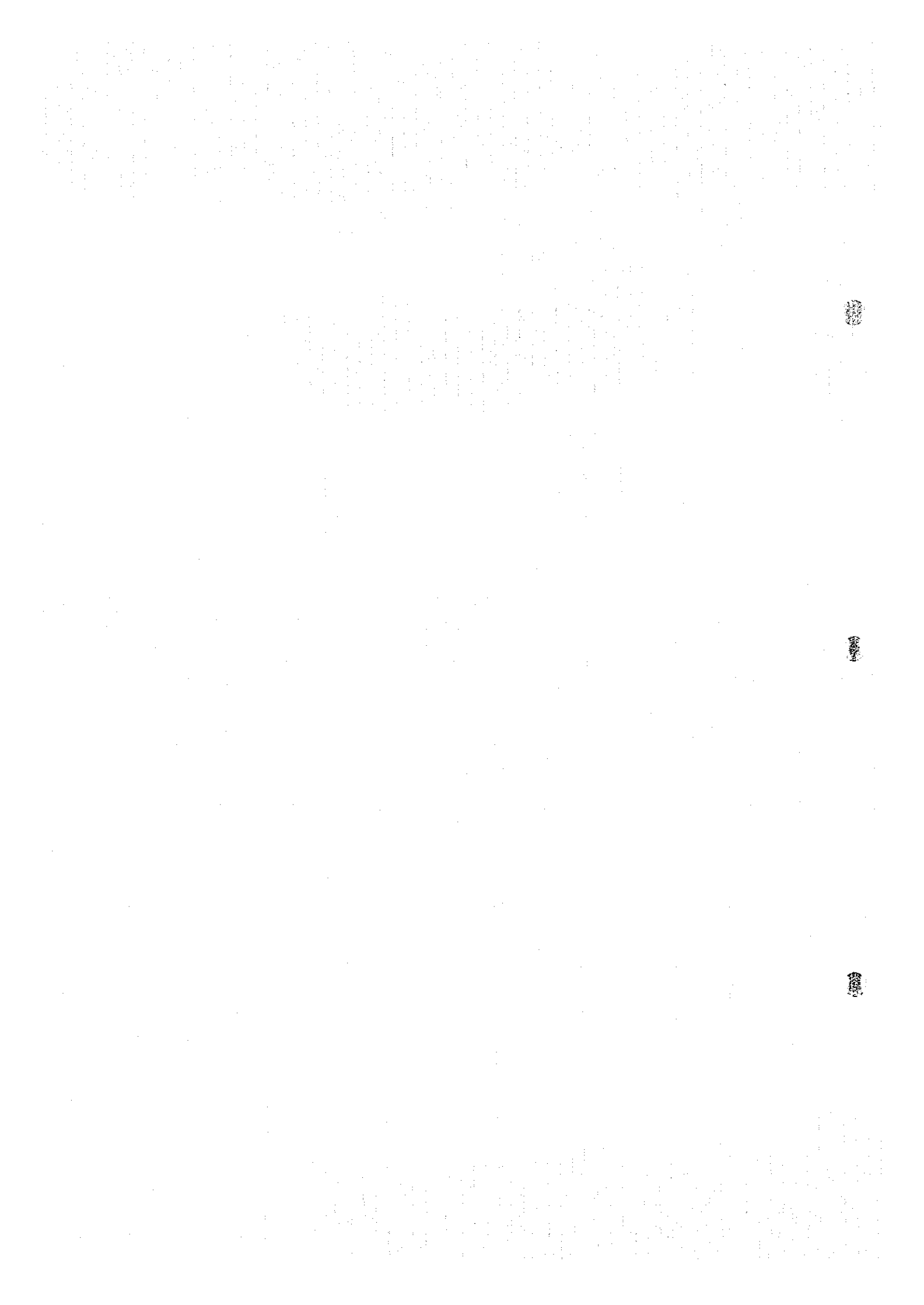
200  
100  
0



300  
200  
100  
0

Level 0.000 0.000 0.000

0.000 0.000 0.000 0.000 0.000 0.000 0.000 0.000 0.000 0.000



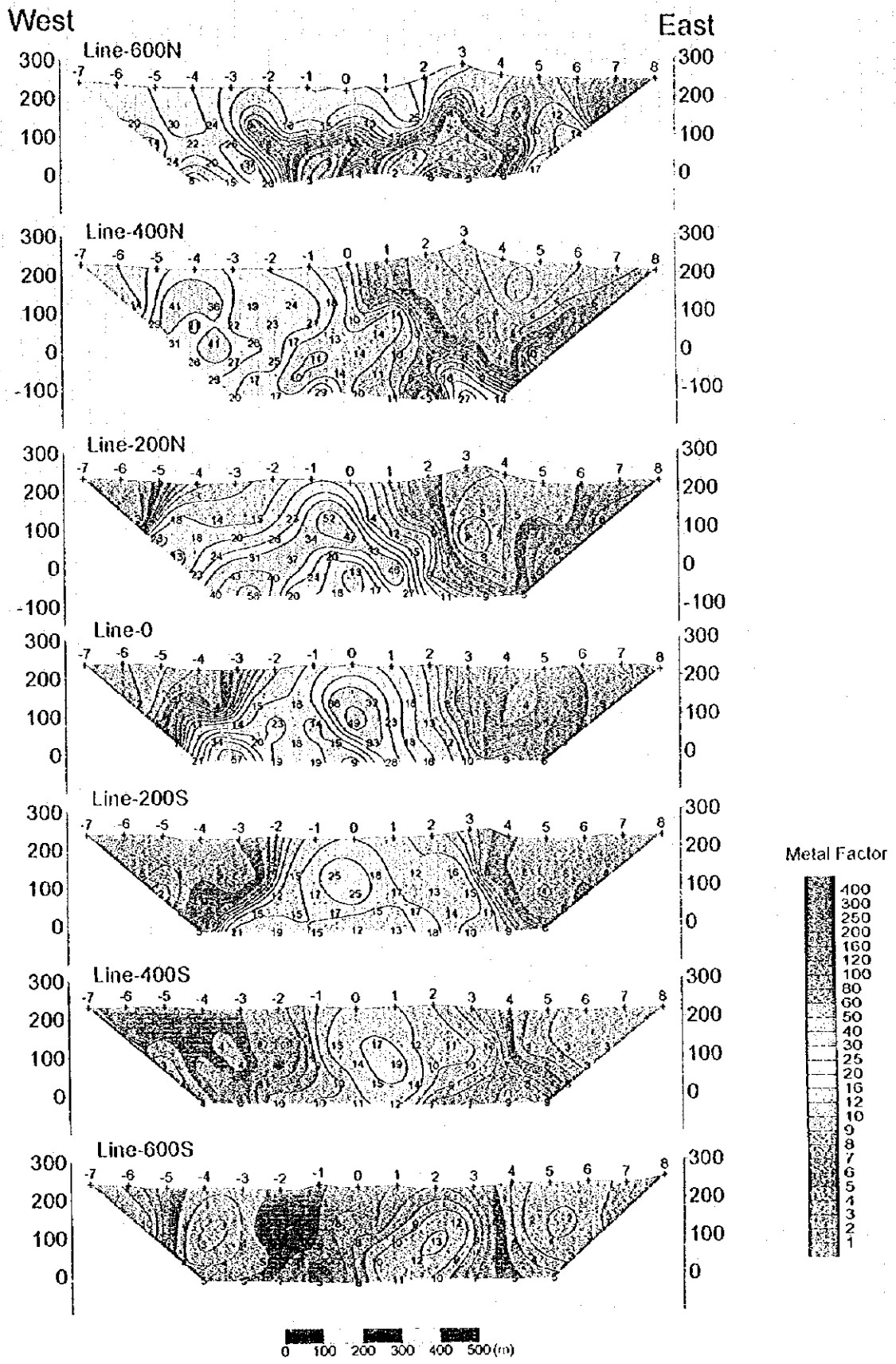


Fig. II-2-34 Metal factor pseudo-sections in Doqal area

West

East

1000 1000 2000

900

800

700

1000 1000 2000

900

800

700

600

1000 1000 2000

900

800

700

600

1000 1000 2000

900

800

700

1000 1000 2000

900

800

700

1000 1000 2000

900

800

700

1000 1000 2000

900

800

700

1000 1000 2000

Figure 1. Map of the study area showing the location of the study sites.

Faint, illegible text at the top of the page, possibly a header or title.

Central block of faint, illegible text.

Small, dark mark or stamp on the right margin.

Small, dark mark or stamp on the right margin.

Small, dark mark or stamp on the right margin.

Faint, illegible text at the bottom of the page, possibly a footer or concluding text.

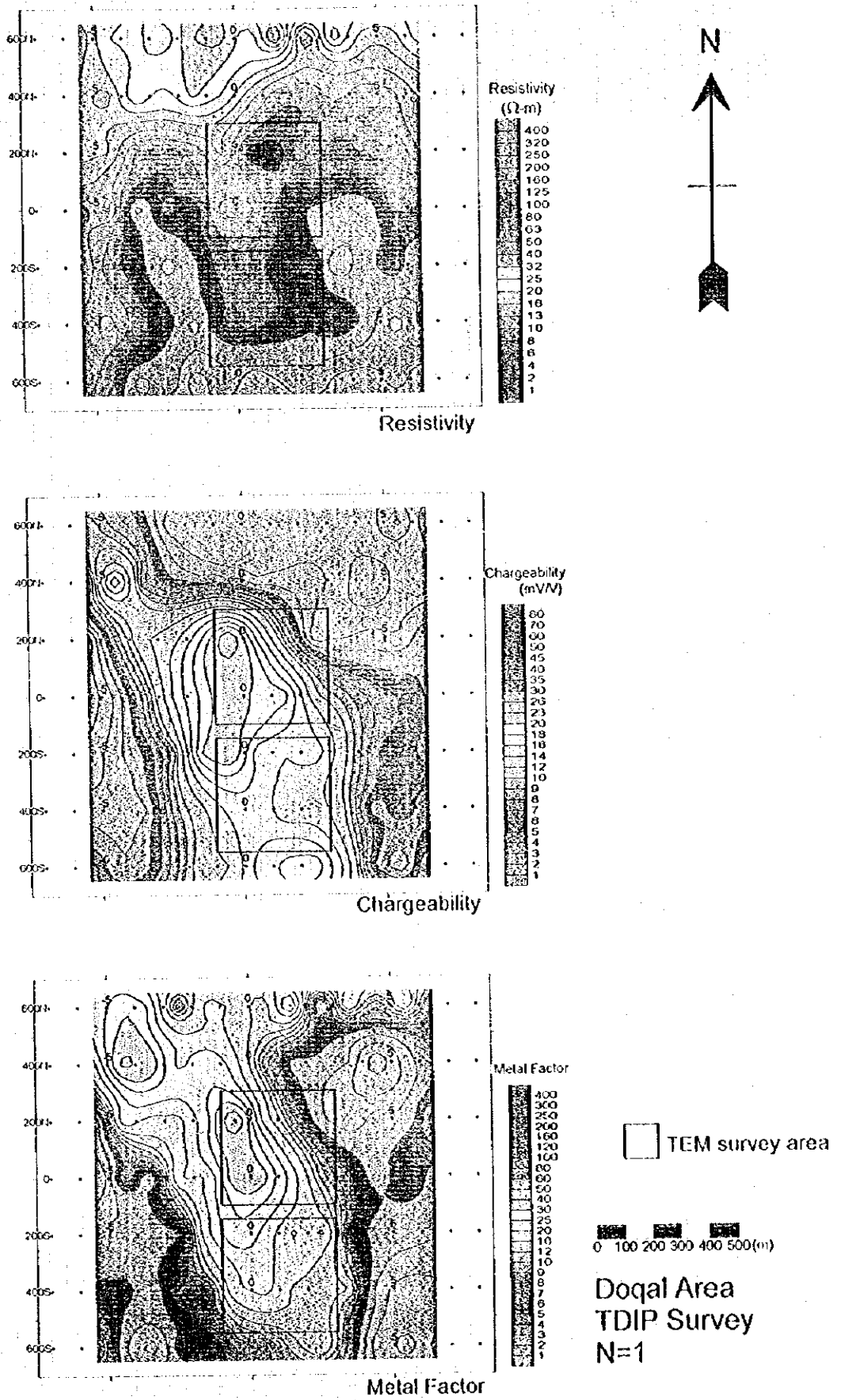


Fig.II-2-35 IP plane map of n=1 in Doqal area

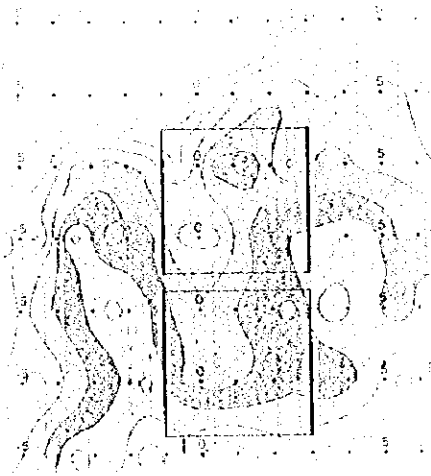


Figure 1a

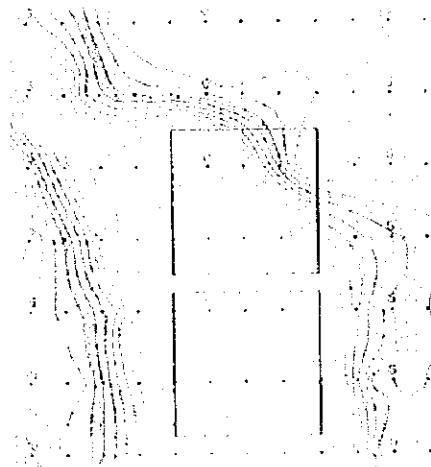


Figure 1b

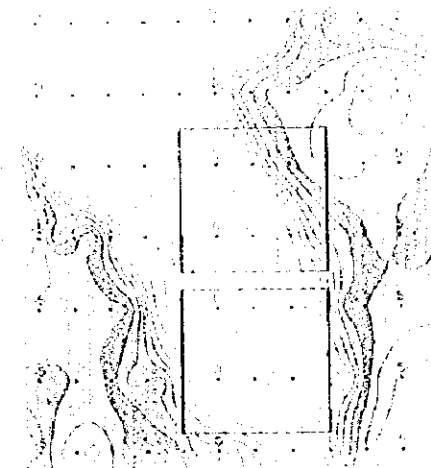
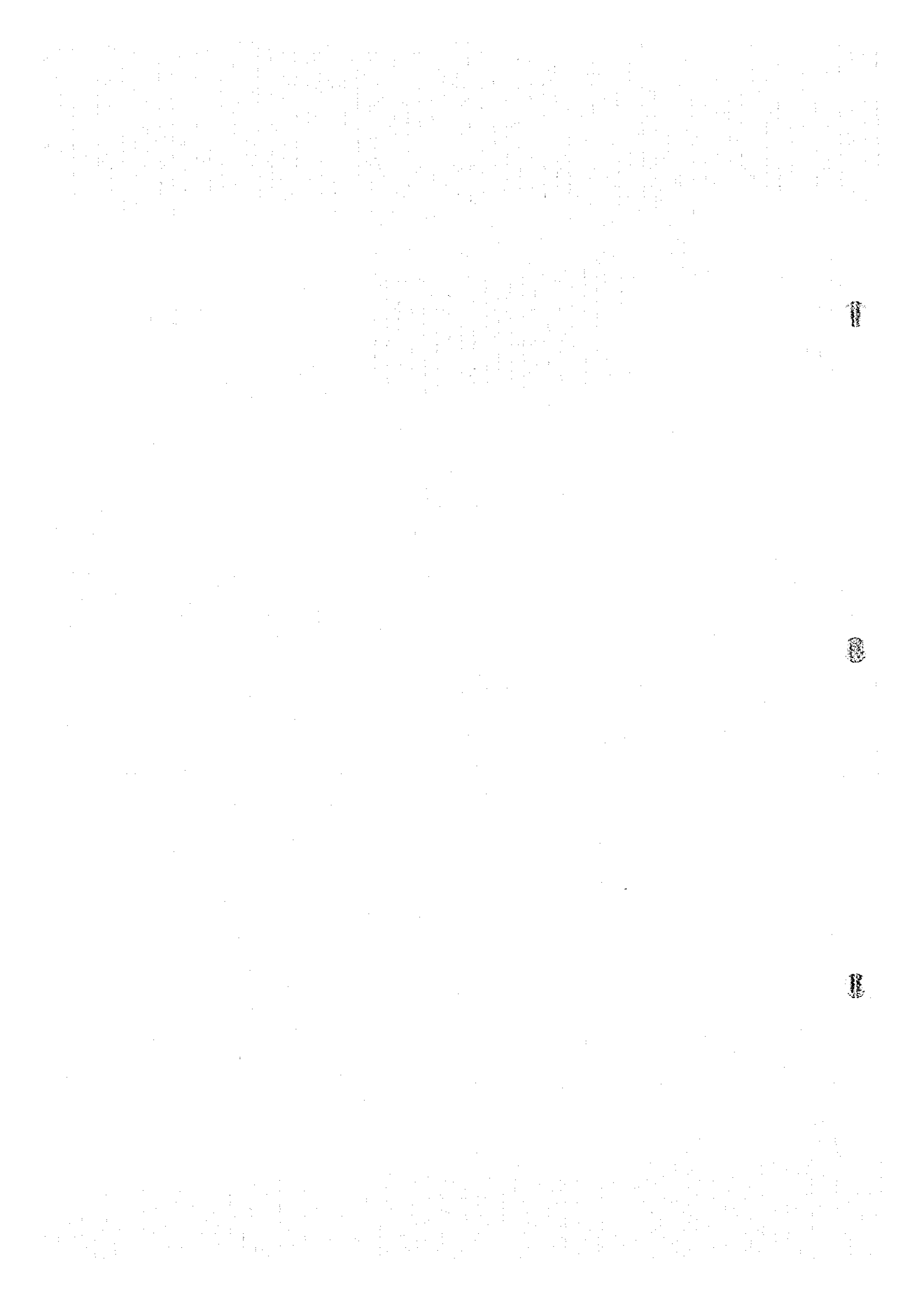


Figure 1c

Journal of

Journal of  
 1000  
 1000





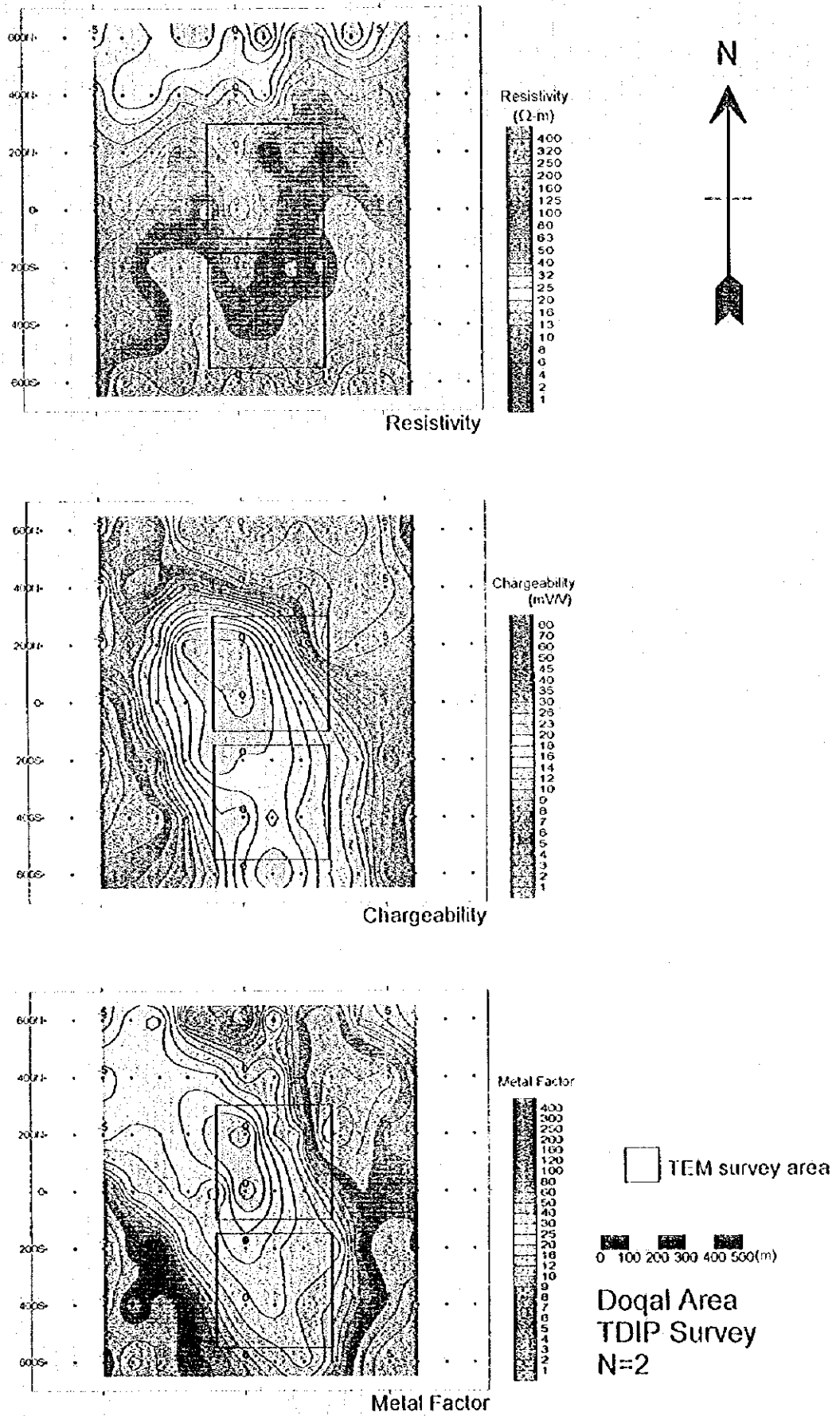
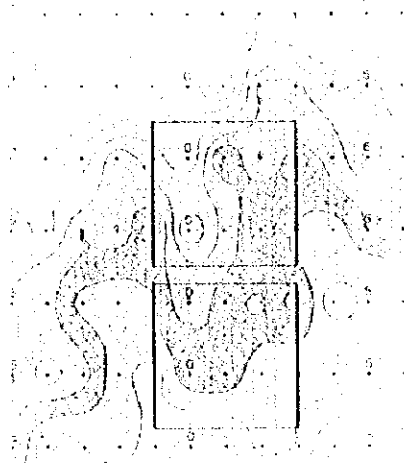
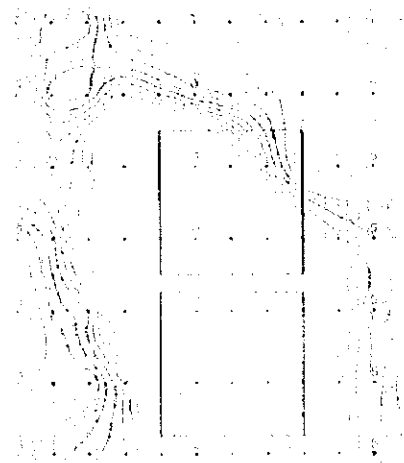


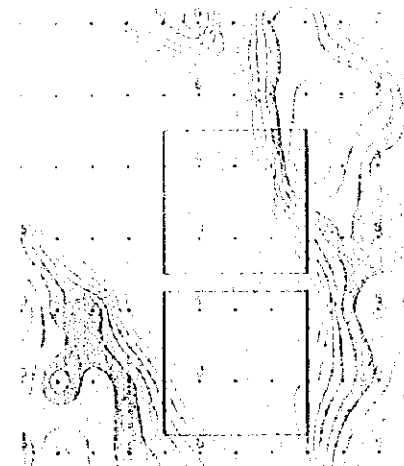
Fig.H-2-36 IP plane map of  $n=2$  in Doqal area



Deep Area

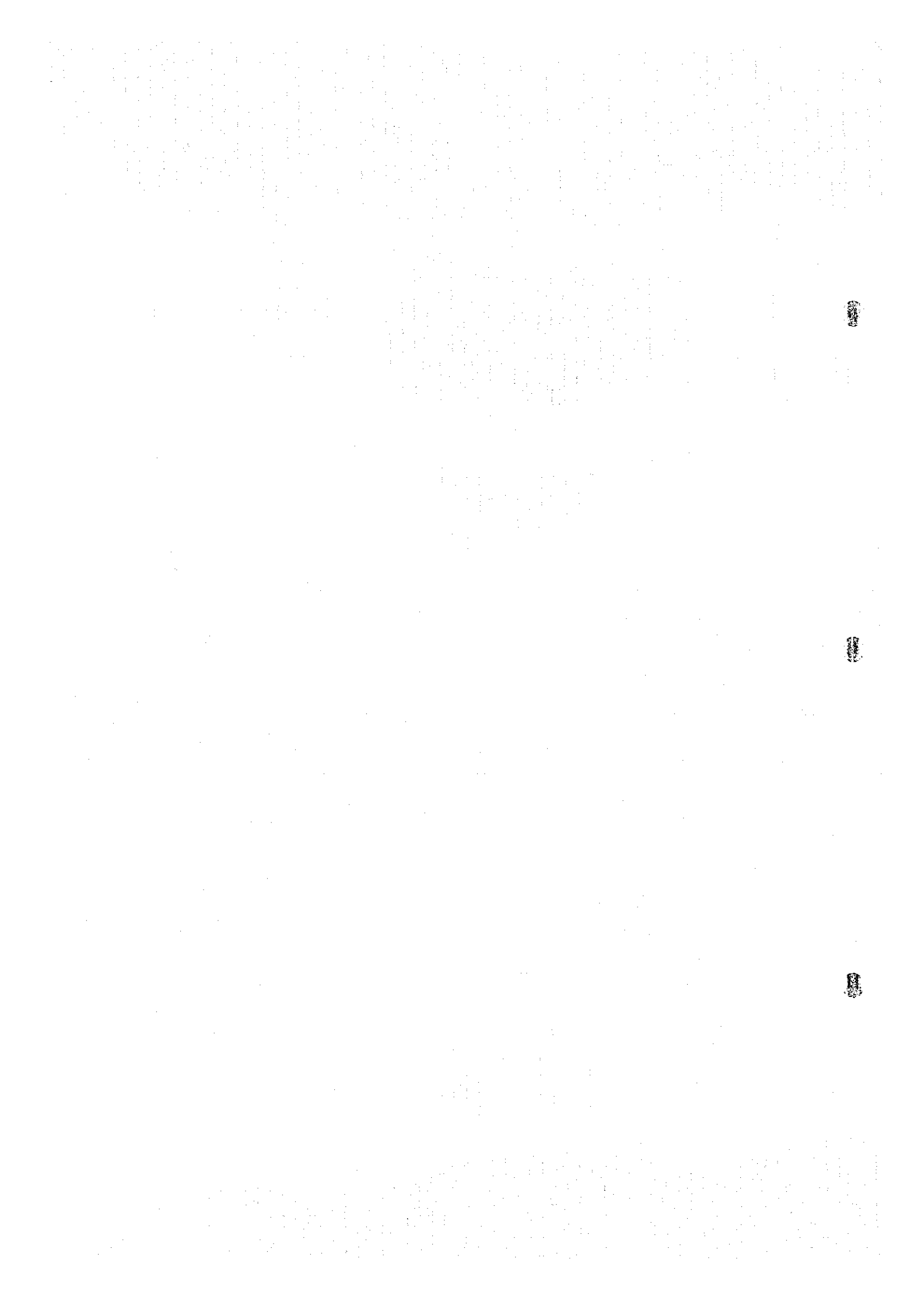


Deep Area



Deep Area

100' Contour  
 Deep Area  
 TDM Survey  
 11/2/02



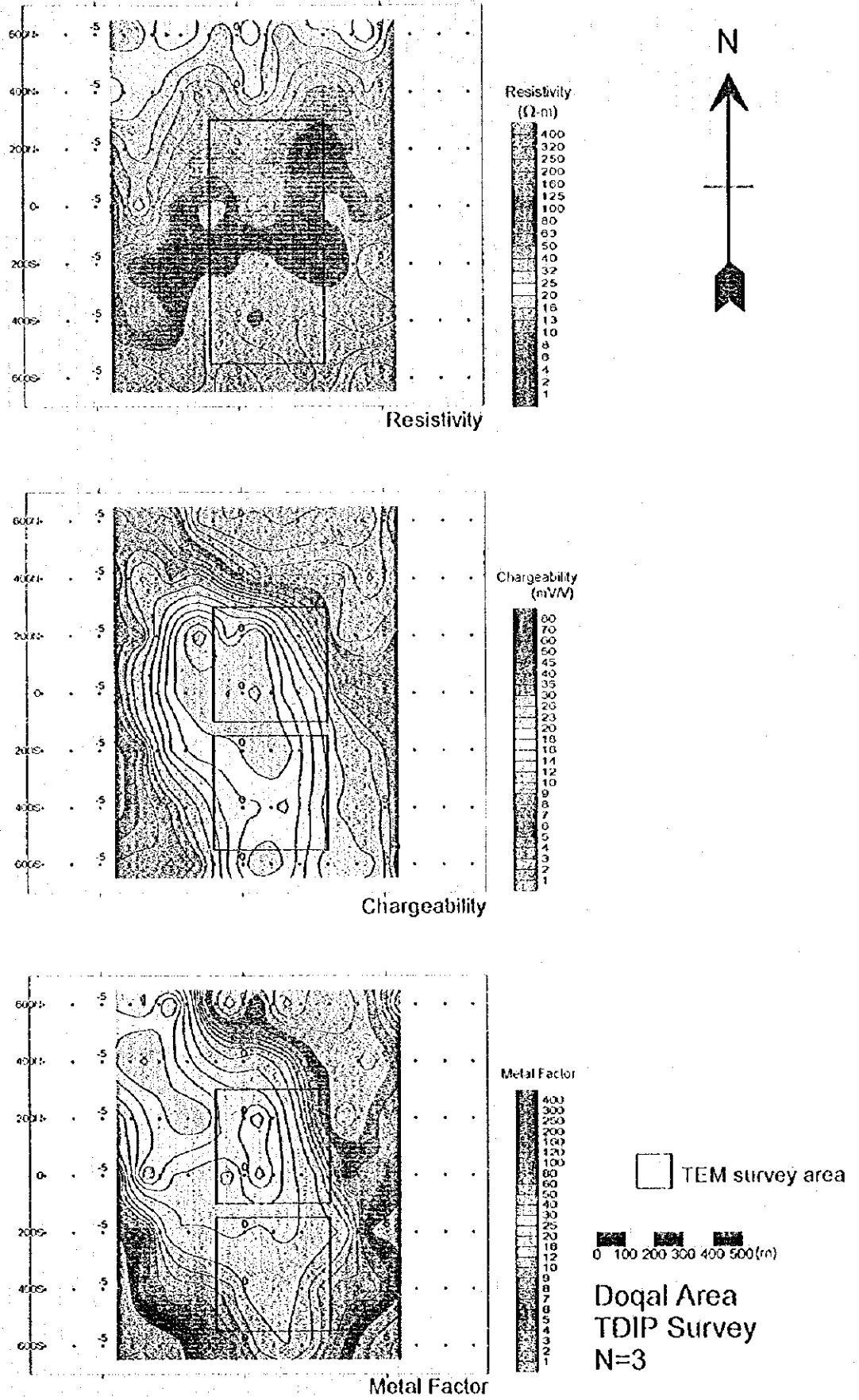


Fig.H-2-37 IP plane map of n=3 in Doqal area

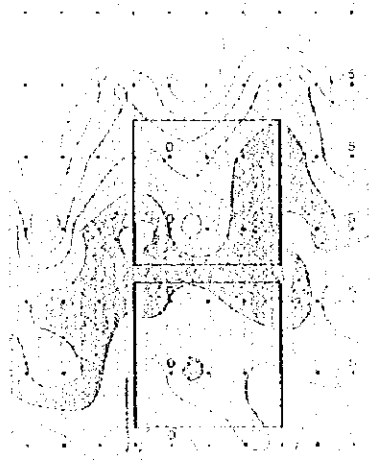


Figure 1

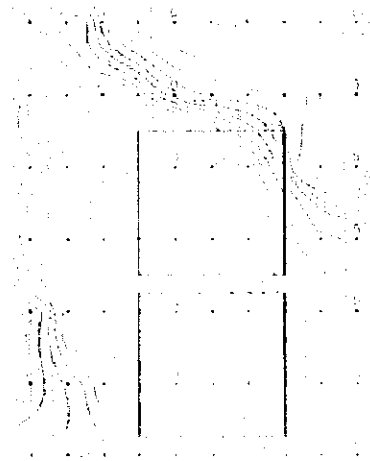


Figure 2

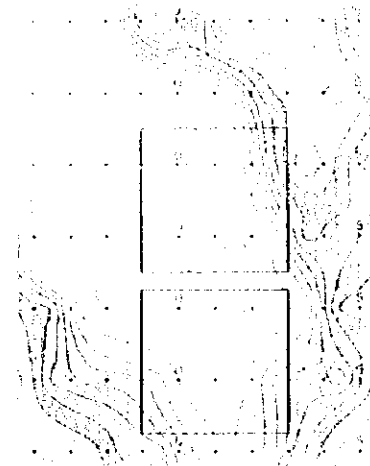


Figure 3

100 200 300  
 400 500 600  
 700 800 900  
 1000

